Rare Earth and Other Critical Element Concentrations in the Sentinel Butte Formation, Tracy Mountain, North Dakota

by

Levi D. Moxness, Edward C. Murphy, and Ned W. Kruger

REPORT OF INVESTIGATION NO. 128
NORTH DAKOTA GEOLOGICAL SURVEY
Edward C. Murphy, State Geologist
Lynn D. Helms, Director Dept. of Mineral Resources
2021

Table of Contents

Tables

Figures

Abstract

High rare earth element concentrations (>300 ppm) were found in a thin lignite bed at Tracy Mountain during reconnaissance sampling in southern Billings County, North Dakota in 2016. Tracy Mountain is a series of buttes comprised of alternating beds of sandstone, siltstone, mudstone, claystone, lignite, and clinker representing roughly the lower two-thirds of the Sentinel Butte Formation of the Fort Union Group (Paleocene). A dozen carbonaceous beds and bentonites were traced across the study area. In total, 15 geologic sections were measured across Tracy Mountain and the surrounding area, and 169 rock samples were submitted for critical element ICP-MS analysis, most of which (155) were lignites and carbonaceous claystones or mudstones. Tracy Mountain samples were analyzed for the rare earth elements including yttrium and scandium, 26 additional elements deemed critical to the economic security of the United States, and noncritical elements molybdenum and thorium. Between 21 and 169 analyses of each element were acquired, with the more economically promising elements receiving more focus. Extensive sampling revealed that high rare earth concentrations (>300 ppm) occur in multiple thin carbonaceous beds over an area of approximately 25 acres, with multiple beds exhibiting spot concentrations over 1000 ppm on a whole coal basis. The highest rare earth concentrations occur in the stratigraphically highest carbonaceous beds, carbonaceous beds immediately below bentonites, and in carbonaceous beds associated with white, greasy claystones and mudstones. In samples with rare earth element concentrations >300 ppm, the high-demand elements dysprosium, neodymium, scandium, and terbium make up 25.7% of the total rare earth elements. Magnesium, zirconium, molybdenum, vanadium, gallium, and uranium are also enriched at Tracy Mountain relative to other US coals. Many critical elements, most notably gallium, vanadium, and uranium, are strongly correlated with the rare earths and may have become enriched via the same pathways. Establishing the presence of these elements in North Dakota lignites and the tendency for each to co-occur has implications in identifying the feedstocks, target mineral commodities, and extraction methods for any future commercial production.

Acknowledgements

Analytical and field costs for this project were financially supported by one-time appropriated state funds (funded as special projects) for the 2015-2017 and 2019-2021 bienniums and a 2020 EPP grant from the North Dakota Lignite Research Council. Rock samples collected from U.S. Forest Service were done so under a collecting permit and the Survey wishes to thank USFS personnel Martina Thornton, Sabre Hanna, Shannon Boehm, and Misty Hays. The Survey also wishes to thank Kim Shade for allowing access to his property.

Introduction

The North Dakota Geological Survey began a critical elements investigation in the fall of 2015. Rock samples (primarily lignites) were collected for rare earth element (REE) analysis from outcrops in the Little Missouri River badlands in southwestern North Dakota. During the first two years of the study, 65 geologic sections were measured, and 352 samples were analyzed for rare earth element concentrations. The results were reported in Kruger and others (2017), which documented the first detailed occurrences of rare earth enrichment in North Dakota. Murphy and others (2018) reported on high concentrations and lateral variability of REE within lignites at Logging Camp Ranch in Slope County after measuring 20 additional geologic sections and submitting 113 samples for analysis. Since 2018, 1,056 samples have been analyzed and 184 additional geologic sections have been measured. Additionally, in recent years the rock samples have been routinely analyzed for other select critical elements. The primary study area encompasses a 30 x 150 mile (9 x 46 km) rectangle stretching from the North Dakota-South Dakota border in Bowman County to Tobacco Garden Creek in McKenzie County. More recently, the study has been expanded to include central and south-central North Dakota (Figure 1).

Samples were collected across an 1,800-foot (550 m)-long stratigraphic interval from the Fox Hills Formation (Cretaceous) through the Arikaree Formation (Miocene), encompassing 10 of the 12 bedrock formations that are exposed at the surface in western and south-central North Dakota. The focus of the study has been the coal-bearing rocks of the Fort Union Group (Figure 2). The vast majority of analyzed

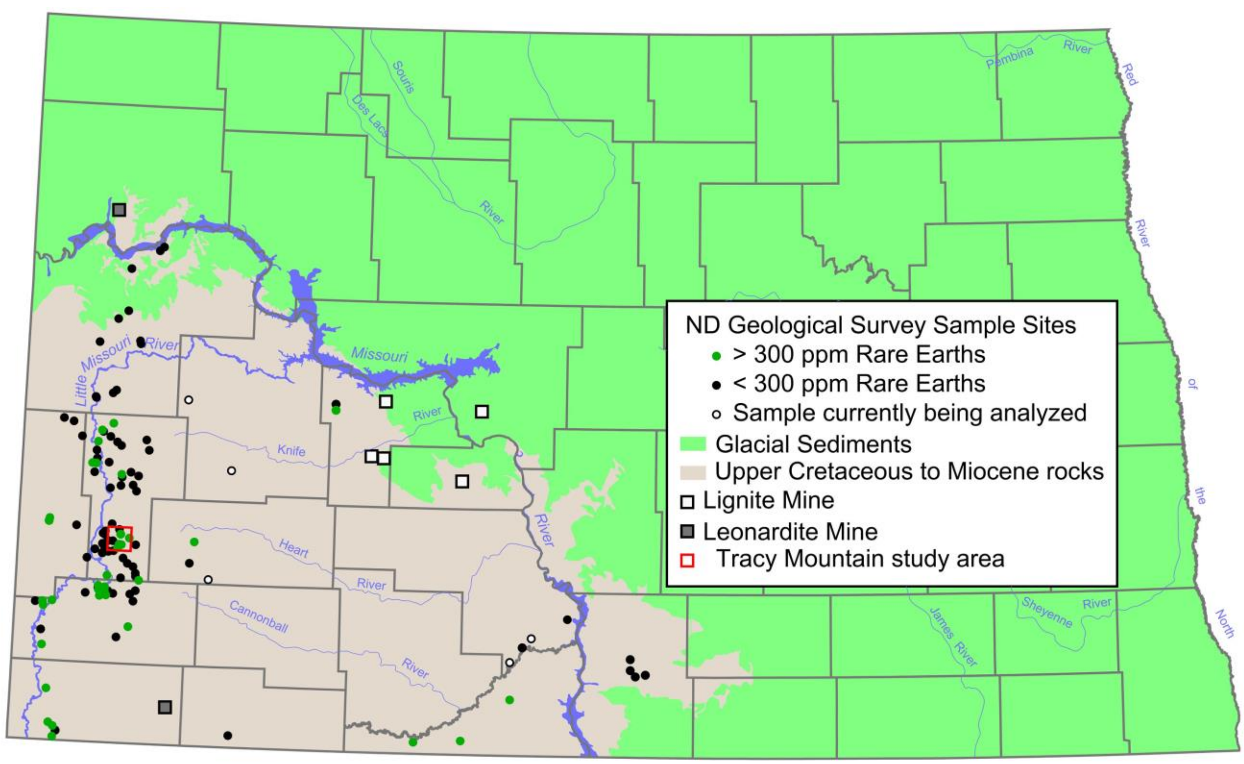

▲ **Figure 1.** North Dakota Geological Survey critical element study sample sites. Existing mines are included as points of reference.

samples have been organic-rich rocks (91%), either lignites (72%) or carbonaceous claystones and mudstones (19%). Volcanic ash (tuffs) or altered volcanic ash (tonsteins and bentonites), clinker (scoria), natural coal ash, both iron and manganese nodules, and sandstone concretions have also been analyzed (Table 1). The majority of samples have come from five areas: west-central Billings County, Tracy Mountain, Logging Camp Ranch, the type section of the Slope Formation, and Mud Buttes.

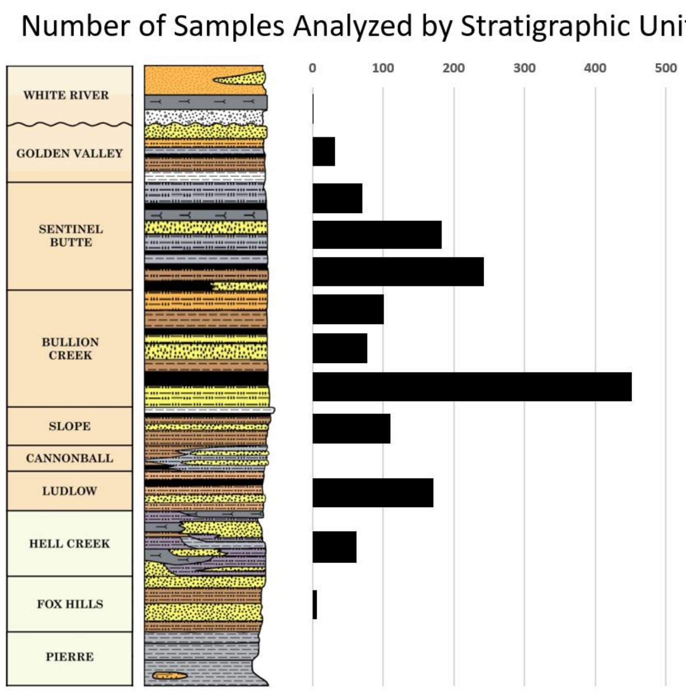

◀ **Figure 2.** The number of samples analyzed for critical elements for the entire NDGS study by stratigraphic position. The Fort Union Group consists of the rocks from the Ludlow Formation up through the Sentinel Butte Formation.

▼ **Table 1.** The number of samples analyzed for REE and other critical elements by lithology.

Entire Project (2015-2021)	Tracy Mtn. (This Report)	Lithology
1,089	110	Lignites
292	45	Carbonaceous clay/mudstones
25	1	Claystones and mudstones
25	7	Bentonites
22		Tonsteins
22	4	Nodules or concretions
20		Volcanic tuffs
12	2	Natural coal ash
11		Sandstones and siltstones
3		K/Pg ejecta
1,521	**169**	**Total**

Fieldwork

Tracy Mountain consists of roughly a half dozen flat-topped buttes or mesas rising 200 to 300 feet (60-90 m) above the surrounding badlands topography in south-central Billings County, approximately 13 miles (21 km) southwest of the town of Belfield (Figure 3). This butte complex trends from the southwest to the northeast covering approximately 1,160 acres (4.7 km^2) in portions of sections 9, 10, 15, and 16 (Township 138N, Range 101W) and has a maximum elevation of approximately 2,900 feet (884 m).

Ned Kruger first measured a geologic section and collected lignite samples for rare earth analysis along the southeast corner of the Tracy Mountain complex in the fall of 2016 (measured section 7 of this report, section 37 of Kruger et al., 2017). The site was chosen for study due to the presence of an old upland surface and the excellent outcrops exposed along the butte slopes. Samples of the upper coal had high rare earth element concentrations in excess of 300 parts per million (ppm) on a whole rock basis (the economic threshold suggested by the U.S. Department of Energy). As a result, an additional section was measured (section 4 of this report, section 38 of Kruger et al., 2017) and two more lignite samples were collected and submitted for analysis in 2017, those samples also contained high concentrations. In 2018, a third geologic section (section 2) was measured 1,700 feet (520 m) to the northwest of measured section 7 and a dozen more rock samples were collected in the upper coals. Consistently high critical element

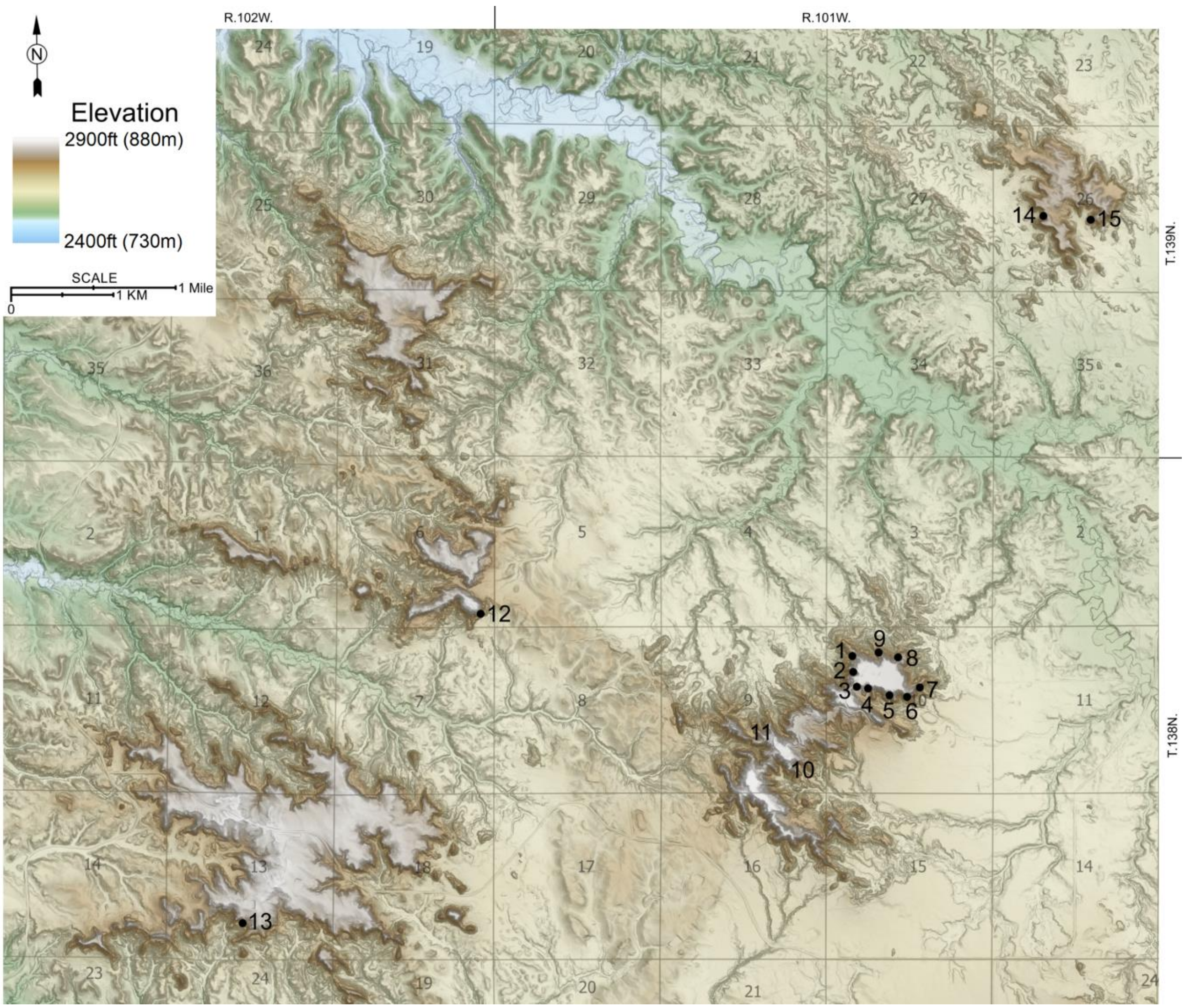

▲ **Figure 3**. The topography of the Tracy Mountain area and the locations of the 15 measured sections and sample sites in this study. The exact locations of measured sections 10 and 11 were not plotted on this map.

concentrations in those well-exposed, laterally continuous, upper carbonaceous beds led to the expansion of the project at Tracy Mountain. Previous investigations into the lateral extent of REE enrichment zones had been limited by the exposure of outcrops or the extents of the lignites themselves (Murphy et al., 2018). In 2020 and 2021, 13 more geologic sections were measured and 150 additional rock samples were collected. The 15 geologic sections plot along a seven-mile-long (11 km), two-to-three-mile-wide (3-5 km) transect centered on Tracy Mountain (Figure 3). Measured sections 1-9 were concentrated around the perimeter of the largest mesa in the Tracy Mountain complex (the northwest quarter of section 10, T138N, R101W). Most of the measured sections on this mesa are spaced 300 to 500 feet (90-150 m) apart (Figure 3). Two additional geologic sections are located 0.6 miles (1 km) southwest of the main butte and four sections are located on isolated buttes or uplands beyond the Tracy Mountain complex; one approximately two miles (3 km) to the northwest, another four miles (6 km) to the southwest, and two more roughly three miles (5 km) to the northeast (Figure 3).

A team of three geologists typically performed the fieldwork with one measuring section and the other two collecting the rock samples. Whenever possible, geologic sections were measured along steep, poorly vegetated slopes to minimize the amount of colluvium obscuring the underlying lithologies. A pick was used to dig down to fresh rock so that bed thickness and characteristics of the freshly exposed rock could be recorded in a field notebook. All rock samples were collected in approximately three-inch-thick (8 cm) stratigraphic intervals after a minimum of six inches (15 cm) was removed from the outcrop in order to minimize the collection of weathered rock. A typical sample weighed approximately 3.3 pounds (1,500 g) and was stored in a gallon-size Ziplock bag. Samples were generally taken from the top three inches (8 cm) of a bed or wherever the most carbonaceous rocks were present.

In total, 175 rock samples were collected from the Tracy Mountain study site. The vast majority of these were either from lignites (116 samples) or carbonaceous claystones or mudstones (45 samples). Additionally, one sample was collected from a mudstone, seven samples were collected from bentonites, four from iron-oxide nodules, barite nodules, or sandstone concretions, and two samples were taken of coal ash beneath clinker deposits. Carbonaceous beds in close proximity to the base of bentonites were specifically targeted for sampling.

Laboratory Analysis

Upon return from the field, rock samples were split into a 2.2 pound (1,000 g) sample that was shipped to Standard Laboratories in Casper, Wyoming and a 1.1 pound (500 g) sample that was archived in the Geological Survey warehouse. Tracy Mountain rock samples were submitted to the laboratory for analysis in 2016, 2017, 2018, 2020, and 2021. In total, 169 of the 175 samples collected were submitted to the laboratory for analysis (Table 1).

The initial focus of the Geological Survey's critical elements project was on rare earths. In 2016, all rock samples, including the first nine samples collected from Tracy Mountain, were analyzed only for rare earth element concentrations (Kruger et al., 2017). The analyses included the fourteen stable lanthanide series elements (lanthanum, cerium, praseodymium, neodymium, samarium, europium, gadolinium, terbium, dysprosium, holmium, erbium, thulium, ytterbium, and lutetium) and yttrium. All concentrations were reported on a whole rock basis. The NDGS added scandium to its analyses in 2017, and it is considered a REE in this report.

On May 18, 2018, the Secretary of the Interior finalized a list of 35 mineral commodities deemed critical: aluminum (bauxite), antimony, arsenic, barite, beryllium, bismuth, cesium, chromium, cobalt, fluorspar, gallium, germanium, graphite (natural), hafnium, helium, indium, lithium, magnesium, manganese, niobium, the platinum group metals, potash, the rare earth elements group, rhenium, rubidium, scandium, strontium, tantalum, tellurium, tin, titanium, tungsten, uranium, vanadium, and zirconium (Interior Dept., 2018). Subsequently, the NDGS expanded the scope of its investigation.

From 2018 on, in addition to REE, Tracy Mountain samples were also analyzed for some of the additional critical elements. The NDGS was also able to obtain additional critical element analyses on some of the previous year's submissions for which the lab had retained sufficient amounts of sample material. Initially, those samples were analyzed for a subset of 26 critical elements; antimony (analyzed for in 81 samples), arsenic (73 samples), barium (81), beryllium (34), bismuth (21), cesium (34), chromium (108), cobalt (55), gallium (128), germanium (130), hafnium (137), indium (21), lithium (34), magnesium (127), manganese (24), niobium (126), rubidium (24), strontium (34), tantalum (108), tellurium (21), tin (21), titanium (34), tungsten (154), uranium (157), vanadium (126), and zirconium (127) along with the noncritical elements molybdenum (157) and thorium (24). Molybdenum, while not considered a critical element in the United States, is a potential value-added product from coal and has been the subject of past commercial exploration in North Dakota lignites, along with uranium and germanium (Murphy, 2005). Thorium, by contrast, is a troublesome contaminant in traditional rare earth ores and can be difficult to separate from the REEs during refinement. Its presence is a consideration in the economic assessment of any REE ore. Due to limitations of the analytical budget, all samples were not analyzed for all 28 elements plus the rare earths. Criteria for which elements to investigate were based upon concentrations relative to lignites from elsewhere in North Dakota, the U.S., and an economic assessment of each element by Dai and Finkelman (2018). In general, more promising elements received more analyses, although some elements considered less promising when produced from coal received additional focus when concentrations were among the highest reported from a North Dakota lignite.

Laboratory analyses for all REE, excluding scandium from six pre-2017 samples, were obtained from 72 of the 169 samples, including all for which ∑REE>300ppm. For the other samples, it was determined that reliable estimates of total REE concentrations could be made by analyzing just seven (lanthanum, cerium, neodymium, gadolinium, erbium, yttrium, and scandium) of the sixteen REEs. These estimates appear in italics in Appendix A. Estimates were calculated using linear regression formulas based on the trendlines from scatter plots of each unknown element compared to its closest-affiliated element(s) with a known concentration, obtained from a database containing a full suite of REE analyses from 828 samples from this and previous studies. The linear regressions were found to produce total REE concentrations within a deviation range of -2.6 to 1.8% from the laboratory measurements and an average deviation of ±0.37%. (Kruger, 2020).

Throughout the project the focus has remained on critical elements. Major ions, including sodium, calcium, potassium, and sulfate were not analyzed to enable funding to be focused on determining the extent of high critical element concentrations.

Geology

Tracy Mountain and the surrounding area consist of alternating beds of claystone, mudstone, siltstone, sandstone, lignite, and clinker (scoria) of the Sentinel Butte Formation, Fort Union Group (Paleocene) (Figures 4 and 5, Appendix A). A six-foot (1.82 m) thick exposure of the HT Butte lignite, the base of which marks the contact of the Sentinel Butte Formation with the underlying Bullion Creek Formation, is present in a ravine in the northeast quarter of section 10. For several miles to the north of Tracy Mountain, the HT Butte lignite has burned, forming low, clinker-capped knolls and ridges at an approximate elevation of 2,600 feet (792 m) above sea level. The HT Butte bed is also present at an elevation of approximately 2,650 feet (808 m) at the base of a ravine below measured section no. 13 (Figure 5). The HT clinker caps ridges and small buttes for several miles (kilometers) to the south of this location. The HT Butte lignite is approximately 14 feet (4.3 m) thick in this area and is traceable through the shallow subsurface on gamma ray logs from coal exploration holes and oil wells. The roughly 300 feet (90 m) of Sentinel Butte strata that comprise Tracy Mountain represents approximately 60% of the total formation thickness in this area. The Sentinel Butte Formation is 512 feet (156 m) thick at Square Butte in Golden Valley County (Murphy et al., 1993, figs. 51 and 97).

The HT Butte bed is the thickest lignite in the Tracy Mountain complex with an exposed thickness of six feet (1.8m). None of the other coals in this complex are more than four feet (1.2 m) thick, although buttes to the north (measured section nos. 14 and 15) contain a 6.5-foot (2.0 m) lignite. More than a dozen thin lignites and carbonaceous claystones are exposed on the slopes of Tracy Mountain or in adjacent drainages. For the purposes of this study, these thin lignite and carbonaceous beds were given letter designations A thru S in descending order from the top of the main mesa in the study area (Figure 4). The HT sample designation was used for samples collected from the HT Butte bed. Additionally, a generalized stratigraphic column was constructed for Tracy Mountain and the positions of the upper carbonaceous beds (A-K) were plotted on it (Figure 6). Lithologic description, bed thickness, and sample position are also noted for these carbonaceous beds. Thin lignites are typically difficult to trace laterally for any distance because they can suddenly pinch out, but many of these thin coals could be traced throughout the relatively closely spaced measured sections (nos. 1-9). While traceable, many of these thin coals transitioned from lignite into carbonaceous claystones and mudstones. Thin lignite layers and/or lignite stringers were typically present in these carbonaceous beds (Figures 7-9).

More than a dozen gray to bluish-gray swelling claystones are present in the Sentinel Butte Formation at Tracy Mountain (Figures 4, 5 and 10). These claystones have an irregular, granular weathering surface that results from the swelling and shrinking that occurs when the clays alternately hydrate and dehydrate. In the field, this weathering surface is typically referred to as popcorn texture (Figure 11). The gray to bluish-gray claystones with the well-developed popcorn surface were assumed to be bentonites, but were not confirmed as such by petrographic analysis (Forsman, 1985). Several of these “bentonites” were traceable through measured section nos. 1-9 (Figure 4). Lignites and carbonaceous mudstones that were overlain by bentonites were specifically targeted for sampling (Figures 12 and 13). Forsman (1985) determined that Sentinel Butte claystones and mudstones are typically composed of a mixture of montmorillonite, illite, chlorite, and kaolinite. As a result, Sentinel Butte claystones and mudstones typically contain a swelling clay component.

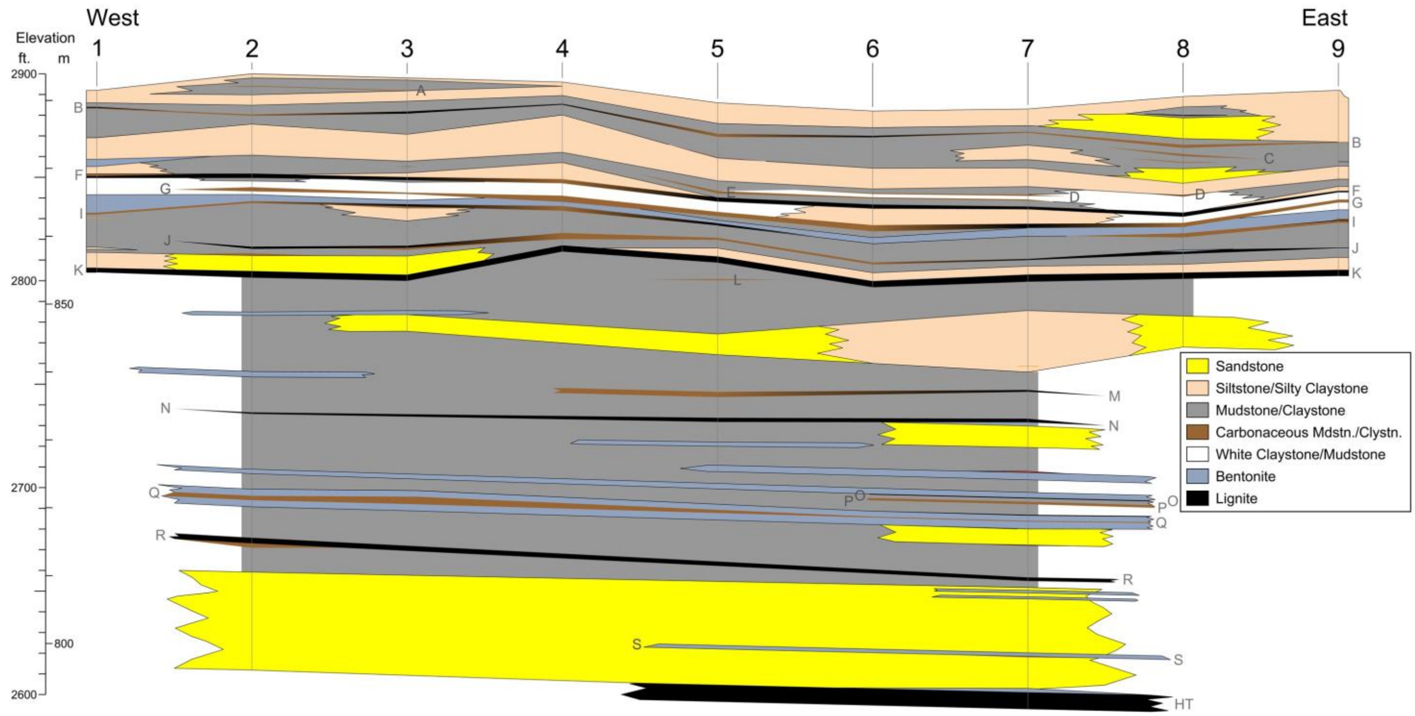

▲ **Figure 4.** A geologic cross-section of measured sections 1-9 in the Tracy Mountain study. See Figure 3 for the location of the measured sections.

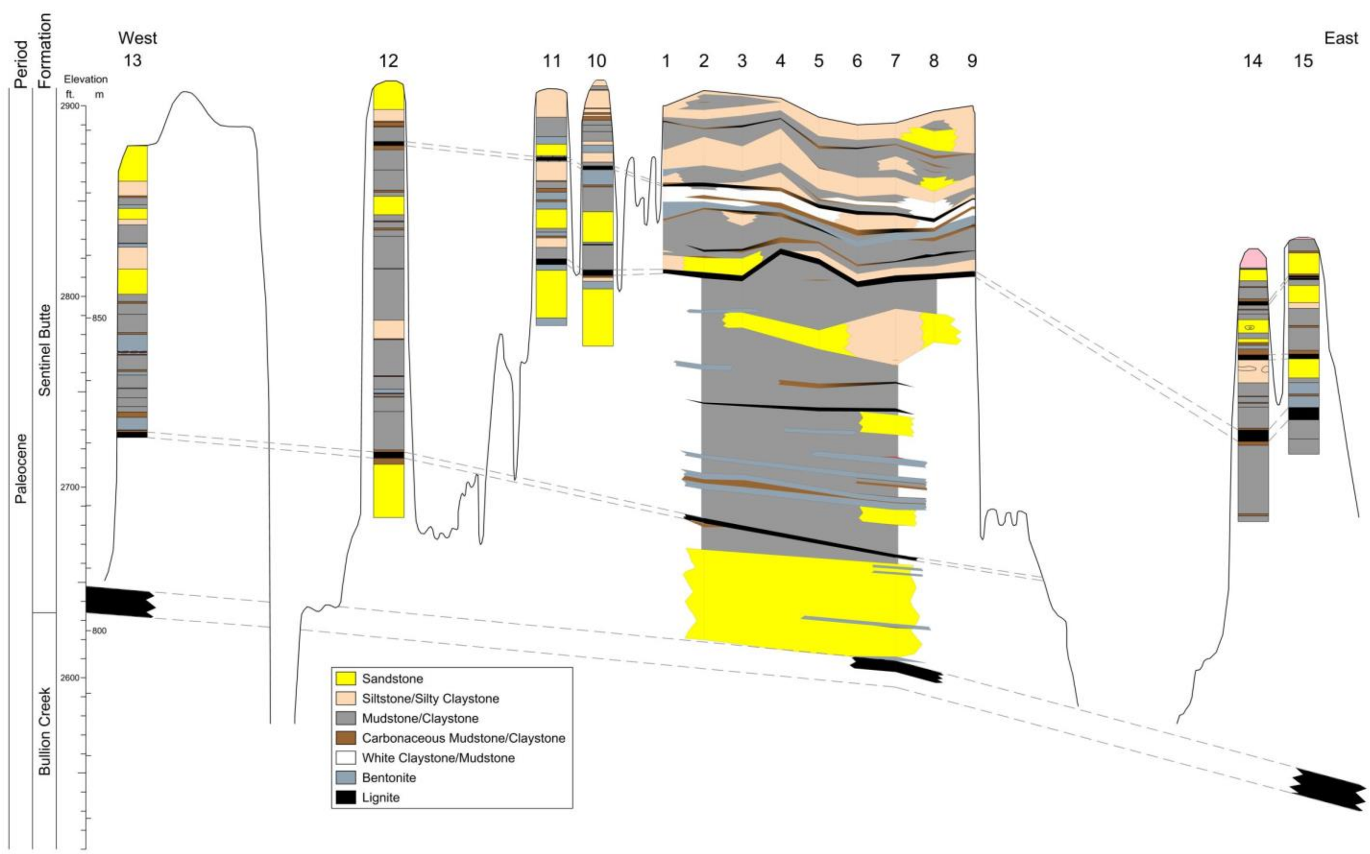

▲ **Figure 5.** A geologic cross-section of measured sections 1-15 in the Tracy Mountain study. See Figure 3 for the location of the measured sections.

Tracy Mountain
Generalized Stratigraphic Column

Main butte (Measured sections 1 through 9)
Upper 100 ft / 30 meters

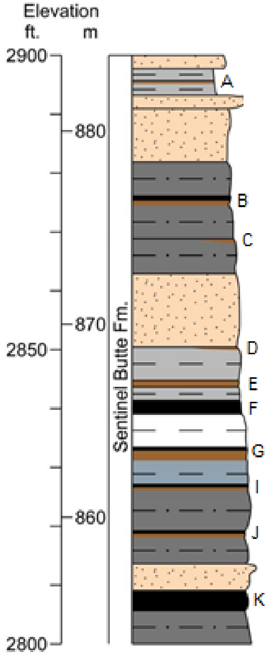

Bed	Bed thickness in	Bed thickness cm	Lithologic Description
A	0 to 2	0 to 5	Carbonaceous mudstone, dark brown, soft
B	8 to 16	20 to 41	Lignite, black, soft, grades down to carb. mudstone, brown, soft and then to carbonaceous claystone, dark brown
C	0 to 2	0 to 5	Carbonaceous mudstone, brown, soft
D	0 to 2	0 to 5	Carbonaceous mudstone, brown, soft
E	0 to 2 0 to 2	0 to 5 0 to 5	Thin coal stringers, black, soft, near the top and base of a 3ft (1m) zone of weakly carbonaceous mudstone, gray-brown
F	10 to 18	25 to 46	Lignite, black, soft
G	1 to 3	2 to 5	Lignite, black, soft at/near top of 3ft (1m) carb mudstone, soft, brown
			C.f. bentonite, carbonaceous base in places
I	0 to 14	0 to 36	Lignite, dark brown to black, clay-rich, grades to carbonaceous mudstone at base
J	0 to 20	0 to 20	Lignite, black, powdery, grades to carb. mudstone at base
K	32 to 42	81 to 107	Lignite, black, hard

▲ **Figure 6.** Generalized descriptions for the upper carbonaceous beds at Tracy Mountain.

◄ **Figure 7.** Approximately 3.4 feet (1.04 m) of lignite is exposed after the colluvium was scraped off of measured section 6. Sample 6K2t was obtained from the top two inches (5 cm) and sample 6K2b from the basal two inches (5 cm) of the coal.

▲ **Figure 8.** A three-inch (7.6 cm) thick coal stringer (sample G) within a four-foot (1.2 m) thick carbonaceous mudstone at measured section no. 6.

▲ **Figure 9.** Sample B, measured section no. 2, was taken from the top two inches (5.1 cm) of this one-foot (0.3 m) thick organic-rich bed. As is typical of many of these thin carbonaceous beds, it consists of a mixture of thin lignite layers and even thinner lignite stringers. This bed is overlain by silty mudstone.

▲ **Figure 10.** A drone photograph looking southwest across the main study site at Tracy Mountain to Bullion Butte in the distance. Thick, bluish-gray swelling claystones (assumed to be bentonites) in the Sentinel Butte Formation cap many of the knolls and ridges adjacent to Tracy Mountain in this area.

▲ **Figure 11**. Popcorn texture of the surface of a bentonite layer resulting from the shrinking and expanding of the swelling clays as they alternately hydrate and dehydrate. A penny in the lower left for scale.

▲ **Figure 12.** In the foreground, a thin, carbonaceous bed (Sample O) at the base of a bentonite in measured section no. 7. Bentonite is draped over the underlying mudstone. Another prominent bentonite is present just below the break in slope. The photograph was taken looking to the northeast.

◄ **Figure 13.** A thin, carbonaceous bed (sample 8I2) beneath a bentonite (8I2r) in measured section 8.

A white to light gray claystone or mudstone was traceable throughout most of measured section nos. 1-9 (Figures 4 and 14). The bed ranges in appearance from a dazzling white, iron-oxide stained, well-indurated, well-exposed claystone to a light gray, moderately exposed mudstone. Wherever traceable, the one consistent trait throughout the bed was the greasy feel of the rocks which was assumed to indicate an elevated presence of kaolinite similar to what is found in the Rhame Bed of the Slope Formation (Paleocene) and the Bear Den Member of the Golden Valley Formation (Paleocene\Eocene) (Murphy, 2013).

The top of the main butte at Tracy Mountain, as well as much of the surrounding uplands, is capped by yellow to yellowish-gray siltstone, clayey siltstone, or silty mudstone (Figure 4). The clay fraction of the capstone is variable and the distinction between clayey siltstone and silty mudstone is less straightforward than the cross-section implies (Figures 15 and 16). The siltstone is typically poorly cemented, but eight of the 15 measured sections recorded flaggy, well-cemented siltstone beds within three feet (0.9 m) of the tops of buttes (Figure 17). Although there may have been some reworking of the poorly cemented siltstone by the wind, it was not evident in the measured sections along the perimeter of the buttes. Pliocene gravel is often present as lag deposits at the top of the major buttes of western North Dakota, but none was observed at Tracy Mountain nor on the adjacent uplands.

Nodules and concretions are relatively common in the Sentinel Butte Formation. Calcite-cemented sandstone and siltstone concretions, along with iron-oxide nodules, were collected for analysis to investigate if critical elements were mobilized with cementing agents (Figure 18). Barite nodules are less common, well-rounded, and are typically smaller in size in comparison to the other nodules and concretions. A fist-sized barite nodule was collected while measuring section no. 7 (Figure 19).

Sample Results

A summary of concentrations is presented in Table 2. Individual analyses are plotted along the corresponding measured section in Appendix A and listed in a comprehensive table in Appendix B. The stratigraphic position of the rock samples was also plotted on the two cross-sections generated across the study area and color-coded based on those samples meeting or exceeding 300 ppm for total rare earth element concentrations and those concentrations falling near or below that threshold (Figures 20 and 21). In addition, the maximum and mean rare earth concentrations of samples A-K were plotted on the generalized stratigraphic section of Tracy Mountain (Figure 22). In all of these figures and tables, several patterns are evident: the highest rare earth concentrations at Tracy Mountain occur in the stratigraphically highest carbonaceous beds (A-I), high REE concentrations are sometimes found in carbonaceous zones immediately underlying bentonite beds (I and O), as well as carbonaceous beds associated with white (possibly kaolinite-rich) beds (D and E).

Two generalized targets for economic concentrations of REE in coal are referenced in the literature: 1) 300 ppm in whole coal, proposed by the U.S. Dept. of Energy, and 2) 0.1% rare earth oxide (REO) content in the ash (which excluded scandium) suggested by Seredin and Dai (2012). Both of these thresholds are referenced in this report as each examines a unique subset of samples, which is useful as it is yet unknown whether any future extraction methods will utilize feedstocks of whole coal or coal ash (see REE Composition). Many of the samples that contain over 300 ppm on a whole coal basis are rich in clay (e.g., sample 9Ir is 639 ppm REE but 92% ash), and conversely some samples that are below 300 ppm

▲ **Figure 14.** A bright, white, mudstone (sample 1(sil)) in measured section 1 at Tracy Mountain. The mudstone is greasy to the touch. The yellow beds cap the ridge in the background.

▲ **Figure 15.** A drone photograph looking northwest to the main mesa at Tracy Mountain and beds of the Sentinel Butte Formation. Yellow beds cap the mesa and dark, bluish-gray swelling claystones (bentonites) are visible along the lower one third of the exposed rocks. Square Butte and Sentinel Butte in the background.

▲ **Figure 16.** The capping yellow beds at Tracy Mountain consist of siltstone, silty mudstone, and silty claystone. The iron-stained rocks contain round iron-oxide spheres and iron-oxide layers.

▲ **Figure 17.** Flaggy siltstone caps the top of measured section no. 3 and litters the underlying slope. The thin, carbonaceous claystone (sample 3A), partially exposed in the center foreground, is high in critical elements.

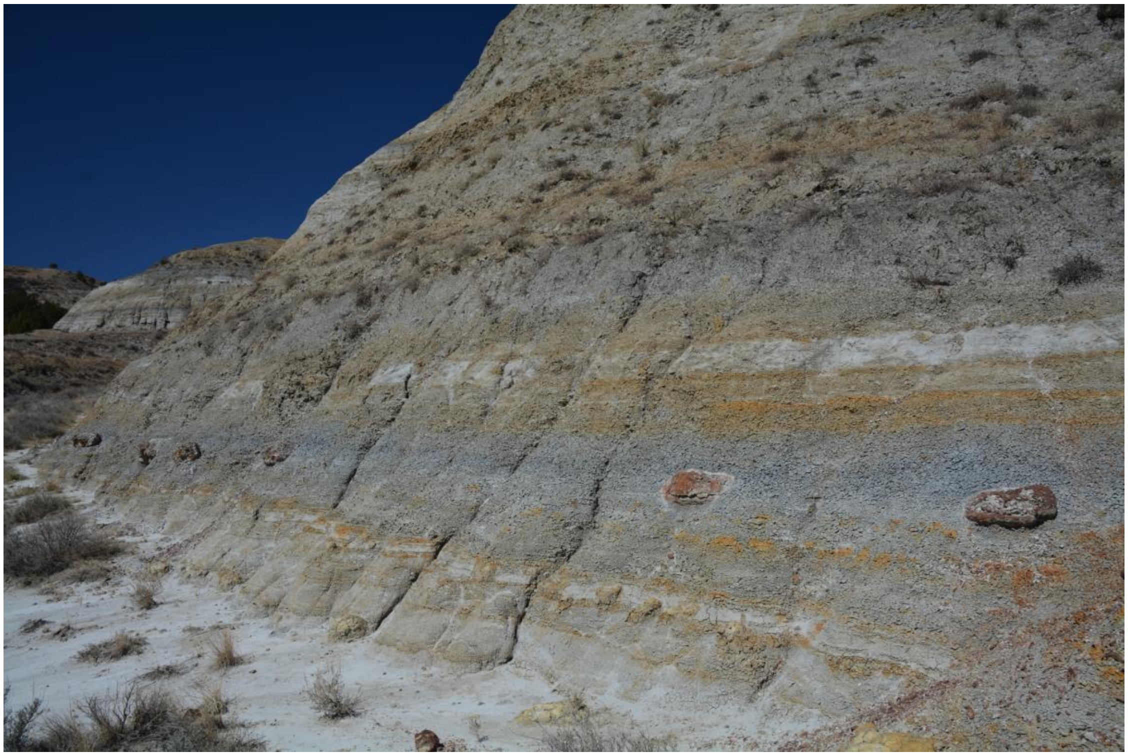

▲ **Figure 18.** Alternating layers of claystone, mudstone, siltstone, sandstone, and lignite in the Sentinel Butte Formation are visible in this photograph of the base of measured section no. 5. A half dozen limonite nodules occur along the same approximate stratigraphic position within a swelling claystone.

▲ **Figure 19.** A barite nodule (left of pick) from measured section no. 7. The nodule was found lying on an iron-oxide concretionary layer.

▼ **Table 2.** Summary of results of sample analyses from the Tracy Mountain study area.

Chemical Group		Element	Symbol	A	Tracy Mountain Analyses (concentrations in ppm)						
						Whole Rock Basis			Ash Basis		
					n	MAX	MIN	MEAN	MAX	MIN	MEAN
Alkali Metals		Lithium	Li	3	34	76.6	1.3	29.9	92.5	4.3	42.2
		Rubidium	Rb	37	24	108	11	61	134	25	83
		Cesium	Cs	55	34	9.88	0.14	4.77	12.3	0.46	6.8
Alkaline Earth Metals		Beryllium	Be	4	34	7.6	0.4	3.9	20.3	0.4	6.5
		Magnesium	Mg	12	157	28800	1580	9020	53300	1600	14600
		Strontium	Sr	38	34	587	34	309	1320	35	545
		Barium	Ba	56	81	32000	222	3954	37800	373	6500
Rare Earth Elements	Lanthanides	Lanthanum	La	57	169	148	4.0	35	285	6.7	56
		Cerium	Ce	58	169	361	7.1	79	695	12.8	131
		Praseodymium	Pr	59	72	46.7	1.3	16.8	89.2	4.3	29.5
		Neodymium	Nd	60	169	199	3.5	43	415	6.4	73
		Samarium	Sm	62	72	49.3	1.6	16.6	96.4	5.3	29.8
		Europium	Eu	63	72	11.5	0.53	3.9	24.7	1.45	7.1
		Gadolinium	Gd	64	169	42.2	0.7	9.5	103	1.2	17
		Terbium	Tb	65	72	6.46	0.39	2.47	15.1	0.91	4.5
		Dysprosium	Dy	66	72	34.8	2.5	13.8	82.2	5.7	25.7
		Holmium	Ho	67	72	6.19	0.48	2.65	15.3	1.11	5.0
		Erbium	Er	68	169	16.7	0.36	4.8	40.7	0.58	8.5
		Thulium	Tm	69	72	2.21	0.19	1.01	5.37	0.49	1.92
		Ytterbium	Yb	70	72	13.6	1.20	6.4	33.2	3.12	12.1
		Lutetium	Lu	71	72	2.00	0.18	0.97	5.06	0.46	1.84
Rare Earth Elements	Transition Metals	Scandium	Sc	21	163	41.5	0.9	17.9	120	3.1	30
		Yttrium	Y	39	169	143	3.9	41	409	5.4	73
Transition Metals		Titanium	Ti	22	34	6930	257	2190	7040	849	3150
		Vanadium	V	23	126	405	5	140	732	27	211
		Chromium	Cr	24	108	167	8	71	298	12	102
		Manganese	Mn	25	24	1310	22	120	1740	31	170
		Cobalt	Co	27	55	253	1.9	20	354	1.9	32
		Zirconium	Zr	40	157	1150	10.1	310	2080	19.9	560
		Niobium	Ni	41	126	30.8	0.8	14.2	97.1	3.2	23.3
		Molybdenum	Mo	42	157	233	<0.2	46	402	<0.3	81
		Hafnium	Hf	72	137	19	0.4	5	34	0.6	8
		Tantalum	Ta	73	108	2.83	0.07	0.82	3.19	0.23	1.13
		Tungsten	W	74	154	83.5	0.1	7.7	151	0.1	13
Post-Transition Metals		Gallium	Ga	31	128	44.2	4.1	19.7	92.7	5.2	30.1
		Indium	In	49	21	0.17	0.02	0.10	0.28	0.09	0.15
		Tin	Sn	50	21	2.7	0.8	2.0	4.2	1.6	2.9
		Bismuth	Bi	83	21	1.21	0.21	0.60	2.29	0.42	0.90
Metalloids		Germanium	Ge	32	128	64	<1	10	100	<2	17
		Arsenic	As	33	73	698	1.7	104	1260	1.7	180
		Antimony	Sb	51	81	25.0	0.29	7.8	44.9	0.29	14.0
		Tellerium	Te	52	21	0.64	<0.1	0.23	0.84	<0.2	0.33
Actinides		Thorium	Th	90	24	45.9	1.9	18.2	55.1	1.9	25.3
		Uranium	U	92	157	200	1	27	304	1	43

A = atomic number

n = number of samples analyzed

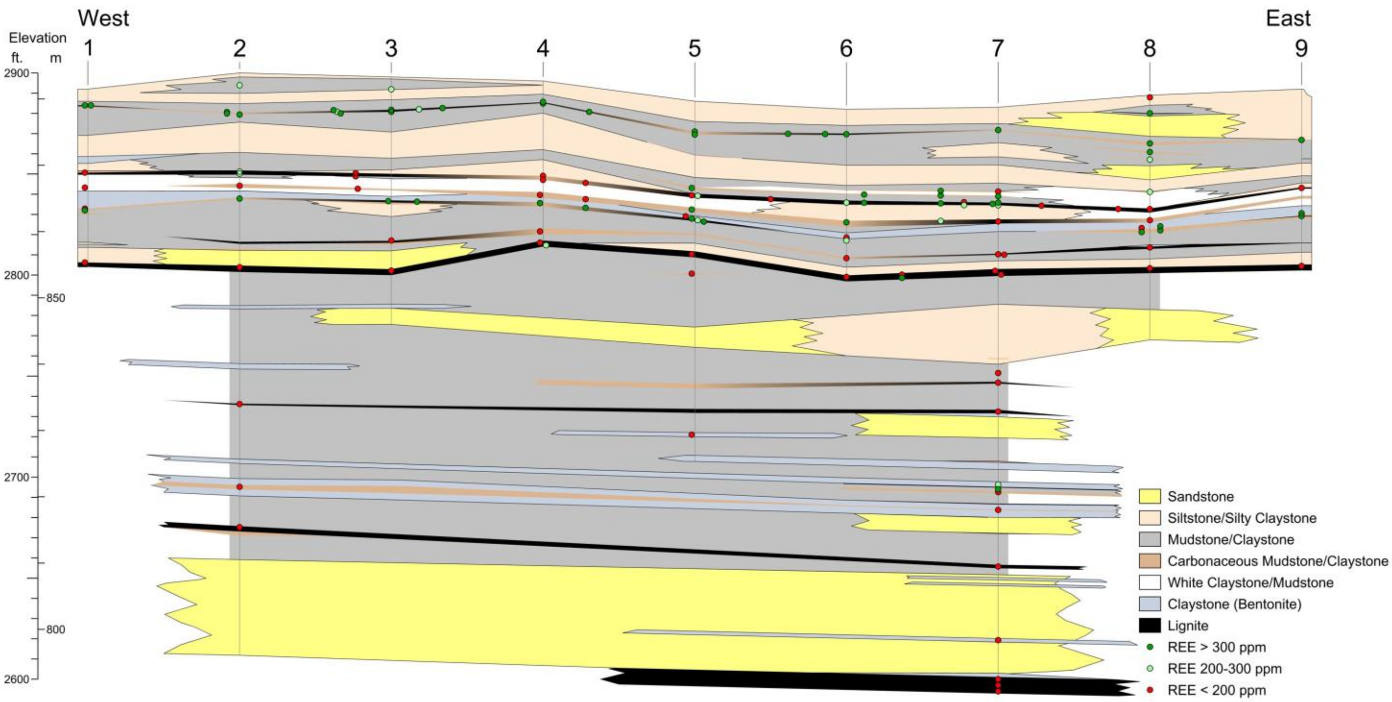

▲ **Figure 20.** A geologic cross-section of measured sections 1-9 in the Tracy Mountain study along with the stratigraphic position of samples submitted for analysis. See Figure 3 for the location of the measured sections.

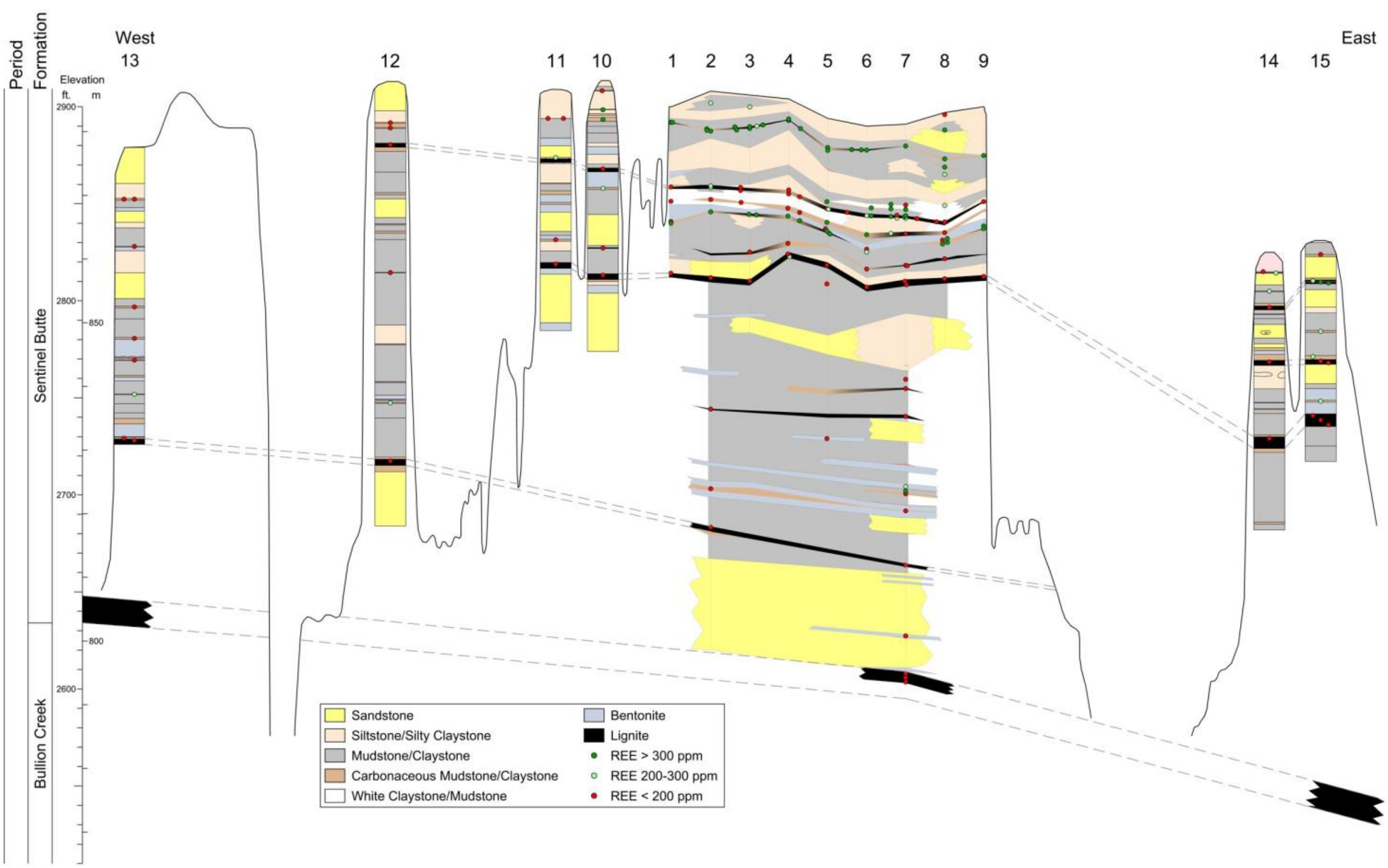

▲ **Figure 21.** A geologic cross-section of measured sections 1-15 in the Tracy Mountain study. See Figure 3 for the location of the measured sections.

Tracy Mountain
Generalized Stratigraphic Column

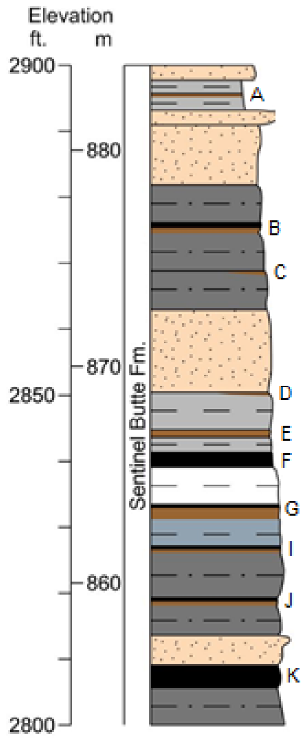

Main butte (Measured sections 1 through 9)
Upper 100 ft / 30 meters

Bed	Bed thickness in	Bed thickness cm	Samples	Sample Position	ASH% MEAN	∑REE Conc. (ppm) MAX	∑REE Conc. (ppm) MEAN
A	0 to 2	0 to 5	3	whole	67%	524	404
B	8 to 16	20 to 41	17	top	73%	**1054**	**511**
			5	bottom	77%	642	473
C	0 to 2	0 to 5	1	whole	85%	622	-
D	0 to 2	0 to 5	2	whole	61%	205	191
E	0 to 2	0 to 5	4	top	75%	646	466
	0 to 2	0 to 5	2	bottom	59%	782	564
F	10 to 18	25 to 46	18	top	43%	402	215
			5	bottom	44%	282	217
G	1 to 3	2 to 5	9	whole	61%	412	219
			6	roof	93%	639	282
I	0 to 14	0 to 36	11	top	70%	**1089**	**681**
			1	bottom	88%	413	-
J	0 to 20	0 to 20	6	top	87%	195	163
K	32 to 42	81 to 107	10	top	57%	134	96
			3	bottom	20%	365	232

▲ **Figure 22.** General stratigraphy and REE concentrations of the REE-enriched carbonaceous beds (samples A-K) in the upper 100 ft (30 m) at Tracy Mountain. See Appendix A for full stratigraphic columns.

contain the highest ash-basis concentrations (sample 4Kb contains only 220 ppm on a whole basis, but is low-ash at 16.5%). Of the 169 samples in this report, 53 contained whole-basis concentrations above 300 ppm REE, and 23 contained ash concentrations of 0.1% REO or greater, which here includes scandium.

There are fewer generally accepted economic thresholds for the other 28 elements investigated in this report. These elements are produced from a wide variety of ores, have supply/demand dynamics controlled by a plethora of industries, and are economic at concentrations of different orders of magnitude. In lieu of this, results can be contextualized in terms of enrichment over a baseline. A common standard for this is upper continental crust (UCC). This is not necessarily an economic proxy, however, as each element is economic at a unique ratio to UCC. The rare earths are well-known for not being “rare” in the earth’s crust, but for rarely concentrating into economic deposits, thus the REE are economic at relatively low UCC multiples. Other elements naturally occur in deposits with much higher ratios and coals need to be highly enriched to be competitive, i.e., a coal that is enriched 100 fold over UCC is still not a promising source if existing ores are 1,000 times UCC. Dai and Finkelman (2018) examined concentrations of traditional ore sources vs. those reported from coals and attempted to classify the prospects for each element to be competitively produced from coal. It is therefore also relevant to contextualize concentrations of North Dakota lignites vs the average world coal (AWC). Thus the most promising critical elements would be elements that both 1) Dai and Finkelman identified as potentially competitive and 2) North Dakota lignites are especially enriched in (see Non-REE Critical Elements).

REE Composition

Although there are commercial applications for each of the rare earth elements, market prices vary significantly between them. Many of the more naturally abundant elements (e.g., cerium and lanthanum) are overproduced relative to global demand, thus the value of a given deposit depends not only on its total REE concentration, but the relative percentages of the surplus elements to those in high demand (e.g., dysprosium, neodymium, terbium). The Mountain Pass mine, the U.S.'s only major historical source of REE, targets an igneous carbonatite deposit with a rare earth composition of approximately 49.6% and 33.8% low-value cerium and lanthanum, respectively. The laterite clay deposits of southeast China, conversely, contain cerium and lanthanum values as low as 0.4% and 1.8% of total REE (Gschneidner and Pecharsky, 2019). Given the variability in compositions, the potential of two deposits that contain "economic" concentrations of 300 ppm ΣREE could be drastically different depending on the relative abundance of the individual elements.

A more detailed examination of the individual element distribution is thus required to assess the economic potential of a deposit, especially the behavior of the most economic REEs. The simplest classification scheme divides the REEs into heavy (dysprosium, erbium, gadolinium, holmium, lutetium, terbium, thulium, ytterbium, and yttrium) and light (cerium, europium, lanthanum, neodymium, praseodymium, samarium, and scandium) elements, although the point of division varies. The heavy elements have traditionally been considered the more valuable group, but light elements neodymium, praseodymium, and scandium have seen increased commercial use and are now among the most economically important. Seredin and Dai (2012) created a coefficient designed to illustrate the economic value of a given concentration by representing the relative abundance of elements with high demand to those produced in excess. This outlook coefficient of rare earth ores (C_{outl}), listed below, groups the REE into critical (neodymium, europium, terbium, dysprosium, erbium, and yttrium), uncritical (gadolinium, lanthanum, praseodymium, and samarium), and excessive (cerium, holmium, thulium, ytterbium, and lutetium).

$$C_{outl} = (Nd + Eu + Tb + Dy + Er + Y / \Sigma REY)/(Ce + Ho + Tm + Yb + Lu/\Sigma REY)$$

This coefficient has been a useful qualitative proxy used by many authors since its creation in 2012, however, there have been significant changes in market conditions over the last decade as both supply and demand dynamics have evolved. Prices of lanthanum and samarium are now on par with cerium (excessive) (Table 3). Prices of yttrium, one of the more abundant elements in the critical REE group, have fallen to similar levels. Critical REE europium and erbium have also seen market prices fall below uncritical elements praseodymium and gadolinium and excessive elements lutetium and holmium which have all risen appreciably. Seredin and Dai also did not include scandium in their review, as it does not occur in most conventional REE ores, but may currently be the most valuable single rare earth element in many coals.

Table 3 also includes the theoretical maximum value of each element in one metric ton of ore based on the most enriched sample from Tracy Mountain at 2021 market prices. Although it is unlikely that ore volumes on the order of metric tons will contain concentrations on par with the maximum spot

▼ **Table 3.** Rare earth oxide (REO) market prices from 2011 to September 2021 and the theoretical value of one ton of ore if it were to contain the highest REE concentrations found at Tracy Mountain.

Seredin & Dai Economic Classification		REO	Market Price (USD/kg REO)			Max values of concentrations identified in this study					
						Whole coal basis			Ash basis		
		$[REE]_2O_3$	2011*	2021**	%Change	Max (REO)	Value/mt	%Value	Max (REO)	Value/mt	%Value
Seredin & Dai Economic Classification	"Critical"	Terbium oxide	$ 557.00	$ 1,743.88	313%	7.44	$ 12.97	8.6%	17.4	$ 30.28	7.9%
		Neodymium oxide	$ 50.64	$ 142.97	282%	232	$ 33.19	22.0%	484	$ 69.17	18.1%
		Dysprosium oxide	$ 235.00	$ 454.04	193%	39.9	$ 18.13	12.0%	94.3	$ 42.82	11.2%
		Erbium oxide	$ 90.00	$ 54.20	-40%	19.1	$ 1.04	0.7%	46.5	$ 2.52	0.7%
		Europium oxide	$ 553.00	$ 30.64	-94%	13.3	$ 0.41	0.3%	28.6	$ 0.88	0.2%
		Yttrium oxide	$ 143.00	$ 11.39	-92%	182	$ 2.07	1.4%	520	$ 5.92	1.6%
	"Uncritical"	Gadolinium oxide	$ 10.71	$ 71.33	666%	48.6	$ 3.47	2.3%	119	$ 8.48	2.2%
		Praseodymium oxide	$ 49.34	$ 138.25	280%	54.7	$ 7.56	5.0%	104	$ 14.43	3.8%
		Samarium oxide	$ 16.00	$ 4.16	-74%	57.2	$ 0.24	0.2%	112	$ 0.47	0.1%
		Lanthanum oxide	$ 23.82	$ 1.35	-94%	174	$ 0.23	0.2%	334	$ 0.45	0.1%
	"Excessive"	Holmium oxide	$ 41.00	$ 200.31	489%	7.1	$ 1.42	0.9%	17.5	$ 3.50	0.9%
		Lutetium oxide	$ 274.00	$ 848.38	310%	2.27	$ 1.93	1.3%	5.75	$ 4.88	1.3%
		Ytterbium oxide	$ 27.00	$ 21.21	-27%	15.5	$ 0.33	0.2%	37.8	$ 0.80	0.2%
		Cerium oxide	$ 23.10	$ 1.44	-94%	423	$ 0.61	0.4%	814	$ 1.17	0.3%
		Thulium oxide	-	-	-	2.52	-	-	6.13	-	-
		Scandium oxide	-	$ 1,060.47	-	63.7	$ 67.50	44.7%	184	$ 195.36	51.3%

*https://www.statista.com/statistics/449834/average-rare-earth-oxide-prices-globally/
**https://www.metal.com/Rare-Earth-Oxides (Prices as of Dec 23, 2021)

concentration, the values do illustrate that even with full recovery, the economic potential of a REE deposit is largely controlled by a handful of the REE (scandium, neodymium, dysprosium, terbium, and perhaps praseodymium).

Another informative look at composition involves correlating the individual elements to total rare earth concentrations, i.e., do all elements undergo linear enrichment or are some more relatively abundant in the more enriched samples? Sixty-six samples in the Tracy Mountain study area were analyzed for all 16 rare earth elements, including scandium and yttrium. While this sample subset is biased toward enriched samples, and thus not representative of the average lignite in the study area, it does offer an opportunity to examine compositional change across a more evenly distributed range of ΣREE concentrations from 62 to 1,089 ppm (whole coal basis). Increased REE fractionation is observable in more enriched samples, represented graphically in Figure 23 and numerically as *r* in Table 4. Compositional trends in Tracy Mountain lignites show preferential enrichment in the light REEs. Note that heavy REE concentrations also increase as total REE concentrations increase, but not to the same rate of lighter REEs, e.g., although scandium increases from an average of 13.7 to 35.0 ppm between the bottom ten and top ten ΣREE samples, its average as a percentage of ΣREE decreases from 9.0% to 4.2%, a strong negative correlation. Conversely, cerium has a moderately strong positive correlation, increasing from 23.5% to 31.9% across the same samples. These trends have implications for modeling recovery of the most economic elements. As bulk ore quality increases (higher ΣREE concentrations), proportionally less of that total will consist of scandium, dysprosium and terbium, while neodymium and praseodymium will make up larger proportions.

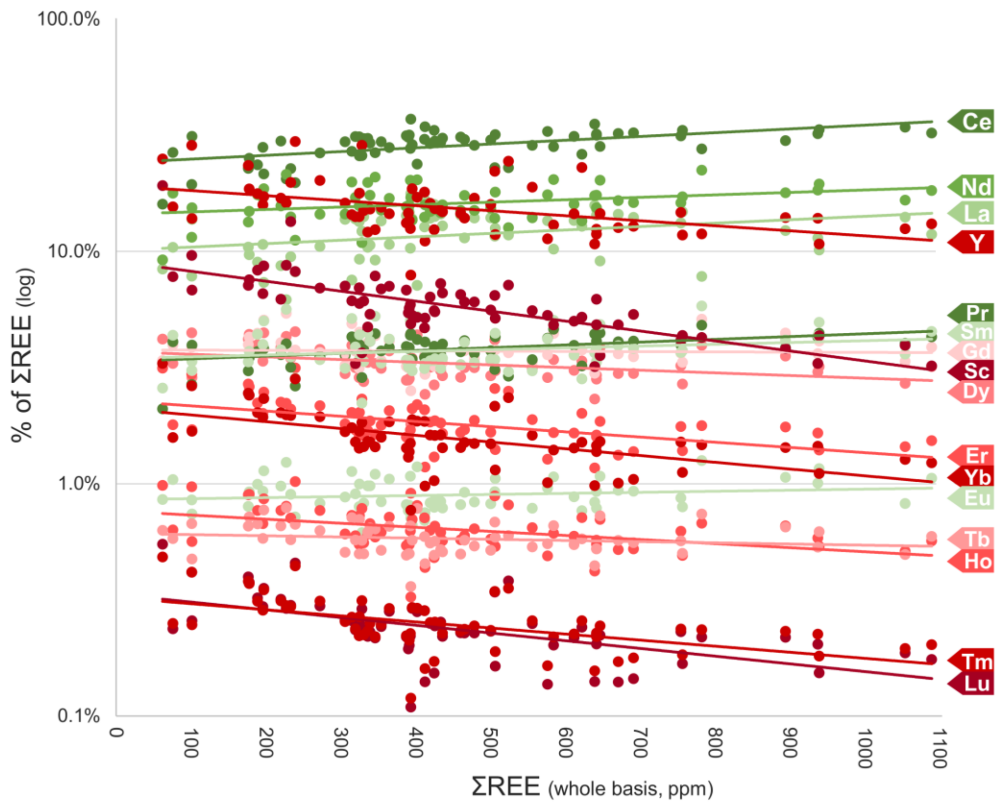

▲ **Figure 23.** Compositional trends in the REEs across a subset of 66 samples with analyses of all 16 REE. Elements in green make up a larger proportion of total rare earths as the samples become more enriched, while elements in red show the opposite trend.

▼ **Table 4.** Compositional data for the subset of 66 samples with analyses of all 16 REE. The light REEs make up a larger proportion of the total rare earth concentrations the more a sample is enriched.

	Element		Concentrations (ppm)			Compostistion (% of total REE)				
			MAX	MEAN	MIN	MAX	MEAN	MIN	*r* %ΣREE	
Light REEs	Cerium	Ce	361	135	9.9	37.1%	28.8%	16.0%	0.55	Higher rate of enrichment
	Praseodymium	Pr	46.7	17.8	1.3	4.8%	3.8%	2.1%	0.44	
	Neodymium	Nd	199	75	5.7	22.4%	16.3%	9.2%	0.32	
	Lanthanum	La	148	56	5.2	17.7%	12.1%	6.2%	0.31	
	Samarium	Sm	49.3	17.5	1.6	5.8%	3.8%	2.2%	0.19	
	Europium	Eu	11.5	4.1	0.53	1.3%	0.9%	0.6%	0.16	
Heavy REEs	Gadolinium	Gd	42.2	16.9	2.1	5.4%	3.8%	2.5%	-0.05	Lower rate of enrichment
	Terbium	Tb	6.46	2.60	0.39	0.8%	0.6%	0.4%	-0.19	
	Dysprosium	Dy	34.8	14.5	2.5	4.5%	3.3%	1.8%	-0.38	
	Yttrium	Y	143	67	11.8	29.7%	15.9%	7.9%	-0.43	
	Holmium	Ho	6.19	2.78	0.48	1.0%	0.7%	0.3%	-0.47	
	Erbium	Er	16.7	7.8	1.36	3.1%	1.9%	0.9%	-0.52	
	Thulium	Tm	2.21	1.06	0.19	0.5%	0.3%	0.1%	-0.56	
	Ytterbium	Yb	13.6	6.7	1.20	3.3%	1.6%	0.8%	-0.58	
	Lutetium	Lu	2.00	1.01	0.18	0.5%	0.2%	0.1%	-0.58	
	Scandium	Sc	41.5	24.3	5.9	19.2%	6.1%	3.2%	-0.62	

r is the correlation coefficient (from +1 to -1)

Non-REE Critical Elements

Regardless of the final economic outlook for producing rare earths alone from coal, its prospects could increase substantially if additional valuable minerals were present that could be co-produced from the same coal. Several mineral commodities are already commercially produced from coal or coal ash, including aluminum, gallium, germanium, magnesium, silicon, selenium, and vanadium (Dai and Finkelman, 2018). Extraction methods are being developed for additional highly promising elements like gold, silver, platinum, palladium, molybdenum, niobium, rhenium, and zirconium. Highly elevated concentrations of antimony, beryllium, chromium, cesium, iridium, iron, hafnium, lithium, osmium, rhodium, ruthenium, tantalum, titanium, and tungsten have been found in coal or coal ash that could be competitive with conventional ores and are potentially one supply/demand disruption away from receiving commercial interest.

Some concentrations of these elements in North Dakota lignites have been reported, as summarized in the USGS's COALQUAL database (Palmer et al., 2015; Lin et al., 2018b). Many critical elements are strongly represented with as many as 7,600 analyses reported, but less than 200 represent North Dakota coals. With so few samples, it is not surprising none of the critical element concentrations in North Dakota's lignites are among the top in the COALQUAL database, which is primarily bituminous Appalachian coals. These 200 entries also likely do not reflect the state's most mineralized seams, instead being full-bed samples of the thick, low-ash coals preferred for supplying thermal power plants. Furthermore, representing the full thickness of a major lignite with one mixed concentration is likely to dilute any signal from enriched zones at the top or bottom of the bed, if present. Concentrations from thin lignites at Tracy Mountain represent new highs for essentially all of the elements reported from North Dakota coals and are higher than any in the national COALQUAL database for magnesium, molybdenum, vanadium, zirconium and many of the REEs (terbium, dysprosium, holmium, samarium, erbium, thulium, ytterbium, and scandium) (Lin and others 2018a, 2018b). Gallium and uranium concentrations reported here are also within 10% of the highest in the database (Figure 24).

In their review of elemental concentrations reported from coal, Dai and Finkelman (2018) classified the potential of each element to be produced from coal based on its competitiveness with currently utilized ore sources for each element. The elements enriched at Tracy Mountain (vs the most enriched US coals reported in the COALQUAL database) fall in the most favorable categories: already commercially produced from coal (gallium, magnesium, vanadium), historical production from coal (uranium), or enriched coals are very promising to be competitive with traditional ores (REE, molybdenum, zirconium).

Organic Association

Another consideration when identifying mineral commodities to potentially co-produce with REEs is the inferred organic affinity of the element. Coals with a low ash yield have been considered the favored targets for potential REE extraction, not only because burning these coals can concentrate non-combustible mineral matter twenty-fold or more, but because this coal type is already utilized for thermal power generation, thus offering opportunity for an additional revenue stream utilizing existing mining

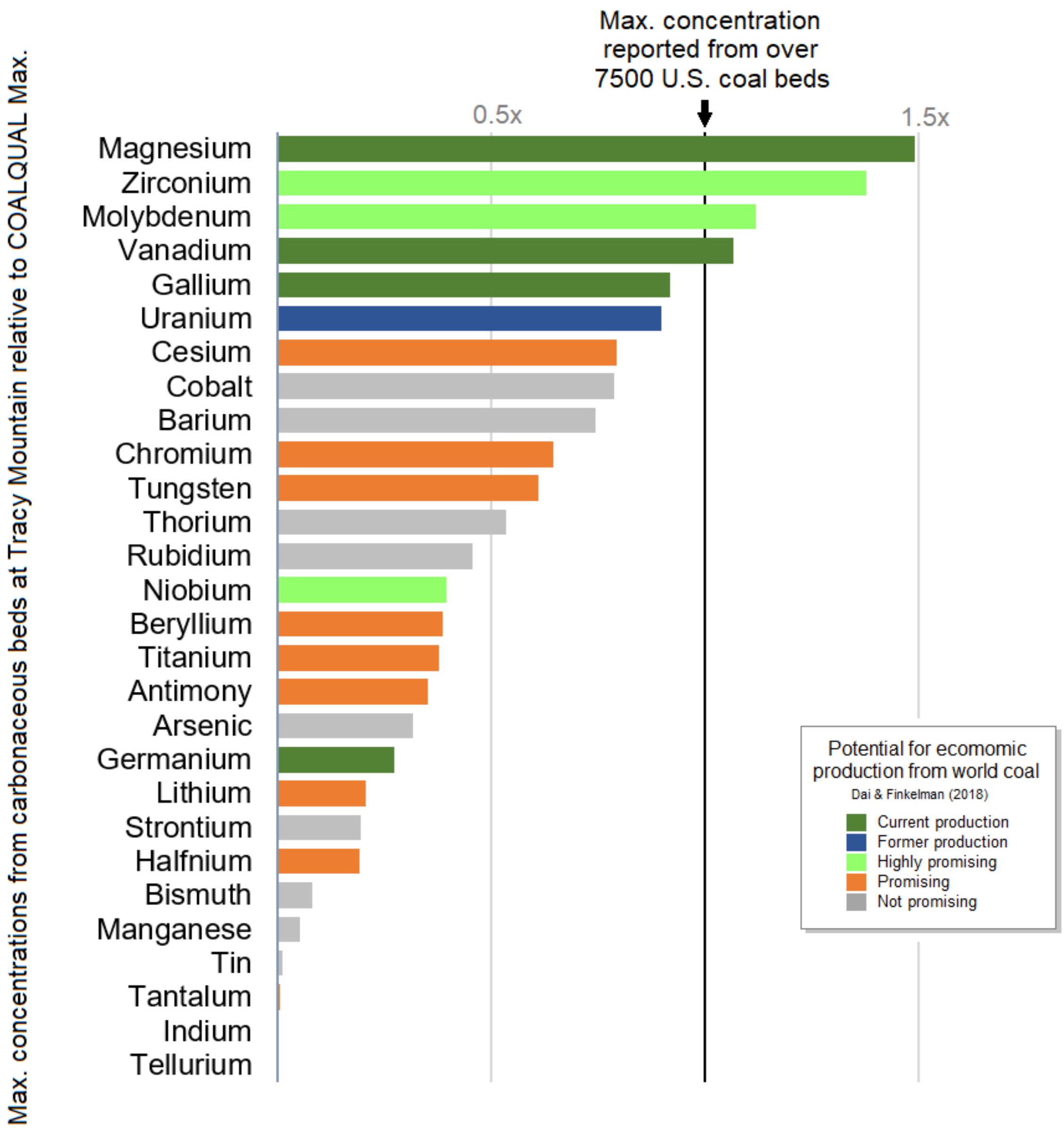

▲ **Figure 24.** The highest concentrations at Tracy Mountain (21 to 157 analyses per element) compared to the highest concentration in the USGS COALQUAL database (often over 7,500 analyses per element). Note: higher concentrations of magnesium, titanium, and barium from natural coal ash, bentonite, and a barite nodule, respectively, from Tracy Mountain are not included.

infrastructure. REE extraction from coal ash can be problematic however, as acid-leaching studies have found that a portion of the REE becomes immobilized in glassy matrix during burning (Taggart and others 2016). REE recovery therefore could be more effective on whole coal in some basins, in which case the more desirable feedstocks may include clay-rich coals, partings, seam roofs and floors, which often have higher whole-basis REE content and a separate group of associated minerals. A large portion of the REE in North Dakota lignites have been shown to be organically associated and easily recovered from pre-combustion coal feedstocks (Laudal et al., 2018).

Organic beds at Tracy Mountain are relatively clayey: 43 of 53 samples >300 ppm ∑REE on a whole basis contain ash yields over 50% by weight. Lithologies of these samples are predominantly coaly stringers in dark brown carbonaceous mudstone (B and E beds) or black clayey coal (I bed) and carbonaceous lenses in its bentonite roof (Ir samples). Despite the higher clay content of beds B, E, and I, six, two, and six samples from these beds, respectively, exceed 0.1% REO on an ash basis. Samples >300 ppm ∑REE and <50% ash yield occur in the more coal-rich F and G beds, but whole basis REE concentrations are generally lower and only two ash samples from each bed exceed 0.1% REO.

Using the ash yield as a general proxy for clay content, many critical elements reported in this study are associated with inorganic fractions of the sample and are unlikely candidates for REE co-production in low ash lignites in North Dakota. The elements titanium, cesium, and lithium have a very strong positive correlation with the ash yield, represented as *r* ASH% in Table 5. Also strongly correlated are gallium, rubidium, tin, tantalum, and thorium (a contaminant). None of these elements with strong or very strong inorganic associations are current targets of production nor were they considered highly promising by Dai and Finkelman (2018), with the exception of gallium. Of the other more promising elements, magnesium and vanadium had moderate positive correlations, niobium had a weak positive correlation, and germanium, molybdenum, niobium, uranium, and zirconium had very weak to negative correlation with the ash yield. The inorganic associations inferred for samples at Tracy Mountain are largely consistent with other lignites from North Dakota, although zirconium and niobium show a stronger positive correlation to ash yield across other sites (Moxness, 2020).

The rare earth elements show mostly weak correlations to ash yield at Tracy Mountain. This is to be expected, as the occurrence of moderate to high REE concentrations in low-ash coals (that become high to very high REE concentrations in coal ash) is the primary reason the rare earths in coal have attracted recent interest in the U.S. as opposed to clays or other siliciclastic deposits. Elements with similarly low inorganic affinities are not necessarily enriched via the same pathways as the rare earths, however, which is a primary consideration in identifying elements for co-production. Column *r*∑REE in Table 5 indicates the correlation coefficient between each element and the total REE. The individual REEs, intuitively, exhibit a very strong positive correlation while uranium, antimony, indium, beryllium, and chromium also exhibit a strong positive correlation to ∑REE. Highly promising elements vanadium and gallium (moderately strong) molybdenum, zirconium, and niobium (weak), and germanium and magnesium (very weak) all show at least some positive correlation to coals enriched in rare earths.

Enrichment Models

Identifying the mechanism(s) by which lignites become enriched in rare earths and other critical elements is an important step in modeling the geologic context of potential ore sources in North Dakota. Seredin and Dai (2012) recognized four main genetic types of REE-enriched coals: terrigenous, tuffaceous, infiltrational, and hydrothermal. Terrigenous and tuffaceous enrichment are proposed to have occurred during deposition, where REE were transported to the peat bog in surface water, often in association with the leaching of tuffaceous sediment. Infiltrational enrichment occurs post-deposition via descending groundwater flows and is consistent with the model for uranium enrichment in coals in North Dakota identified by Denson and Gill (1965). Hydrothermal enrichment is associated with ascending fluids transporting REE into a coal at any stage of its development.

▼**Table 5.** The likelihood of each critical element to be enriched with the REE (left) and whether each element is more enriched in low- or high-ash lignites (right) at Tracy Mountain.

Correlation with total REE (Increasing co-enrichment with ∑REE; rows Cerium to Scandium grouped as Rare Earth Elements)

Element		n	r ∑REE
Cerium	Ce	70	0.99
Praseodymium	Pr	70	0.98
Neodymium	Nd	70	0.97
Terbium	Tb	70	0.97
Dysprosium	Dy	70	0.96
Gadolinium	Gd	70	0.96
Europium	Eu	70	0.96
Holmium	Ho	70	0.95
Samarium	Sm	70	0.95
Lanthanum	La	70	0.95
Erbium	Er	70	0.93
Thulium	Tm	70	0.92
Ytterbium	Yb	70	0.91
Yttrium	Y	70	0.89
Lutetium	Lu	70	0.87
Scandium	Sc	64	0.84
Uranium	U	143	0.69
Indium	In	21	0.67
Chromium	Cr	97	0.63
Beryllium	Be	31	0.63
Antimony	Sb	75	0.61
Vanadium	V	113	0.60
Gallium	Ga	115	0.54
Titanium	Ti	31	0.54
Thorium	Th	21	0.50
Lithium	Li	31	0.50
Cesium	Cs	31	0.48
Hafnium	Hf	125	0.48
Molybdenum	Mo	143	0.41
Zirconium	Zr	143	0.40
Tellerium	Te	21	0.29
Niobium	Nb	113	0.29
Tungsten	W	140	0.24
Arsenic	As	67	0.22
Bismuth	Bi	21	0.18
Barium	Ba	75	0.17
Tantalum	Ta	97	0.14
Magnesium	Mg	143	0.13
Cobalt	Co	51	0.13
Germanium	Ge	115	0.11
Tin	Sn	21	0.09
Rubidium	Rb	21	-0.02
Strontium	Sr	31	-0.09
Manganese	Mn	21	-0.29

Correlation with ash yield (Relative enrichment in low-ash coals ↑; Relative enrichment in clay-rich coals ↓)

Element		n	r ASH%
Zirconium	Zr	143	-0.14
Molybdenum	Mo	143	-0.10
Germanium	Ge	115	-0.04
Tungsten	W	140	-0.02
Hafnium	Hf	125	0.00
Strontium	Sr	31	0.01
Arsenic	As	67	0.06
Manganese	Mn	21	0.10
Cobalt	Co	51	0.10
Uranium	U	143	0.15
Lutetium (REE)	Lu	66	0.16
Ytterbium (REE)	Yb	66	0.17
Thulium (REE)	Tm	66	0.19
Erbium (REE)	Er	66	0.20
Antimony	Sb	75	0.20
Barium	Ba	75	0.21
Holmium (REE)	Ho	66	0.21
Niobium	Nb	113	0.21
Dysprosium (REE)	Dy	66	0.21
Gadolinium (REE)	Gd	66	0.23
Terbium (REE)	Tb	66	0.23
Samarium (REE)	Sm	66	0.25
Yttrium (REE)	Y	66	0.25
Europium (REE)	Eu	66	0.25
Tellerium	Te	21	0.28
Neodymium (REE)	Nd	66	0.31
Indium	In	21	0.33
Praseodymium (REE)	Pr	66	0.36
Cerium (REE)	Ce	66	0.41
Magnesium	Mg	143	0.41
Scandium (REE)	Sc	64	0.42
Bismuth	Bi	21	0.47
Vanadium	V	113	0.47
Chromium	Cr	97	0.51
Beryllium	Be	31	0.52
Lanthanum (REE)	La	66	0.53
Thorium	Th	21	0.63
Gallium	Ga	115	0.69
Tantalum	Ta	97	0.72
Tin	Sn	21	0.77
Rubidium	Rb	21	0.78
Lithium	Li	31	0.90
Cesium	Cs	31	0.93
Titanium	Ti	31	0.96

n is the number of analyses
r is the correlation coefficient (from +1 to -1)

Potential for ecomomic production from world coal
Dai & Finkelman (2018)

- Current production
- Former production
- Highly promising
- Promising
- Not promising

Seredin and Dai (2012) also described three REE distribution patterns (L-type (light), M-type (medium), and H-type (heavy)) in high-REE coals based on the preferential transport and sorption of certain element groups corresponding to the different genetic types of enrichment. These patterns are classified using the ratios of individual REE concentrations normalized to upper continental crust ($[REE]_N$) (Taylor and McLennan, 1985). In this study, 70 of 169 samples were analyzed for all of the lanthanide elements (excluding promethium) and yttrium, including all 53 samples projected to contain concentrations over 300 ppm on a whole basis (see Laboratory Analysis). Twenty-three samples meet the Seredin and Dai (2012) criteria for high rare earth accumulation in coal of 0.1% REO (rare earth oxide) content in the ash, which here includes scandium.

Seven of the 53 enriched samples in this study classify as L-type ($La_N/Lu_N > 1$), all from the I bed. The I bed is a clayey carbonaceous bed up to 14 inches (36 cm) in thickness and is overlain by a prominent bentonite (weathered volcanic ash). This is consistent with the description of L-type distributions that are a product of tuffaceous enrichment via volcanic ash input into the peat. The seven L-type samples are clay-rich portions of the I bed (76% to 96% ash), including two roof samples of carbonaceous lenses in bentonites. The REE concentrations of these samples range from 394 to 691 ppm. One sample reaches 0.1% REO in the ash, although less-clayey areas of this bed contain the highest REE concentrations in the Tracy Mountain study area and lower La_N/Lu_N ratios.

The most enriched samples in this study, including 19 of 23 samples over 0.1% REO on an ash basis, are consistent with M-type distribution patterns (Fig. 4B), with $La_N/Sm_N < 1$ and $Gd_N/Lu_N > 1$ and a consistent Eu_N-maximum (Figure 25). This enrichment pattern was also attributed to natural acidic water interacting with tuffaceous sediment during the peat bog stage, and the higher concentrations of the medium-REEs is likely due to higher humic matter in these samples relative to the clayier L-type samples.

Three of the 23 samples over 0.1% ash REO and three of the 53 samples over 300 ppm REE contain concentrations of $La_N/Lu_N < 1$ and $Gd_N/Lu_N < 1$, which classify as H-type. Heavy enrichment can occur in any of the genetic types where more alkaline waters transport REE in terrigenous, tuffaceous, infiltrational, or hydrothermal settings.

In addition to identifying light, medium, and heavy distributions, which are each associated with multiple genetic types, Seredin and Dai also used associated non-rare earth elements as an additional line of evidence in determining the source of enrichment of high-REE coals: terrigenous (aluminum, gallium, barium, strontium), tuffaceous (zirconium, hafnium, niobium, tantalum, gallium), infiltrational (uranium, molybdenum, selenium, rhenium), and hydrothermal (arsenic, antimony, mercury, silver, gold).

Although the presence of bentonite and predominately medium-light fractionation of the REE suggest tuffaceous enrichment, samples from Tracy Mountain do not contain high normalized concentrations of zirconium, hafnium, niobium, tantalum, or gallium. The ash samples most enriched with these elements contain concentrations 3.2 (Ta_N), 4.5 (Ga_N), 5.9 (Hf_N), 8.1 (Nb_N), and 10.9 (Zr_N) times that of the upper continental crust (UCC) (Table 6). Some elements associated with the hydrothermal genetic type, by contrast, are abundant. Antimony in the ash is up to 225 times UCC and arsenic is up to 840 times UCC. Elements associated with the infiltration model are also considerably more abundant. The highest normalized uranium concentrations approach 109 times UCC and molybdenum is up to 268 times UCC.

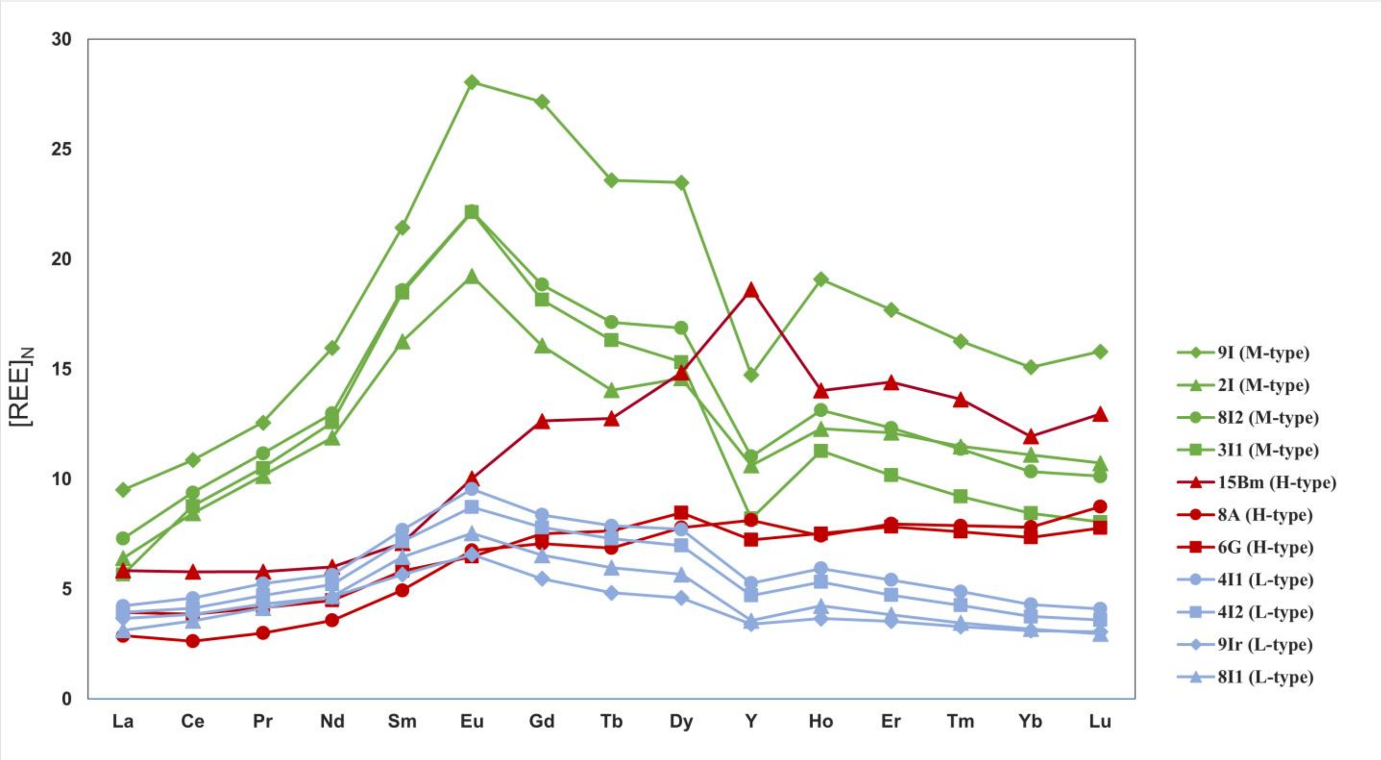

▲ **Figure 25.** Enrichment in Tracy Mountain samples (ash basis) relative to upper continental crust. Samples variably contain relative enrichment in light (blue), medium (green), or heavy (red) REE.

A more targeted examination of co-enriched critical elements involves comparing concentrations from Tracy Mountain lignites to the average values for world coal (Ketris and Yudovich 2009). Among coal ash samples >0.1% REO in this study, arsenic and antimony (associated with hydrothermal enrichment) average only 4.0 and 3.5 times the average world coal (AWC), while uranium and molybdenum (associated with infiltrational enrichment) average 6.3 and 10.7 times AWC. At Tracy Mountain, the concentrations of several critical elements (antimony, arsenic, barium, germanium, molybdenum, and uranium) average over 5X the upper continental crust in coal and 10X on an ash basis (Table 6), although this does not necessarily indicate they are enriched in the same pathways as the REE. In the 23 most REE-enriched coal ashes at Tracy Mountain, average concentrations of beryllium, bismuth, lithium, manganese, rubidium, strontium, tantalum, tin, and titanium are still below the average world coal ash. In the clayier whole coal subset of 53 REE-enriched samples, only bismuth and manganese average concentrations are below the average world coal.

▼ **Table 6**. Tracy Mountain elemental concentrations normalized to upper continental crust and world coals.

		Enrichment coefficients vs Upper Continental Crust (UCC)																	Enrichment coefficients vs Average World Coal (AWC)							
			All Tracy Mountain lignite samples							REE-enriched Tracy Mountain lignite samples									AWC (ppm)		REE-enriched Tracy Mountain lignite samples					
		UCC (ppm)	Whole coal basis				Ash basis			>300 ppm ΣREE (whole)				>0.1% REO (ash)							>300 ppm ΣREE (whole)			>0.1% REO (ash)		
	Element		n	MAX	MEAN	MIN	MAX	MEAN	MIN	n	MAX	MEAN	MIN	n	MAX	MEAN	MIN	whole	ash	MAX	MEAN	MIN	MAX	MEAN	MIN
Rare Earth Elements	Lanthanum	30	155	4.9	1.2	0.1	9.5	1.9	0.4	51	4.9	2.2	0.8	23	9.5	4.7	2.6	11	69	13.5	6.0	2.2	4.1	2.0	1.1
Rare Earth Elements	Cerium	64	155	5.6	1.3	0.1	10.9	2.1	0.4	51	5.6	2.5	1.3	23	10.9	5.7	3.2	23	130	15.7	6.8	3.6	5.3	2.8	1.6
Rare Earth Elements	Praseodymium	7.1	70	6.6	2.3	0.2	12.6	4.2	0.6	51	6.6	2.9	1.3	23	12.6	6.9	3.8	3.5	20	13.3	5.9	2.7	4.5	2.5	1.4
Rare Earth Elements	Neodymium	26	155	7.7	1.7	0.1	16.0	3.0	0.5	51	7.7	3.4	1.4	23	16.0	8.2	4.5	12	67	16.6	7.3	3.0	6.2	3.2	1.7
Rare Earth Elements	Samarium	4.5	70	11.0	3.7	0.4	21.4	6.7	1.2	51	11.0	4.5	1.6	23	21.4	11.3	5.8	2.0	13	24.7	10.2	3.7	7.4	3.9	2.0
Rare Earth Elements	Europium	0.88	70	13.1	4.4	0.6	28.0	8.1	1.6	51	13.1	5.5	2.3	23	28.0	13.6	6.5	0.47	2.5	24.5	10.2	4.3	9.9	4.8	2.3
Rare Earth Elements	Gadolinium	3.8	155	11.1	2.6	0.2	27.2	4.7	0.5	51	11.1	5.2	2.6	23	27.2	13.0	7.5	2.7	16	15.6	7.3	3.7	6.4	3.1	1.8
Rare Earth Elements	Terbium	0.64	70	10.1	3.9	0.6	23.6	7.1	1.4	51	10.1	4.7	2.4	23	23.6	11.8	7.1	0.32	2.1	20.2	9.4	4.8	7.2	3.6	2.2
Rare Earth Elements	Dyspros	3.5	70	9.9	4.0	0.7	23.5	7.3	1.6	51	9.9	4.8	2.6	23	23.5	12.1	7.0	2.1	14	16.6	8.0	4.3	5.9	3.0	1.7
Rare Earth Elements	Yttrium	22	155	6.5	1.9	0.2	18.6	3.3	0.2	51	6.5	3.5	1.9	23	18.6	8.5	4.7	8.4	51	17.0	9.1	4.8	8.0	3.7	2.0
Rare Earth Elements	Holmium	0.8	70	7.7	3.3	0.6	19.1	6.2	1.4	51	7.7	4.0	2.2	23	19.1	10.0	5.7	0.54	4.0	11.5	5.9	3.3	3.8	2.0	1.1
Rare Earth Elements	Erbium	2.3	155	7.3	2.2	0.2	17.7	3.7	0.3	51	7.3	3.9	2.1	23	17.7	9.7	5.4	0.93	5.5	18.0	9.6	5.2	7.4	4.1	2.3
Rare Earth Elements	Thulium	0.33	70	6.7	3.1	0.6	16.3	5.8	1.5	51	6.7	3.7	2.0	23	16.3	9.2	4.9	0.31	2.0	7.1	3.9	2.1	2.7	1.5	0.8
Rare Earth Elements	Ytterbium	2.2	70	6.2	2.9	0.5	15.1	5.5	1.4	51	6.2	3.4	1.8	23	15.1	8.7	4.3	1.0	6.2	13.6	7.6	4.0	5.4	3.1	1.5
Rare Earth Elements	Lutetium	0.32	70	6.3	3.1	0.6	15.8	5.8	1.5	51	6.3	3.6	1.8	23	15.8	9.0	4.1	0.20	1.2	10.0	5.7	2.9	4.2	2.4	1.1
Rare Earth Elements	Scandium	13.6	149	3.1	1.3	0.1	8.8	2.2	0.2	50	3.1	2.0	0.8	22	8.8	4.5	2.7	3.9	23	10.6	6.9	2.7	5.2	2.6	1.6
	Antimony	0.2	75	125	40.3	1.5	225	73.6	9.1	27	125	54.2	4.5	13	225	109	19.6	0.92	6.3	27.2	11.8	1.0	7.1	3.5	0.6
	Arsenic	1.5	67	465	71.8	3.4	840	127	4.5	25	309	87.0	8.2	12	323	126	31.1	8.3	47	55.9	15.7	1.5	10.3	4.0	1.0
	Barium	550	75	31.8	6.5	0.4	68.6	11.5	0.7	27	25.1	8.5	0.6	13	55.4	16.5	1.2	150	940	92.0	31.0	2.1	32.4	9.6	0.7
	Beryllium	3	31	2.5	1.4	0.4	6.8	2.3	1.1	19	2.5	1.6	1.0	8	3.6	3.0	1.7	1.6	9.4	4.8	3.0	1.8	1.2	0.9	0.6
	Bismuth	0.127	21	9.5	4.9	1.7	18.0	7.1	3.3	17	9.5	5.1	2.3	7	18.0	7.9	4.8	0.97	5.9	1.2	0.7	0.3	0.4	0.2	0.1
	Cesium	4.6	31	2.1	1.0	0.0	2.7	1.5	0.1	19	2.1	1.4	0.2	8	2.3	1.5	0.6	1.0	6.6	9.9	6.2	0.9	1.6	1.1	0.4
	Chromium	83	97	2.0	0.8	0.1	3.6	1.3	0.2	39	2.0	1.1	0.3	16	3.6	2.0	1.0	16	100	10.4	5.9	1.7	3.0	1.7	0.8
	Cobalt	17	51	14.9	1.2	0.1	20.8	2.0	0.2	23	14.9	1.5	0.4	10	5.0	2.2	0.5	5.1	32	49.6	5.0	1.4	2.7	1.2	0.3
	Gallium	17	115	2.6	1.2	0.2	5.5	1.8	0.5	42	2.6	1.5	0.5	19	5.5	2.7	1.3	5.8	33	7.6	4.3	1.4	2.8	1.4	0.7
	German	1.6	115	40.0	6.7	0.6	62.7	11.5	1.3	42	26.3	6.6	1.9	19	45.6	16.3	4.1	2.2	15	19.1	4.8	1.4	4.9	1.7	0.4
	Hafnium	5.8	125	3.3	0.9	0.1	5.9	1.5	0.4	45	2.6	1.2	0.5	19	3.7	2.4	0.7	1.2	8.3	12.5	5.6	2.4	2.6	1.7	0.5
	Indium	0.05	20	3.4	2.1	1.0	5.7	3.1	1.7	17	3.4	2.3	1.4	7	5.7	4.1	2.5	0.031	0.16	5.5	3.7	2.3	1.8	1.3	0.8
	Lithium	20	31	3.8	1.5	0.1	4.6	2.2	0.2	19	3.8	2.1	0.3	8	4.3	2.5	0.8	12	66	6.4	3.4	0.5	1.3	0.8	0.2
	Magnesium	13300	143	1.8	0.7	0.1	4.0	1.1	0.2	48	1.8	0.7	0.2	22	4.0	1.4	0.5	n/a	n/a	-	-	-	-	-	-
	Manganese	600	21	2.2	0.2	0.0	2.9	0.3	0.1	17	0.4	0.1	0.0	7	0.3	0.2	0.1	86	490	2.7	0.8	0.3	0.3	0.2	0.1
	Molybdenum	1.5	143	155	32.3	0.7	268	58.0	0.8	48	155	47.3	4.8	22	232	99.9	12.4	2.2	14	106	32.3	3.3	24.8	10.7	1.3
	Niobium	12	113	2.6	1.2	0.1	8.1	2.0	0.4	41	2.6	1.4	0.4	18	6.5	3.0	1.0	3.7	20	8.3	4.4	1.4	3.9	1.8	0.6
	Rubidium	112	21	1.0	0.6	0.1	1.2	0.8	0.2	17	1.0	0.6	0.1	7	0.9	0.6	0.2	14	79	7.7	4.6	0.8	1.3	0.9	0.3
	Strontium	350	31	1.7	0.9	0.2	3.8	1.6	0.3	19	1.6	0.9	0.2	8	3.1	1.6	0.7	110	740	5.0	2.8	0.8	1.5	0.8	0.3
	Tantalum	1	97	2.8	0.8	0.1	3.2	1.2	0.2	39	1.6	0.9	0.2	16	2.2	1.2	0.4	0.28	1.7	5.8	3.3	0.6	1.3	0.7	0.3
	Tellerium	n/a	21	-	-		-	-	-	-	-	-	-	-	-	-	-	n/a	n/a	-	-	-	-	-	-
	Thorium	10.7	21	4.3	1.9	0.3	5.1	2.6	0.7	17	4.3	2.1	1.1	7	4.1	3.2	2.4	3.3	21	13.9	6.7	3.5	2.1	1.6	1.2
	Tin	5.5	21	0.5	0.4	0.1	0.8	0.5	0.3	17	0.5	0.4	0.2	7	0.8	0.6	0.4	1.1	6.4	2.5	1.9	1.0	0.7	0.5	0.4
	Titanium	4100	31	0.9	0.5	0.1	1.0	0.7	0.2	19	0.9	0.6	0.1	8	1.0	0.8	0.3	800	4650	4.5	3.2	0.7	0.9	0.7	0.3
	Tungsten	2	140	41.8	3.9	0.3	75.4	7.0	0.5	47	18.3	5.4	0.8	21	23.0	9.0	1.4	1.1	6.9	33.3	9.9	1.5	6.7	2.6	0.4
	Uranium	2.8	143	71.4	10.2	0.4	109	16.4	1.6	48	71.4	19.9	1.8	22	109	36.1	11.3	2.4	16	83.3	23.2	2.1	19.0	6.3	2.0
	Vanadium	107	113	3.8	1.3	0.0	6.8	2.1	0.3	41	3.8	1.9	0.2	18	6.8	3.4	0.7	25	155	16.2	7.9	0.7	4.7	2.3	0.5
	Zirconium	190	143	6.1	1.7	0.1	10.9	3.2	0.3	48	6.1	2.1	0.7	22	10.9	5.6	0.9	36	210	31.9	11.0	3.4	9.9	5.1	0.9

UCC values from Taylor and McLennan (1985) and McLennan (2001); AWC values from Ketris and Yudovich (2009)
n is number of samples analyzed

Conclusions

Tracy Mountain is noteworthy for its consistent lateral rare earth element enrichment across multiple thin lignite beds. Although these beds are too thin to be economically mined for their critical element contents, they provide new insights into the variability and mineral associations within REE-enriched lignites in North Dakota and the geologic context in which these deposits occur. The upper perimeter (roughly 4,500 ft or 1,400 m) of the main butte of Tracy Mountain contains multiple thin (~1 ft) lignites that are consistently enriched in REE (over 300 ppm, up to 1,000 ppm whole coal basis). The area encompassed by this butte is roughly 25 acres (100,000 square meters), suggesting high REE concentrations in North Dakota lignites can occur over a more widespread area than would be expected if enrichment were the product of localized vertical groundwater flows.

High REE concentrations are found in carbonaceous beds immediately underlying bentonite beds (I and O), as well as carbonaceous beds associated with white (possibly kaolinite-rich) beds (D and E), suggesting enrichment occurred from volcanic input directly into the peat or the weathering of adjacent volcanic sediments, perhaps as soon as immediately after during the Paleocene. Although this enrichment model is consistent with tuffaceous enrichment proposed by Seredin and Dai (2012), high to very high REE concentrations also occur in stratigraphically higher beds (A, B, and C) with no immediate proximity to bentonites or the white (weathered) zone. Furthermore, lignites below bentonites lower in section do not show similarly high enrichment. Enrichment in the upper beds may have occurred later as overlying volcanogenic sediment of the White River Group was eroded post-Miocene, or it may reflect Quaternary leaching from the weathering of a long-lived upland surface.

This upland proximity hypothesis was tested by sampling the stratigraphically highest carbonaceous beds in the areas adjacent to the badlands topography. Uppermost carbonaceous beds on nearby buttes were often not enriched, and no samples approached the 1000 ppm REE seen in multiple beds on the main butte of Tracy Mountain. REE enrichment in the uppermost sample is not uncommon from other sites in North Dakota (Kruger et al, 2017), but input from Quaternary weathering is likely not a factor in other exceptionally enriched lignites like the H bed in Slope County, which has hundreds of feet of overburden, including 25 or more feet of other non-enriched coals, where it contains REE concentrations in excess of 1000 ppm (Murphy et al., 2018). Results from the Tracy Mountain area, as well as the authors' previous reports suggest multiple pathways of rare earth enrichment in North Dakota lignites.

The bulk of the market value of a REE deposit comes from a small number of the 16 rare earth elements. In the 53 samples over 300 ppm total REE at Tracy Mountain, the four most economic elements (dysprosium, neodymium, scandium, and terbium) make up 25.7% of the total REE, a significant improvement over the 15.3% in the U.S.'s traditional source of REE, Mountain Pass Mine. Other economically important elements are also enriched in these lignites. Spot concentrations of gallium, magnesium, molybdenum, vanadium, uranium, and zirconium at Tracy Mountain are nearly as high or higher than any beds in the USGS COALQUAL national database. These elements could thus be potential candidates for co-production with REE if similar co-enrichment trends extend to other North Dakota lignites. At Tracy Mountain, gallium, vanadium, and uranium especially tend to be enriched in the same samples as the REEs. The most promising of the elements investigated are generally considered to be gallium, germanium, magnesium, molybdenum, niobium, vanadium, uranium, and zirconium, but the ultimate prospects for each will depend not only on bulk concentration but on the ease of co-production by newly developed REE extraction technologies.

Ongoing research is examining the REE recovery economics from raw clay-rich coal vs coal ash. At Tracy Mountain, elevated concentrations of the more promising elements gallium, magnesium, scandium, and vanadium correlate with the ash yield, suggesting these elements may be more abundant in clay-rich lignites. Conversely, molybdenum, niobium, germanium, uranium, zirconium and many of the heavy REE have very weak to negative correlation with the ash yield, suggesting more organic association and higher potential from low-ash coals. The rare earth elements have been shown to have multiple modes of occurrence in North Dakota lignites, with the heavy REEs associated with organic complexes in the coal and the lighter REEs with mineral matter (UND-IES, 2021). Titanium, cesium, lithium, and rubidium are very strongly correlated to ash yield. Establishing the presence of these elements in North Dakota lignites and the tendency for each to co-occur has implications in identifying the feedstocks, target mineral commodities, and extraction methods for any future commercial production.

References

Dai, S., and Finkelman, R.B., 2018, Coal as a promising source of critical elements: Progress and future prospects; International Journal of Coal Geology, no. 186, p. 155–164

Denson, N.M., and Gill, J.R., 1965, Uranium-bearing lignite and carbonaceous shale in the southwestern part of the Williston Basin – a regional study: United States Geological Survey Professional Paper 463, 75 p.

Forsman, N.F., 1985, Petrology of the Sentinel Butte Formation (Paleocene), North Dakota: Unpublished PhD Dissertation, University of North Dakota, 222 p.

Gschneidner, K. A. , Jr., and Pecharsky, V.K., 2019 "rare-earth element". Encyclopedia Britannica, https://www-britannica-com.ezproxy.library.und.edu/science/rare-earth-element. Accessed 1 December 2021.

Interior Department, 2018, Final list of critical minerals: 83 FR 23295, FR Document no. 2018-10667, Filed 5-17-18, 8:45 am.

Ketris, M.P., Yudovich, Y.E., 2009, Estimation of Clarkes for carbonaceous biolithes: world average for trace element contents in black shales and coals: International Journal of Coal Geology, v. 78, p. 135-148.

Kruger, N.K., 2020, Reducing Laboratory Costs by Estimating Total Rare Earth Concentrations from Seven or Fewer Analyzed Elements in Western North Dakota Coals: Geological Society of America Abstracts with Programs, v. 52, no. 6.

Kruger, N.W, Moxness, L.D., and Murphy, E.C., 2017, Rare Earth Element Concentrations in Fort Union and Hell Creek Strata in Western North Dakota: North Dakota Geological Survey Report of Investigation no. 117, 104 p.

Laudal, D.A., Benson, S.A., Addleman, R.S., and Palo, D., 2018. Leaching behavior of rare earth elements in Fort Union lignite coals of North America: International Journal of Coal Geology, v. 191. P. 112-124.

Lin, R., Soong, Y., Granite, E.J., 2018. Evaluation of trace elements in U.S. coals using the USGS COALQUAL database version 3.0. Part I: Rare Earth Elements and Yttrium (REY). International Journal of Coal Geology, v. 192, p. 1-13.

Lin, R., Soong, Y., and Granite, E.J., 2018, Evaluation of trace elements in U.S. coals using the USGS COALQUAL database version 3.0. Part II: Non-REY critical elements: International Journal of Coal Geology, v. 192, p. 39–50.

Moxness, L.D., 2020, Critical Element Associations with Rare Earths and Ash Yields in Fort Union Group Lignites, Williston Basin, North Dakota: Geological Society of America Abstracts with Programs, v. 52, no. 6.

McLennan, S.M., 2001. Relationships between the trace element composition of sedimentary rocks and upper continental crust. Geochemistry, Geophysics, Geosystems 2, 1021.

Murphy, E.C., 2015, Uranium in North Dakota: North Dakota Geological Survey, Geologic Investigations No. 184, 48 p.

Murphy, E.C., 2013, The alumina content of the Bear Den Member (Golden Valley Formation) and the Rhame Bed (Slope Formation) in Western North Dakota, North Dakota Geological Survey Report of Investigation no. 112, 271 p.

Murphy, E.C., Moxness, L.D., Kruger, N.W., and Maike, C.A., 2018, Rare Earth Element Concentrations in the Harmon, Hanson, and H Lignites, in Slope County, North Dakota: North Dakota Geological Survey Report of Investigation no. 119, 46 p.

Palmer, C.A., Oman, C.L., Park, A.J., Luppens, J.A., 2015. The U.S. Geological Survey coal quality (COALQUAL) database version 3.0. In: Data Series, Reston, VA, pp. 57.

Seredin, V.V., and Dai, S., 2012, Coal deposits as potential alternative sources for lanthanides and yttrium: International Journal of Coal Geology, v. 94, p. 67-93.

Taggart, R.K., Hower, J.C., Dwyer, G.S., Hsu-Kim, H., 2016, Trends in the rare earth element content of U.S.- based coal combustion fly ashes: Environmental Science & Technology. V. 50, p. 5919-5926

Taylor, S.R., and McLennan, S.M., 1985, The Continental Crust – Its Composition and Evolution: Blackwell, Oxford, 312p.

University of North Dakota Institute for Energy Studies, 2021. Investigation of rare earth element extraction from North Dakota coal-related feedstocks. Phase 2 Technical Report. 102 p.

Appendices

Appendix A

Legend for lithologies of measured sections

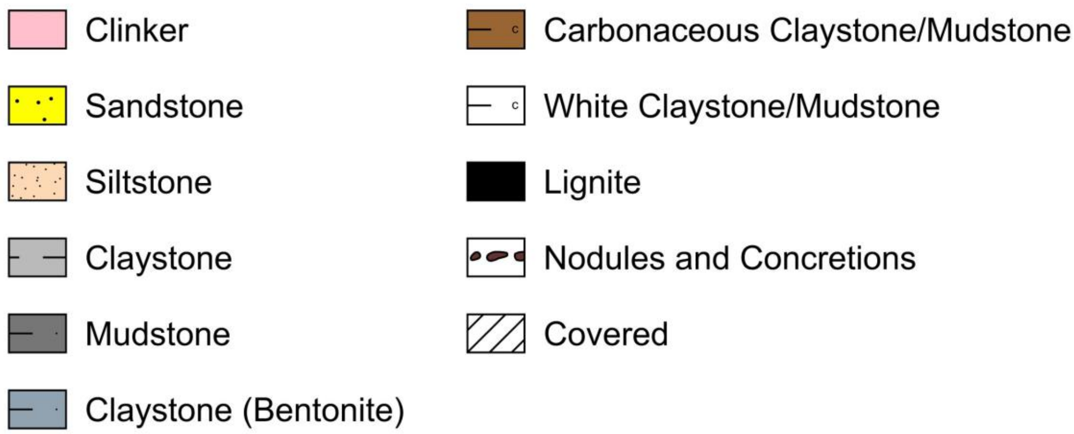

Tracy Mtn. REE Section 1

T.138N., R.101W., Sec.10, SE/NW/NW
Elevation at top 2,892 ft.

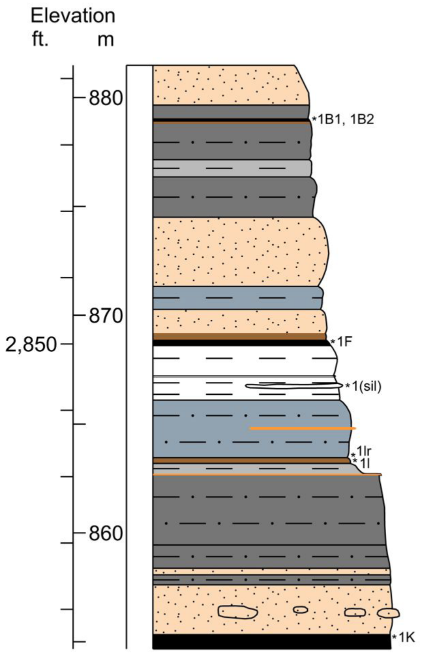

	Lab Analysis (in µg/g)																Total REE	
Sample ID	Cerium	Dysprosium	Erbium	Europium	Gadolinium	Holmium	Lanthanum	Lutetium	Neodymium	Praseodymium	Samarium	Scandium	Terbium	Thulium	Ytterbium	Yttrium	Whole coal	Ash
1B1	191	18.8	10.1	5.37	21.8	3.64	83.1	1.33	97.7	24.1	21.9	30.6	3.34	1.38	8.72	88.7	612	955
1B2	124	11.1	6.01	3.16	13.0	2.14	57.6	0.79	61.7	15.1	13.3	22.3	1.96	0.83	5.37	53.2	392	492
1F	38.8		3.03		6.3		15.2		25.3			18.2				24.6	*156*	*336*
1(sil)	41.1		1.28		2.1		22.4		16.6			6.2				10.7	*112*	*114*
1lr	52.9		2.29		4.4		29.1		24.4			15.2				20.5	169	178
1l	116	21.1	13.0	4.68	21.9	4.48	58.9	1.73	70.3	15.7	17.3	32.7	3.46	1.74	10.9	112	506	879
1K	18.9		1.81		2.6		8.1		10.2			4.9				20.0	*78*	*209*

Sample ID	Lab Analysis (in µg/g)																										
	Antimony	Arsenic	Barium	Beryllium	Bismuth	Cesium	Chromium	Cobalt	Gallium	Germanium	Hafnium	Indium	Lithium	Magnesium	Manganese	Molybdenum	Niobium	Rubidium	Strontium	Tantalum	Tellurium	Thorium	Tin	Titanium	Tungsten	Uranium	Vanadium	Zirconium
1B1							76		22.9	7	6.3			8610		78.0	15.5			0.83					13.3	65.5	165	358
1B2	7.33		4240	3.1		6.33	84		23.8	10	5.4		37.6	11100		47.8	13.8		420	1.02				2740	10.0	70.6	156	288
1F							55		10.1	15	8.7			8010		67.9	15.0			0.33					9.9	27.1	57	739
1(sil)	1.44	2.8	367	0.5		5.29	36	1.9	10.2	2	2.8		33.3	1580	38	1.4	26.1	49	34	1.78		6.8		6930	3.7	3.1	54	97.7
1Ir	1.99	16.1	3680	1.9		6.62	88	12.5	21.3	7	2.5		32.8	9090	157	4.5	13.4	96	173	0.97		9.8		4310	2.2	4.1	138	89.0
1I							157		24.7	42	10			6400		94.4	26.8			0.67					3.4	27.9	405	1150
1K							8		5.5	3	2.9			7550		16.5	4.5			0.16					7.9	6.3	17	298

Tracy Mtn. REE Section 2

T.138N., R.101W., Sec.10, SE/NW/NW
Elevation at top 2,900 ft.

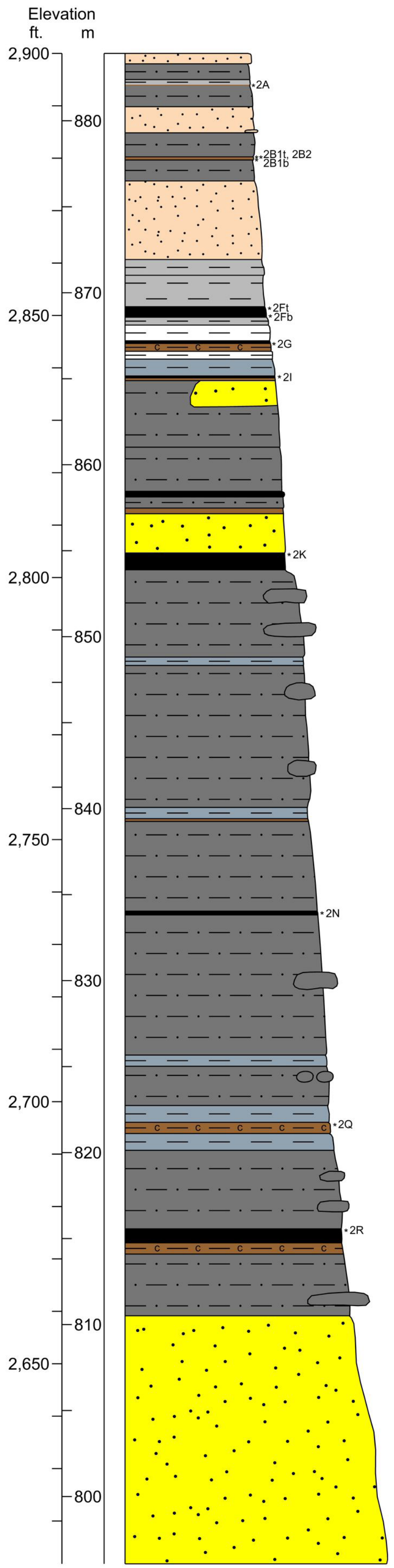

Sample ID	Lab Analysis (in µg/g)																Total REE	
	Cerium	Dysprosium	Erbium	Europium	Gadolinium	Holmium	Lanthanum	Lutetium	Neodymium	Praseodymium	Samarium	Scandium	Terbium	Thulium	Ytterbium	Yttrium	Whole coal	Ash
2A	61.5		5.80		8.6		31.8		32.6			22.8				43.0	*243*	*324*
2B1t	203	18.1	10.2	5.94	23.1	3.52	91.9	1.44	112	26.4	24.6	31.0	3.37	1.46	9.36	76.1	641	862
2B2	361	28.5	15.2	8.67	35.4	5.4	148	1.97	175	42.4	38.1	41.5	5.22	2.06	13.4	132	1054	1508
2B1b	205	18.8	10.4	5.04	21.6	3.67	97.6	1.31	98.9	24.4	21.4	39.9	3.36	1.41	8.83	80.0	642	798
2Ft	50.3		4.82		8.9		19.1		32.5			15.2				37.9	*204*	*492*
2Fb	62.4		4.38		8.3		24.0		35.3			18.0				34.1	*221*	*407*
2G	34.1		3.86		4.0		17.5		15.7			12.0				33.8	*141*	*211*
2I	301	28.4	15.5	9.42	34.0	5.47	107	1.91	172	40.1	40.7	30.9	5.00	2.11	13.6	130	937	1683
2K	31.6	2.9	1.73	0.75	3.1	0.57	13.9	0.26	15.6	4.0	3.4	6.9	0.48	0.25	1.70	14.0	101	225
2N	9.9	2.6	1.95	0.53	2.1	0.61	5.2	0.34	5.7	1.3	1.6	11.9	0.39	0.30	2.04	15.5	62	205
2Q	55.0	6.6	3.94	1.82	7.5	1.32	21.0	0.58	33.3	7.7	7.8	12.9	1.14	0.56	3.79	31.1	196	409
2R	20.2	2.5	1.36	0.79	3.0	0.48	7.9	0.18	13.5	3.1	3.3	5.9	0.44	0.19	1.20	11.8	76	232

Sample ID	Lab Analysis (in µg/g)																											
	Antimony	Arsenic	Barium	Beryllium	Bismuth	Cesium	Chromium	Cobalt	Gallium	Germanium	Hafnium	Indium	Lithium	Magnesium	Manganese	Molybdenum	Niobium	Rubidium	Strontium	Tantalum	Tellurium	Thorium	Tin	Titanium	Tungsten	Uranium	Vanadium	Zirconium
2A	22.4	392	11700	5.4	0.65	6.61	81	100	25.2	14	10	0.07	26.5	18600	1310	139	28.4	87	587	0.74	0.15	11.9	2.0	2420	56.6	18.9	184	480
2B1t	12.8	329	9830	5.0	0.59	5.38	89	9.5	32.6	13	13	0.11	56.4	11400	56	233	22.0	41	523	1.23	0.42	21.6	2.4	2540	24.6	100	241	775
2B2	9.39	285	11500	7.6	0.86	5.77	110	9.5	44.2	15	15	0.14	60.4	15000	22	159	29.1	48	548	1.54	0.59	30.7	2.5	2830	31.2	157	201	959
2B1b	6.9	89.6	1390	5.6	0.65	9.88	118	9.8	34.5	20	8.2	0.12	54.7	11300	35	75.5	19.5	108	353	1.05	0.20	27.9	2.3	3250	18.3	106	206	503
2Ft	9.59	266	1650					10.8			6.9			6030		78.5									15.2	23.1		541
2Fb	6.49	48.4	486					5.7			5.3			4780		42.2									5.1	18.6		292
2G	6.22	43.4	1340					12.7			5.9			11800		35.7									2.8	26.9		299
2I	25.0	270	581	2.9	0.34	4.38	102	16.5	17.5	29	6.2	0.07	20.7	5310	86	58.5	13.4	45	255	0.56	0.11	14.2	1.4	1960	5.7	42.4	160	533
2K	4.88		517	1.9		1.33	19		10.5	10	3.3		9.7	3710		12.5	9.7		320	0.70				900	1.9	6.0	51	219
2N	6.95		775	1.9		0.14	11		6.3	11	2.4		1.3	4260		22.1	9.0		399	0.07				257	4.3	9.1	24	295
2Q	10.5		978	1.9		3.36	44		9.8	14	3.0		7.7	3010		68.3	10.9		204	0.32				1140	9.1	19.4	93	392
2R	6.11		986	1.1		0.87	25		4.3	14	1.9		3.4	1970		11.0	16.8		279	0.18				747	4.2	4.6	68	217

Tracy Mtn. REE Section 3

T.138N., R.101W., Sec.10, SW/NW/NW
Elevation at top 2,898 ft.

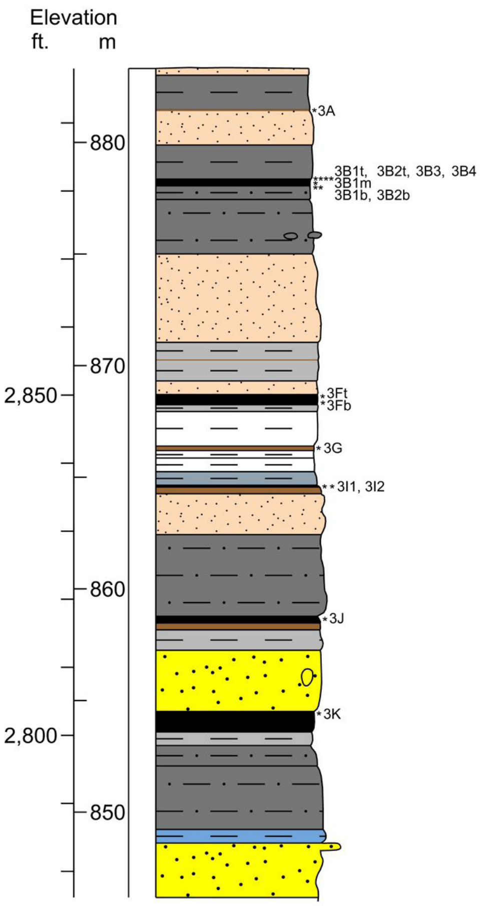

Sample ID	Lab Analysis (in µg/g) Cerium	Dysprosium	Erbium	Europium	Gadolinium	Holmium	Lanthanum	Lutetium	Neodymium	Praseodymium	Samarium	Scandium	Terbium	Thulium	Ytterbium	Yttrium	Total REE Whole coal	Total REE Ash
3A	53.3		9.01		10.9		26.8		30.2			32.7				72.7	*283*	*512*
3B1t	141	14.7	7.95	4.27	17.4	2.78	53.2	1.06	81.0	19.2	18.9	28.2	2.66	1.10	7.00	64.8	465	1077
3B2t	122	10.8	6.16	3.15	12.4	2.10	55.3	0.85	60.4	15.1	13.2	26.4	1.91	0.86	5.52	51.4	388	487
3B3	73.3		5.13		8.5		33.2		38.3			19.2				40.6	*255*	*435*
3B4	90.6	9.1	5.53	2.68	9.9	1.86	42.0	0.79	44.3	10.9	9.6	21.7	1.55	0.78	5.12	49.4	306	416
3B1m	68.0		4.03		7.5		31.1		34.8			16.7				35.9	*230*	*332*
3B1b	122	13.3	7.72	3.47	14.8	2.64	58.2	1.05	62.3	15.2	14.2	26.7	2.33	1.06	6.80	67.6	419	731
3B2b	128	13.3	7.91	3.64	14.3	2.68	62.8	1.10	63.7	15.6	13.6	31.5	2.26	1.08	7.03	65.1	434	555
3Ft	34.9		4.70		6.5		15.9		20.6			14.1				41.7	*166*	*452*
3Fb	29.8		3.75		4.7		14.5		14.9			17.4				32.7	*139*	*338*
3G	46.8		4.34		5.3		23.9		21.6			15.8				38.5	*182*	*265*
3I1	314	30.0	13.1	10.9	38.6	5.05	95.1	1.44	183	41.7	46.5	40.7	5.84	1.70	10.4	101	939	1678
3I2	161	15.5	7.10	5.33	19.1	2.72	63.6	0.83	91.2	21.7	22.5	26.1	2.98	0.96	5.80	59.8	506	612
3J	51.8		1.91		3.4		26.9		21.8			18.0				15.6	*156*	*173*
3K	20.3		0.83		1.5		10.2		8.9			8.7				6.8	*64*	*86*

Sample ID	Lab Analysis (in µg/g)																											
	Antimony	Arsenic	Barium	Beryllium	Bismuth	Cesium	Chromium	Cobalt	Gallium	Germanium	Hafnium	Indium	Lithium	Magnesium	Manganese	Molybdenum	Niobium	Rubidium	Strontium	Tantalum	Tellurium	Thorium	Tin	Titanium	Tungsten	Uranium	Vanadium	Zirconium
3A	16.4	698	16800					57			19			23200		126									83.5	44.4		870
3B1t	6.17	87.0	4860	4.4	0.29	1.37	72	10.9	17.3	6	7.1	0.11	15.4	10300	46	48.1	16.2	11	471	0.45	0.18	12.4	1.1	1270	10.8	60.7	107	334
3B2t	8.66	186	6280	4.6	0.75	7.65	79	12.2	30.8	9	7.4	0.09	58.7	9100	43	85.8	15.9	64	268	1.47	0.26	18.9	2.5	2790	11.0	74.9	185	389
3B3	6.03	175	1590	4.0	0.45	4.80	54	26	21.9	7	6.1	0.05	29.0	9700	39	56.1	14.7	37	252	1.09	0.16	10.0	1.7	1900	9.8	114	117	297
3B4	6.28	86.2	7370	4.2	0.54	8.97	80	17.6	32	8	6.3	0.07	38.1	10300	113	87.8	16.4	69	299	1.16	0.13	13.6	2.0	3000	13.4	76.0	181	283
3B1m	5.11	30.8	2780	3.1	0.72	6.37	50	6.3	31.7	6	4.8	0.06	46.0	5870	30	41.0	10.9	56	242	1.94	0.13	15.9	2.7	2380	8.4	32.7	126	193
3B1b	9.18	42.0	1540	3.8	0.55	5.52	90	16.3	22.9	11	6.2	0.09	18.2	6470	29	62.8	11.5	66	482	0.61	0.23	11.5	1.4	2150	10.4	64.9	227	323
3B2b	13.1	267	13800					9.8			7.6			8130		107									10.9	94.8		494
3Ft	7.06	48.6	1720					8.4			6.5			11300		75.2									12.7	24.5		418
3Fb	6.18	33.4	1580					7.7			4.7			9170		44.1									7.1	12.1		284
3G	8.10	34.9	3210					30.9			5.2			15900		37.9									2.3	22.7		266
3I1	19.3	65.6	376	5.4	0.35	5.97	167	23	25.5	23	6.2	0.12	29.5	5210	86	64.0	9.7	56	199	0.57	0.14	22.4	1.6	2190	2.3	81.4	285	489
3I2							129		29.6	5	3.3			5310		8.7	11.4			0.85					2.3	22.6	202	180
3J							90		26.1	2	3.4			11000		2.3	11.6			0.94					2.0	4.5	150	124
3K							21		22.2	3	3.8			7010		1.5	3.8			1.26					0.7	6.2	37	96.1

Tracy Mtn. REE Section 4

T.138N., R.101W., Sec.10, NE/SE/NW
Elevation at top 2,896 ft.

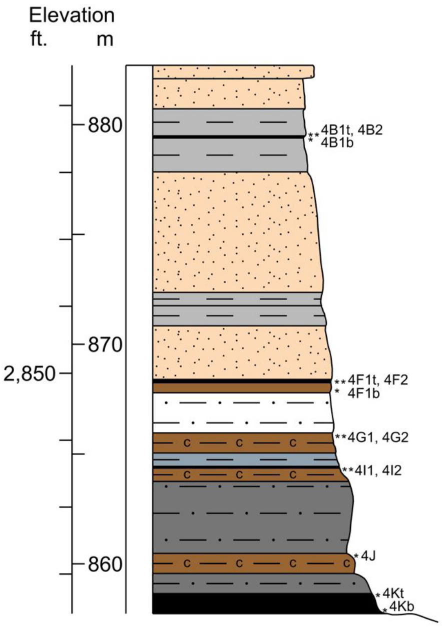

Sample ID	Lab Analysis (in µg/g)																Total REE	
	Cerium	Dysprosium	Erbium	Europium	Gadolinium	Holmium	Lanthanum	Lutetium	Neodymium	Praseodymium	Samarium	Scandium	Terbium	Thulium	Ytterbium	Yttrium	Whole coal	Ash
4B1t	134	12.7	7.18	3.43	14.5	2.48	56.1	0.96	69.2	17.4	15.1	28.9	2.22	0.99	6.23	64.6	436	505
4B2	127	14.0	7.94	3.63	15.4	2.80	60.2	1.04	64.4	15.8	14.7	23.4	2.41	1.08	6.87	65.0	426	607
4B1b	137	15.1	8.97	4.00	16.5	3.06	66.6	1.09	71.9	17.4	15.9	29.0	2.58	1.17	7.13	81.2	479	549
4F1t	46.0		3.56		6.1		22.3		25.5			14.5				29.4	*173*	*271*
4F2	44.7	7.8	4.65	1.64	7.6	1.60	17.2	0.67	26.4	6.2	6.6	13.4	1.28	0.66	4.27	33.0	178	427
4F1b	45.8		4.17		6.9		19.6		25.0			13.9				29.6	*174*	*392*
4G1	34.3		4.82		4.9		19.0		16.0			13.1				46.2	*162*	*249*
4G2	32.7		4.44		4.5		15.8		14.9			14.4				38.3	*147*	*249*
4I1	224	20.6	9.51	6.41	24.3	3.62	96.9	1.00	112	28.4	26.4	37.0	3.85	1.23	7.22	88.5	691	905
4I2	216	20.0	8.91	6.29	24.3	3.49	97.0	0.94	111	27.4	26.4	32.4	3.82	1.15	6.75	84.8	671	818
4J	52.6		2.04		4.0		25.7		23.6			17.0				16.5	*160*	*175*
4Kt	32.0		1.87		3.5		14.4		17.3			12.2				16.2	*113*	*186*
4Kb	65.7	8.5	4.94	2.15	8.9	1.69	19.1	0.70	34.5	7.9	8.3	13.7	1.45	0.69	4.45	37.3	221	1338

Sample ID	Antimony	Arsenic	Barium	Beryllium	Bismuth	Cesium	Chromium	Cobalt	Gallium	Germanium	Hafnium	Indium	Lithium	Magnesium	Manganese	Molybdenum	Niobium	Rubidium	Strontium	Tantalum	Tellurium	Thorium	Tin	Titanium	Tungsten	Uranium	Vanadium	Zirconium
	Lab Analysis (in µg/g)																											
4B1t	13.7	148	747	6.7	0.88	8.67	95	11.2	31.8	8	6.5	0.14	62.4	9990	58	125	20.9	65	275	1.46	0.64	27.1	2.7	3620	20.4	69.3	248	278
4B2																												
4B1b	11.9	142	11200					12			6.7			10400		74.0									16.7	73.8		271
4F1t	8.13	152	1860					10.2			7.5			9780		62.3									14.9	26.6		506
4F2	7.04		4180	3.4		1.47	15		12.2	6	8.4		5.4	9420		99.8	3.6		434	0.17				506	19.3	21.6	58	617
4F1b	8.47	93.2	553					8.5			6.0			8840		108									16.4	34.7		401
4G1	12.0	52.3	9280					30.6			7.3			9040		32.6									6.3	13.0		395
4G2	5.35	31.1	6980					9.8			7.0			17800		11.3									3.0	23.0		397
4I1	7.65	35.6	5560	6.2	0.58	6.75	118	7.1	23.6	5	2.9	0.16	39.6	5380	69	14.2	9.5	68	190	0.65	0.10	29.6	1.8	2810	2.2	44.5	198	137
4I2	8.13	18.1	509	5.4	0.65	7.53	136	8.4	26.7	5	3.2	0.17	49.1	5190	63	13.4	10.8	81	85	0.77	0.12	25.7	2.0	3390	2.2	34.4	205	168
4J	2.18	11.5	937					6.1			3.3			9790		4.4									1.7	5.9		123
4Kt	4.16	37.3	845					3.7			5.0			6540		7.0									2.4	7.4		285
4Kb	5.37	12.7	2730					11.5			3.2			2490		12.6									4.8	5.2		241

Tracy Mtn. REE Section 5

T.135N., R.101W., Sec.10, NW/SE/NW
Elevation at top 2,886 ft.

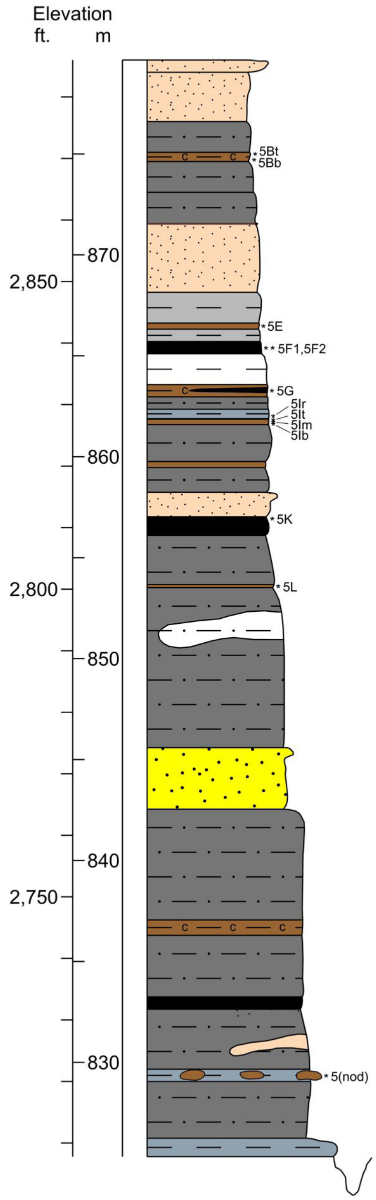

Sample ID	Cerium	Dysprosium	Erbium	Europium	Gadolinium	Holmium	Lanthanum	Lutetium	Neodymium	Praseodymium	Samarium	Scandium	Terbium	Thulium	Ytterbium	Yttrium	Total REE: Whole coal	Total REE: Ash
	Lab Analysis (in µg/g)																	
5Bt	251	20.3	10.5	6.01	25.2	3.72	112	1.27	130	32.5	28.3	32.9	3.79	1.39	8.47	89.0	756	935
5Bb	121	10.9	6.24	2.99	12.3	2.16	61.5	0.76	59.1	14.9	12.4	21.2	1.95	0.84	5.08	57.0	390	463
5E	109	13.5	6.70	4.23	17.3	2.46	40.5	0.87	79.6	17.1	19.8	23.2	2.59	0.89	5.87	49.3	393	503
5F1	42.6		3.90		9.6		13.4		40.1			14.3				30.3	*189*	*452*
5F2	46.6	9.8	5.05	2.81	12.3	1.82	14.1	0.66	48.7	9.1	12.8	19.8	1.79	0.68	4.50	36.8	227	549
5G	125	14.6	8.57	2.86	14.5	2.94	52.5	1.17	57.8	14.4	12.9	19.3	2.44	1.17	7.64	74.1	412	952
5lr	50.6		1.88		3.6		27.4		21.7			19.5				16.6	*158*	*172*
5lt	141	11.3	5.54	3.36	13.6	2.04	67.6	0.65	65.1	16.6	14.4	23.6	2.09	0.73	4.38	52.7	425	500
5lm	79.8		2.38		6.0		38.8		35.3			12.0				21.9	*223*	*234*
5lb	142	10.0	4.87	3.10	12.2	1.80	68.6	0.58	65.5	16.8	13.6	21.3	1.87	0.66	4.03	45.7	413	467
5K	29.9		1.77		3.7		13.7		16.5			7.5				16.8	*105*	*216*
5L	37.5		2.39		3.3		19.6		17.2			16.2				20.5	*133*	*176*
5(nod)	11.8		0.62		1.2		8.1		5.7			2.9				7.2	*43*	*62*

Sample ID	Lab Analysis (in µg/g)																										
	Antimony	Arsenic	Barium	Beryllium	Bismuth	Cesium	Chromium	Cobalt	Gallium	Germanium	Hafnium	Indium	Lithium	Magnesium	Manganese	Molybdenum	Niobium	Rubidium	Strontium	Tantalum	Tellurium	Thorium	Tin	Titanium	Tungsten	Uranium	Vanadium	Zirconium
5Bt							86		28.6	9	7.5			14000		142	18.2			1.24					18.5	99.8	194	297
5Bb							71		30.5	8	4.8			11700		86.7	13.3			1.42					11.6	111	189	228
5E							88		26.5	7	6.3			12300		29.8	15.0			1.03					3.0	31.4	213	345
5F1							36		8.3	4	6.0			6150		89.7	9.7			0.28					21.1	17.4	63	379
5F2																												
5G							53		17.3	4	5.4			5110		50.1	16.6			0.74					2.6	15.5	84	261
5Ir							116		28.4	3	2.9			8930		6.5	14.2			0.91					2.5	3.8	207	98.2
5It							117		35.1	5	3.0			6430		13.0	12.6			0.83					2.7	11.7	209	136
5Im							66		17.8	3	2.3			4500		4.3	11.5			0.83					1.5	4.4	107	79.4
5Ib							100		25.3	4	3.1			7510		7.2	13.2			0.90					2.3	10.6	167	124
5K							24		12.8	8	4.4			5880		7.8	12.2			0.91					2.7	5.6	50	281
5L							98		24.1	28	4.8			18200		45.9	23.9			0.74					2.0	19.6	219	477
5(nod)							98		24.1	28	4.8			18200		45.9	23.9			0.74					2.0	19.6	219	477

Tracy Mtn. REE Section 6

T.135N., R.105W., Sec.9, NE/SE
Elevation at top 2,882 ft.

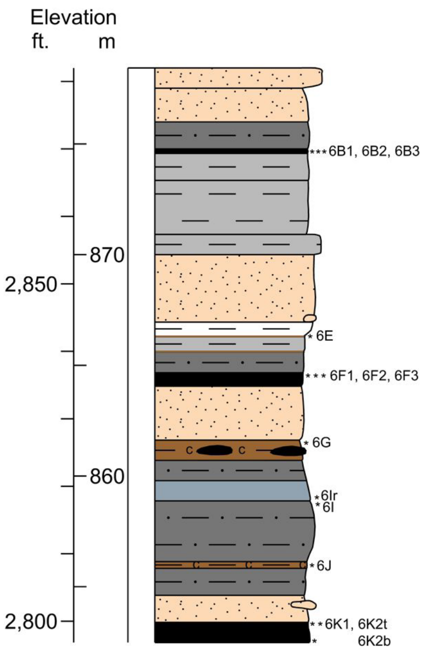

Sample ID	Lab Analysis (in µg/g)																Total REE	
	Cerium	Dysprosium	Erbium	Europium	Gadolinium	Holmium	Lanthanum	Lutetium	Neodymium	Praseodymium	Samarium	Scandium	Terbium	Thulium	Ytterbium	Yttrium	Whole coal	Ash
6B1	143	13.2	7.65	3.74	14.9	2.64	65.9	1.05	69.1	17.0	15	30.0	2.29	1.07	6.59	67.0	460	522
6B2	105	11.1	6.32	2.96	12.0	2.19	47.9	0.86	53.3	13.2	11.7	24.4	1.83	0.88	5.61	54.8	354	438
6B3	159	17.4	10.5	4.36	18.6	3.60	78.1	1.39	77.6	19.0	17	30.9	2.97	1.43	8.98	105	556	759
6E	165	20.0	9.70	6.26	25.9	3.58	59.8	1.18	119	27.0	29.5	28.2	3.86	1.28	8.16	75.9	584	891
6F1	19.6	4.5	2.99	0.86	3.9	0.98	7.9	0.42	11.6	2.7	3.1	9.7	0.68	0.42	2.66	28.9	101	202
6F2	47.2	10.8	7.53	1.72	9.0	2.44	19.5	1.09	26.7	6.3	6.8	19.6	1.60	1.06	6.76	71.0	239	746
6F3	83.7	12.7	6.58	3.24	14.6	2.37	30.1	0.82	57.9	12.9	14.2	19.4	2.28	0.87	5.47	57.8	325	727
6G	114	13.7	8.32	2.63	13.2	2.78	54.6	1.15	53.9	13.6	12.1	21.0	2.26	1.16	7.47	73.6	395	856
6Ir	61.9		2.37		5.0		32.1		28.5			15.0				21.2	*189*	*203*
6I	84.0		3.41		6.5		41.5		36.5			23.2				28.1	*254*	*279*
6J	49.4		2.30		4.1		24.0		22.6			18.6				18.4	*158*	*186*
6K1	19.6		1.03		1.8		9.5		9.5			7.6				8.8	*66*	*112*
6K2t	35.9		1.91		3.7		17.9		18.5			11.6				14.1	*120*	*178*
6K2b	102	13.6	7.52	3.82	15.0	2.62	39.1	1.03	61.7	14.1	15.3	25.8	2.39	1.06	6.74	52.9	365	1551

Sample ID	Lab Analysis (in µg/g)																											
	Antimony	Arsenic	Barium	Beryllium	Bismuth	Cesium	Chromium	Cobalt	Gallium	Germanium	Hafnium	Indium	Lithium	Magnesium	Manganese	Molybdenum	Niobium	Rubidium	Strontium	Tantalum	Tellurium	Thorium	Tin	Titanium	Tungsten	Uranium	Vanadium	Zirconium
6B1							122		36.9	13	6.3			10600		105	20.1			1.18					20.3	69.4	268	302
6B2	10.7	93.8	5740	4.5	0.87	8.32	87	25.8	22.3	7	6.4	0.09	58.3	15000	112	64.7	17.2	96	370	1.63	0.24	21.1	2.6	3000	16.5	63.9	200	331
6B3							70		32.1	7	7.8			13000		178	17.4			1.26					36.1	131	196	442
6E	15.4	67.9	547					32			8.7			11900		51.3									4.5	49.2		524
6F1	7.78	113	3050	3.7		0.64	13	8.3	10.7	6	4.7		6.1	8550		55.8	4.0		318	0.12				436	8.9	14.9	59	297
6F2	9.29	54.9	600	6.5		1.19	23	29.9	17.5	6	6.5		8.7	9600		92.6	5.5		400	0.19				596	10.0	34.7	80	426
6F3							27		8.9	5	5.9			7030		77.2	5.2			0.20					7.3	16.5	47	385
6G	4.50	34.4	1850					16.7			6.8			6670		26.1									2.5	23.7		320
6Ir							84		21.1	3	2.8			20500		1.7	14.6			1.03					2.1	2.9	128	90.6
6I							106		28.4	5	4.5			12500		6.4	13.9			1.03					2.2	15.6	202	254
6J	6.80	23.5	3940					5.9			4.2			13500		11.2									1.9	12.3		214
6K1	4.30	37.8	7510					2			3.2			6730		8.3									1.1	5.0		158
6K2t									18.4	7				6630		9.8										10.3		204
6K2b									21.8	11				4280		9.8										8.0		487

Tracy Mtn. REE Section 7

T.138N., R.101W., Sec.10, NE/SW/NE
Elevation at top 2,883 ft.

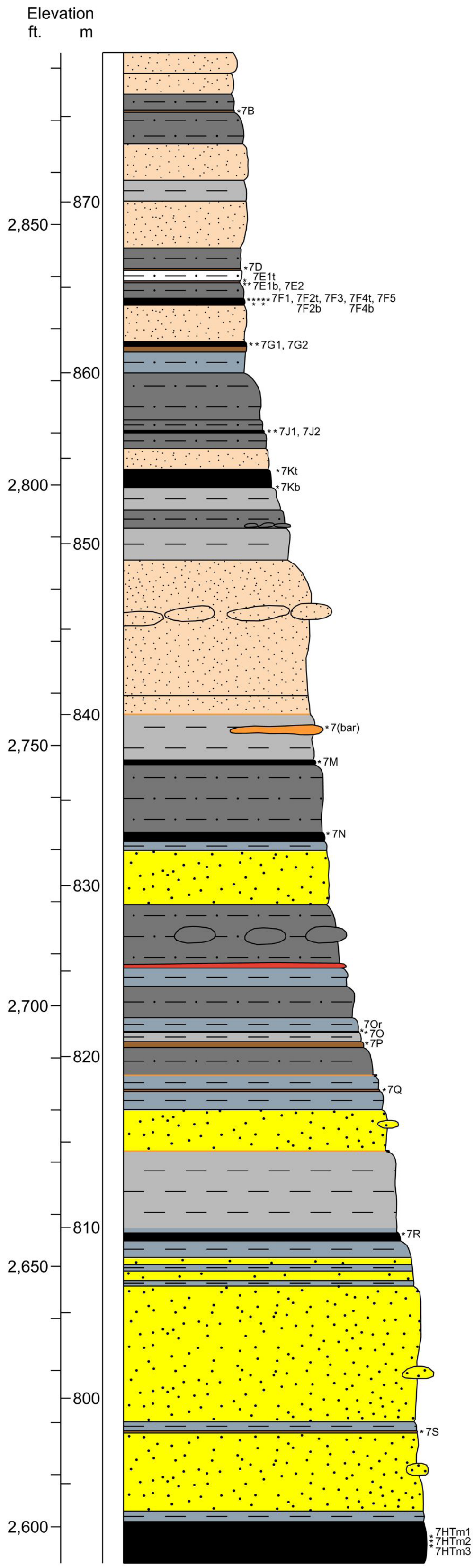

Sample ID	Lab Analysis (in µg/g)																Total REE	
	Cerium	Dysprosium	Erbium	Europium	Gadolinium	Holmium	Lanthanum	Lutetium	Neodymium	Praseodymium	Samarium	Scandium	Terbium	Thulium	Ytterbium	Yttrium	Whole coal	Ash
7B	151	14.6	8.35	4.11	16.9	2.89	69.8	1.16	76.8	18.7	17.2	28.0	2.59	1.17	7.43	79.8	501	605
7D	40.2	7.4	4.74	1.41	7.0	1.58	18.4	0.70	23.6	5.4	5.9	12.6	1.16	0.67	4.33	41.3	176	652
7E1t	183	25.0	12.0	6.96	30.4	4.54	58.8	1.44	131	28.8	31.3	23.0	4.70	1.58	9.83	94.1	646	1022
7E1b	91.9	11.4	5.65	3.80	15.0	2.04	31.7	0.75	72.2	15.3	18.2	27.1	2.21	0.76	4.98	42.9	346	523
7E2	216	30.8	13.9	9.85	40.0	5.29	61.1	1.71	175	37.6	45.5	33.3	5.79	1.84	11.5	93.0	782	1480
7F1	95.5	17.6	8.81	4.75	21.0	3.24	28.7	1.13	81.8	16.8	21.1	20.9	3.15	1.17	7.48	68.8	402	1083
7F2t	18.0		1.99		3.2		6.7		12.7			7.4				17.9	*81*	*181*
7F3	84.8	12.4	6.38	3.55	15.4	2.30	23.7	0.81	62.6	13.5	16.2	19.3	2.25	0.84	5.49	45.3	315	786
7F4t	114	17.3	8.73	4.67	20.0	3.20	36.2	1.13	80.1	17.7	20.1		2.93	1.22	7.43	64.0	399	
7F5	44.6	7.5	4.20	1.88	8.4	1.45	17.0	0.61	33.1	7.0	8.3	15.7	1.27	0.59	3.82	33.5	189	458
7F2b	69.9		6.51		10.2		29.6		37.0			23.6				61.7	*282*	*695*
7F4b	72.2	10.3	5.89	2.24	10.0	2.09	28.6	0.81	39.3	9.6	9.3	18.9	1.71	0.85	5.29	55.0	272	498
7G1	56.8		5.19		6.7		31.3		23.6			13.5				48.9	*217*	*343*
7G2	38.9		3.67		4.4		22.0		16.0			10.3				34.4	*151*	*221*
7J1	45.8	3.3	2.20	0.84	3.5	0.70	23.5	0.37	21.3	5.3	3.8		0.51	0.35	2.35	17.0	131	
7J2	65.0		2.35		4.6		33.8		28.0			19.3				20.0	*195*	*220*
7Kt	26.7	3.4	1.92	0.86	3.6	0.66	12.7	0.28	15.9	3.9	3.8		0.54	0.29	1.85	15.0	91	154
7Kb	35.3	4.0	2.26	1.14	4.3	0.80	15.3	0.31	18.8	4.5	4.4		0.65	0.33	2.02	17.0	*111*	
7(bar)	12.6		0.57		1.2		6.6		6.3			3.1				5.3	*41*	*41*
7M	57.9		3.34		5.4		28.1		26.9			19.2				25.1	*191*	*277*
7N	19.3	5.2	3.95	0.88	3.7	1.23	9.6	0.64	10.4	2.4	2.7		0.68	0.61	3.93	34.0	99	338
7Or	70.8		2.80		5.7		37.4		32.8			13.4				25.7	*215*	*225*
7O	99.6	10.1	5.45	2.89	11.9	1.91	44.1	0.75	54.6	12.9	12.4	10.5	1.83	0.76	4.84	45.1	320	344
7P	48.6		3.19		6.5		19.3		29.7			14.1				25.3	*173*	*332*
7Q	31.7		3.26		3.2		17.6		14.5			16.4				26.2	*130*	*221*
7R	28.5	3.0	1.47	1.13	3.8	0.55	11.4	0.18	18.2	4.1	4.4		0.53	0.20	1.25	12.0	91	
7S	54.8		2.77		5.7		23.4		28.8			16.9				22.0	*179*	*250*
7HTm1	21.5		1.64		2.8		12.8		11.5			5.0				18.2	*85*	*171*
7HTm2	9.3		0.47		0.8		6.4		3.9			1.8				6.0	*32*	*107*
7HTm3	7.1		0.36		0.7		4.0		3.5			2.4				3.9	*25*	*142*

Sample ID	Lab Analysis (in µg/g)																										
	Antimony	Arsenic	Barium	Beryllium	Bismuth	Cesium	Chromium	Cobalt	Gallium	Germanium	Hafnium	Indium	Lithium	Magnesium	Manganese	Molybdenum	Niobium	Rubidium	Strontium	Tantalum	Tellurium	Thorium	Tin	Titanium	Tungsten	Uranium	Vanadium	Zirconium
7B	10.1	164	5630	6.6	0.91	7.62	99	14.5	33	8	7.4	0.11	76.6	8300	33	96.7	20.9	82	322	1.54	0.30	23.8	2.6	2990	20.7	58.8	214	359
7D																												
7E1t							89		34	16	10			12200		124	30.8			0.80					12.6	34.9	382	720
7E1b							107		18.0	6	7.3			10800		51.9	14.5			0.70					3.8	26.5	238	404
7E2	22.6	107	4480	5.6	1.21	4.08	84	45	15.3	14	11	0.15	23.2	9430	43	131	25.8	46	163	0.56	0.32	16.0	2.2	1800	6.4	79.2	387	839
7F1	11.2		11300	3.6		0.94	30		8.1	10	6.6		5.9	7790		110	6.4		203	0.16				520	17.1	25.0	74	372
7F2t							18		5.3	6	4.6			9040		144	6.5			0.15					10.3	7.3	40	324
7F3																												
7F4t																												
7F5																												
7F2b							38		13.8	4	4.2			7970		33.5	13.7			0.88					3.8	19.7	92	199
7F4b																												
7G1							**49**		**11.8**	**7**	**4.7**			**9030**		**28.5**	**20.7**			**0.82**					**3.1**	**7.7**	**156**	**212**
7G2							47		12.7	7	4.5			6300		31.4	17.9			1.05					3.1	6.4	140	193
7J1																												
7J2							89		26.9	3	3.6			12600		1.7	13.3			0.96					1.9	6.9	147	154
7Kt																												
7Kb																												
7(bar)	0.29	1.7	32000	0.4		2.70	12	2.3	5.1	1	0.6		7.8	3150	84	0.5	3.2	28	524	0.24		1.9		930	0.5	1.7	27	19.6
7M							88		20.3	46	4.0			7390		19.6	20.4			0.71					1.7	15.0	200	360
7N																												
7Or							78		20.0	3	3.3			13500		2.3	15.5			0.89					1.5	2.9	121	135
7O							56		16.0	4	3.1			6580		8.5	13.8			0.84					1.6	5.1	103	237
7P							49		11.1	25	3.5			4910		66.7	18.1			0.39					11.4	17.6	97	634
7Q							65		19.9	59	4.1			6950		24.8	29.9			0.53					3.4	14.7	171	469
7R																												
7S							81		19.4	36	2.8			7860		18.8	21.4			0.59					1.5	16.6	211	237
7HTm1	1.94	36.7	2030	1.6	0.21	1.71	23	6.1	6.3	4	1.3	0.02	11.9	4840	118	6.0	5.5	28	330	0.36	<0.1	3.5	0.8	1230	1.6	4.6	35	63.8
7HTm2	0.55	11.2	1620					2			0.8			4580		4.8									1.1	1.7		28.4
7HTm3	0.46	5.1	1780					3.1			0.7			3800		2.3									1.1	1.1		25.4

Tracy Mtn. REE Section 8

T.138N., R.101W., Sec.1, NE/NW/NE
Elevation at top 2,889 ft.

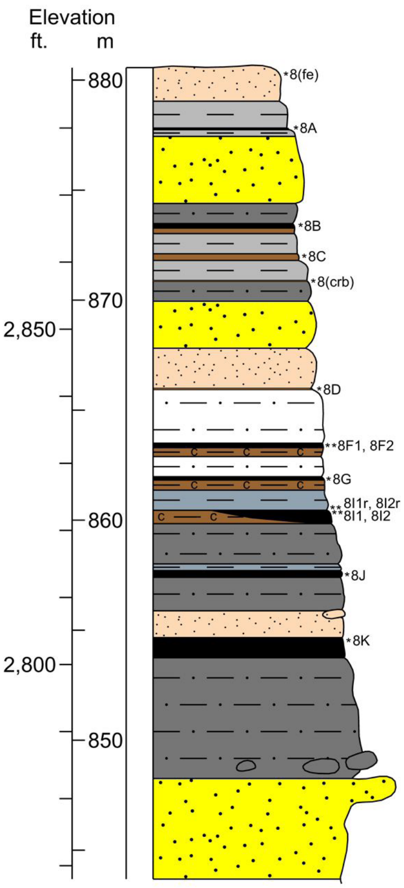

Sample ID	Lab Analysis (in µg/g)															Total REE	
	Cerium	Dysprosium	Erbium	Europium	Gadolinium	Holmium	Lanthanum	Lutetium	Neodymium	Praseodymium	Samarium	Scandium	Terbium	Thulium	Ytterbium	Yttrium	Whole coal	Ash
8(fe)	20.9		1.54		2.4		10.9		10.3			7.7				14.1	*78*	*88*
8A	120	19.5	13.1	4.25	19.2	4.25	61.6	2.00	66.3	15.2	15.9	37.5	3.14	1.86	12.3	128	524	732
8B	101	9.1	5.35	2.73	11.1	1.84	46.6	0.78	51.7	12.5	11.1	20.2	1.65	0.74	4.77	49.5	331	438
8C	163	21.0	12.5	4.76	23.4	4.45	79.7	1.50	84.1	20.0	17.6	32.4	3.60	1.60	9.38	143	622	732
8(crb)	66.2		2.78		5.3		36.0		29.1			12.1				29.4	*205*	*215*
8D	74.4		4.03		6.5		39.6		34.1			17.8				35.3	*242*	*265*
8F1	42.5	8.8	4.89	2.24	10.0	1.70	14.5	0.70	36.7	7.5	9.9	17.1	1.52	0.69	4.59	34.0	197	599
8F2	30.5		3.63		6.0		10.4		21.9			10.6				31.8	*139*	*300*
8G	33.7		4.64		4.6		21.6		14.6			11.2				47.5	*161*	*241*
8I1r	46.5		1.65		3.4		24.3		20.3			19.4				13.8	*145*	*158*
8I2r	146	7.1	3.58	2.80	9.9	1.28	69.8	0.43	67.1	17.4	12.9	19.2	1.42	0.47	3.03	31.1	394	425
8I1	189	16.5	7.35	5.52	20.7	2.82	78.0	0.79	101	24.4	24.2	30.6	3.18	0.95	5.82	65.3	576	692
8I2	352	34.8	16.7	11.5	42.2	6.19	129	1.91	199	46.7	49.3	35.0	6.46	2.21	13.4	143	1089	1848
8J	56.8		2.41		4.1		28.5		24.8			18.8				19.9	*175*	*217*
8K	37.7		2.52		4.7		17.0		20.4			9.9				21.8	*134*	*251*

Sample ID	Lab Analysis (in µg/g)																											
	Antimony	Arsenic	Barium	Beryllium	Bismuth	Cesium	Chromium	Cobalt	Gallium	Germanium	Hafnium	Indium	Lithium	Magnesium	Manganese	Molybdenum	Niobium	Rubidium	Strontium	Tantalum	Tellurium	Thorium	Tin	Titanium	Tungsten	Uranium	Vanadium	Zirconium
8(fe)	13.7	152	614					20.6			1.2			2650		31.3									2.3	22.9		49.9
8A	15.9	464	6020					253			12			23400		39.3									36.6	17.6		599
8B	5.59	146	4940	3.0	0.46	5.02	74	7.1	20.9	8	7.4	0.07	39.4	12500	230	48.8	22.2	60	360	1.06	0.20	14.4	1.9	2820	20.0	44.3	150	337
8C	14.0	32.8	724					15.2			7.3			13000		8.5									3.1	27.2		545
8(crb)	3.15	19.0	618					37.2			3.0			8000		2.9									1.9	8.4		116
8D	7.38	34.4	6920					19.6			6.6			17400		11.7									2.6	12.1		371
8F1	6.74		3580	1.9		0.51	29		6.4	4	5.6		2.6	10400		73.1	5.3		132	0.15				599	14.6	19.9	55	345
8F2	6.88	291	17500					11.8			4.7			8400		53.2									10.0	10.4		332
8G	4.31	23.9	6200					12.9			4.7			7870		18.9										8.8		208
8l1r							104		26	2	2.6			7100		8.9	12.2			0.78					2.1	5.7	181	80.0
8l2r	7.95	23.4	541	3.6	0.62	8.42	117	7.9	24.9	6	3.3	0.12	40.4	6450	56	14.1	11.6	87	107	0.88	0.11	45.9	2.2	3550	2.5	39.7	209	167
8l1							103		28.2	4	2.5			6390		2.9	12.8			0.83					2.2	4.6	172	77.1
8l2							122		33.5	20	4.5			5240		47.0	9.7			0.53					2.2	60.4	230	391
8J							96		28.1	3	3.6			11500		2.8	11.6			0.96					1.9	8.4	162	181
8K							34		11.6	11	2.9			5270		8.7	6.4			0.50					1.2	4.6	72	194

Tracy Mtn. REE Section 9

T.138N., R.101W., Sec.10, SE/NE/NW
Elevation at top 2,892 ft.

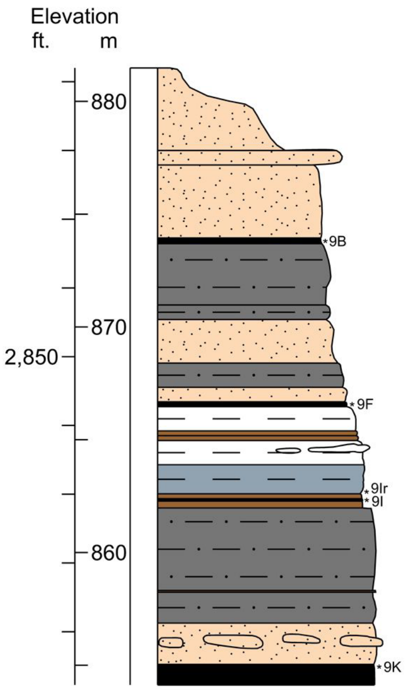

Sample ID	Lab Analysis (in µg/g)															Total REE	
	Cerium	Dysprosium	Erbium	Europium	Gadolinium	Holmium	Lanthanum	Lutetium	Neodymium	Praseodymium	Samarium	Scandium	Terbium	Thulium	Ytterbium	Yttrium	Whole coal	Ash
9B	237	24.3	13.3	6.55	27.5	4.71	100	1.74	122	29.9	27.7	31.3	4.28	1.79	11.4	111	754	1148
9F	44.4		4.49		7.5		17.5		27.2			15.9				39.1	*187*	*419*
9Ir	226	14.8	7.47	5.32	19.1	2.69	101	0.90	111	28.2	23.4	20.4	2.84	1.00	6.28	68.8	639	695
9I	268	31.7	15.7	9.52	39.8	5.89	110	1.95	160	34.4	37.2	34.1	5.82	2.07	12.8	125	894	2317
9K	26.4		1.42		2.7		11.9		13.6			8.0				11.6	*87*	*139*

Sample ID	Lab Analysis (in µg/g)																										
	Antimony	Arsenic	Barium	Beryllium	Bismuth	Cesium	Chromium	Cobalt	Gallium	Germanium	Hafnium	Indium	Lithium	Magnesium	Manganese	Molybdenum	Niobium	Rubidium	Strontium	Tantalum	Tellurium	Thorium	Tin	Titanium	Tungsten	Uranium	Vanadium	Zirconium
9B							85		19.8	10	8.1			15300		175	20.2			0.85					22.2	200	155	413
9F							35		16.0	9	9.7			4590		69.1	10.4			0.23					14.9	26.3	99	741
9Ir							117		32.8	8	2.9			5960		9.2	13.3			0.94					2.4	10.4	189	110
9I							98		21.9	15	6.7			2360		134	18.2			0.26					4.7	51.3	216	697
9K							25		14.3	7	2.9			6090		3.1	4.1			0.67					0.6	4.5	62	117

Tracy Mtn. REE Section 10

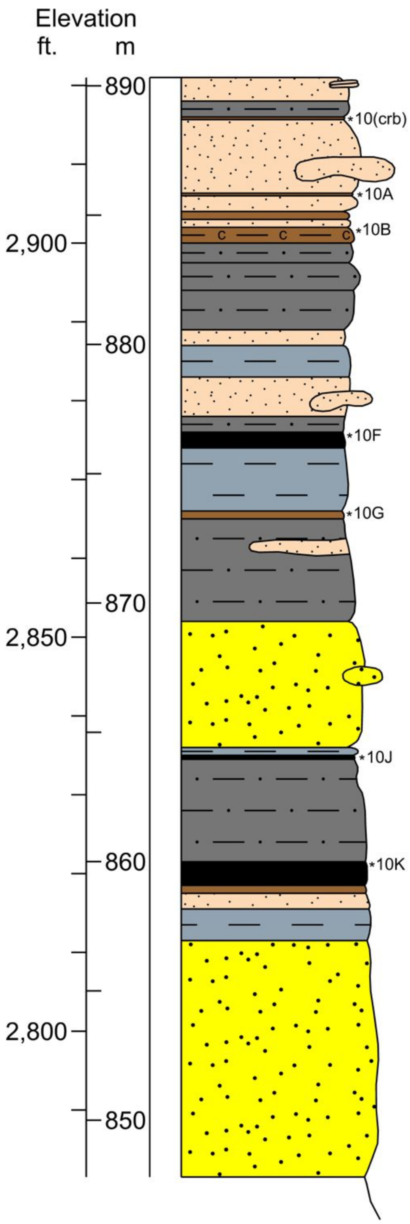

Sample ID	Lab Analysis (in µg/g)																Total REE	
	Cerium	Dysprosium	Erbium	Europium	Gadolinium	Holmium	Lanthanum	Lutetium	Neodymium	Praseodymium	Samarium	Scandium	Terbium	Thulium	Ytterbium	Yttrium	Whole coal	Ash
10(crb)	54.0		2.69		4.9		23.2		24.4			17.5				21.8	*171*	*213*
10A	103	11.2	5.69	3.29	13.6	2.04	35.0	0.74	66.6	15.3	15	15.9	2.08	0.78	5.12	40.7	336	377
10B	101	9.3	5.21	2.59	10.2	1.78	43.6	0.72	51.1	12.7	11.1	22.6	1.62	0.72	4.61	45.8	325	431
10F	51.3		3.03		5.8		23.2		27.6			13.3				26.4	*175*	*285*
10G	88.5		4.33		7.3		43.6		39.7			13.9				37.0	*269*	*303*
10J	49.1		1.91		3.2		24.8		20.9			17.7				15.2	*149*	*163*
10K	32.1		1.21		2.6		16.5		15.4			11.3				10.2	*101*	*149*

Sample ID	Lab Analysis (in µg/g)																											
	Antimony	Arsenic	Barium	Beryllium	Bismuth	Cesium	Chromium	Cobalt	Gallium	Germanium	Hafnium	Indium	Lithium	Magnesium	Manganese	Molybdenum	Niobium	Rubidium	Strontium	Tantalum	Tellurium	Thorium	Tin	Titanium	Tungsten	Uranium	Vanadium	Zirconium
10(crb)							59		20.6	12	9.8			20500		71.6	23.1			0.88					30.1	25.0	103	539
10A							80		27.1	13	5.8			17400		13.6	21.3			0.96					5.9	22.0	236	280
10B							113		25.3	4	4.6			7750		27.9	14.3			1.05					3.9	46.6	249	222
10F							55		16.4	12	5.6			7760		73.9	8.0			0.54					6.2	28.4	133	422
10G							48		33.8	4	5.7			5860		21.2	29.5			2.83					7.7	12.1	95	235
10J							85		26.5	3	3.6			10700		6.3	12.5			1.08					2.2	7.0	145	148
10K							49		18.8	14	3.7			5940		7.7	13.0			1.22					2.0	6.6	120	229

Tracy Mtn. REE Section 11

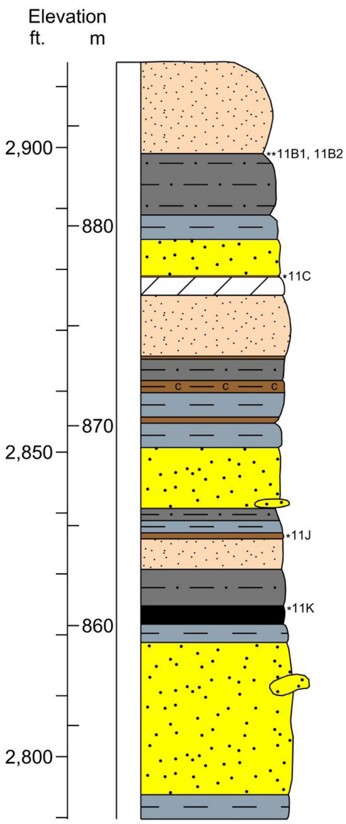

Sample ID	Lab Analysis (in µg/g)																
	Cerium	Dysprosium	Erbium	Europium	Gadolinium	Holmium	Lanthanum	Lutetium	Neodymium	Praseodymium	Samarium	Scandium	Terbium	Thulium	Ytterbium	Yttrium	Total REE Whole coal	Total REE Ash
11B1	49.6		2.32		3.5		25.1		20.1			18.7				14.4	*151*	*172*
11B2	47.0		1.94		3.7		24.7		21.5			13.5				16.6	*146*	*170*
11C	74.6		2.81		6.2		35.0		34.6			10.8				25.3	*217*	*230*
11J	39.9		1.76		2.8		20.2		17.4			11.5				14.3	*122*	*137*
11K	19.9		1.04		2.2		9.1		11.2			9.5				8.6	*71*	*103*

Sample ID	Lab Analysis (in µg/g)																											
	Antimony	Arsenic	Barium	Beryllium	Bismuth	Cesium	Chromium	Cobalt	Gallium	Germanium	Hafnium	Indium	Lithium	Magnesium	Manganese	Molybdenum	Niobium	Rubidium	Strontium	Tantalum	Tellurium	Thorium	Tin	Titanium	Tungsten	Uranium	Vanadium	Zirconium
11B1							108		24.5	3	5.3			11600		33.6	14.0			1.27					3.6	14.1	233	258
11B2							73		25.8	2	3.0			7600		6.3	9.3			1.22					1.9	7.7	147	132
11C							50		17.8	2	2.7			8020		1.1	14.1			1.20					2.6	4.5	74	99.5
11J							71		16.4	7	3.0			10200		1.5	11.2			0.87					1.5	5.5	118	210
11K							25		15.8	11	3.0			6090		9.7	5.4			0.89					2.0	6.3	48	186

Tracy Mtn. REE Section 12

T.138N., R.101W., Sec.6,
Elevation at top 2,913 ft.

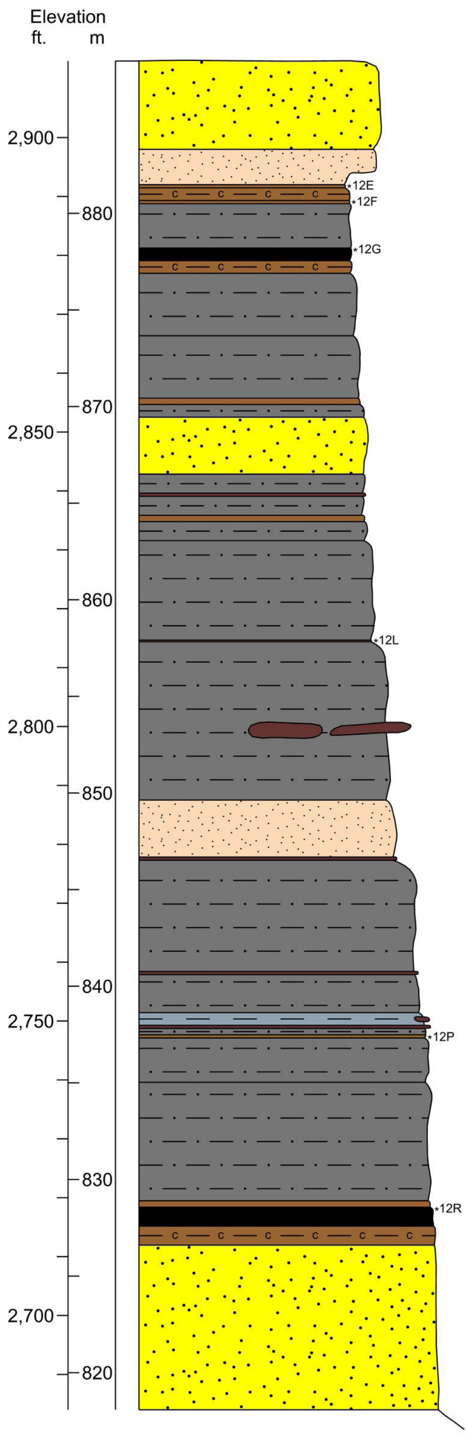

Sample ID	Lab Analysis (in µg/g)																Total REE	
	Cerium	Dysprosium	Erbium	Europium	Gadolinium	Holmium	Lanthanum	Lutetium	Neodymium	Praseodymium	Samarium	Scandium	Terbium	Thulium	Ytterbium	Yttrium	Whole coal	Ash
12E	31.2		1.89		2.4		16.8		13.3			10.5				16.2	*105*	*161*
12F	43.4		1.37		2.6		22.0		18.9			9.3				11.1	*122*	*136*
12G	28.8		1.14		2.1		12.6		12.2			7.5				11.0	*85*	*120*
12L	40.4		2.44		4.2		19.4		21.2			13.4				17.9	*138*	*195*
12P	83.3		4.90		9.3		40.0		42.3			16.4				39.6	*275*	*335*
12R	20.6		1.42		3.4		7.2		15.8			4.7				12.9	*79*	*251*

Sample ID	Lab Analysis (in µg/g)																											
	Antimony	Arsenic	Barium	Beryllium	Bismuth	Cesium	Chromium	Cobalt	Gallium	Germanium	Hafnium	Indium	Lithium	Magnesium	Manganese	Molybdenum	Niobium	Rubidium	Strontium	Tantalum	Tellurium	Thorium	Tin	Titanium	Tungsten	Uranium	Vanadium	Zirconium
12E							67		14.7	15	3.2			11300		11.3	13.5			0.70					2.2	49.3	228	287
12F							56		17.2	3	2.9			8350		2.4	13.1			0.98					2.5	8.0	109	117
12G							13		14.0	4	2.8			11600		11.7	3.1			1.03					1.1	29.0	54	85.9
12L							73		22.3	64	5.0			6230		105	18.4			0.66					8.3	16.3	195	593
12P							97		22.6	30	3.5			7830		17.4	15.1			0.74					1.3	15.2	281	387
12R							29		4.5	6	2.3			2320		17.6	27.4			0.26					5.9	3.6	44	300

Tracy Mtn. REE Section 13

T.138N., R.102W., Sec.13, SW 1/4
Elevation at top 2,879 ft.

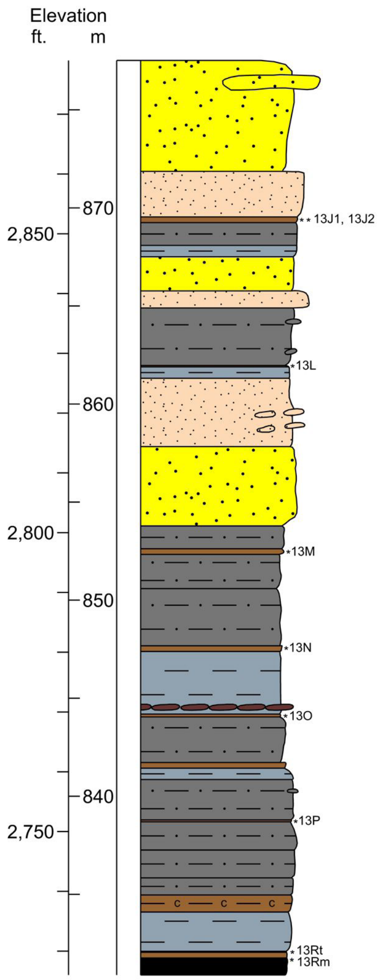

Sample ID	Lab Analysis (in µg/g)																Total REE	
	Cerium	Dysprosium	Erbium	Europium	Gadolinium	Holmium	Lanthanum	Lutetium	Neodymium	Praseodymium	Samarium	Scandium	Terbium	Thulium	Ytterbium	Yttrium	Whole coal	Ash
13J1	26.4		2.02		2.4		13.9		11.1			13.2				17.6	*99*	*112*
13J2	39.1		2.84		3.8		21.1		17.5			16.7				27.8	*147*	*174*
13L	53.6		2.32		4.5		28.8		24.6			14.0				21.2	*169*	*182*
13M	60.0		2.00		4.3		31.4		26.5			14.9				18.3	*177*	*189*
13N	41.4		1.83		2.8		22.7		18.1			10.3				15.3	*127*	*146*
13O	27.4		2.37		3.5		14.2		14.6			11.5				21.1	*110*	*203*
13P	78.3		3.34		6.5		41.5		35.9			17.9				29.5	*243*	*279*
13Rt	39.4		2.03		4.9		17.0		25.4			13.8				15.9	*138*	*276*
13Rm	17.1		1.09		2.2		7.4		10.5			5.3				9.3	*62*	*158*

Sample ID	Lab Analysis (in µg/g)																										
	Antimony	Arsenic	Barium	Beryllium	Bismuth	Cesium	Chromium	Cobalt	Gallium	Germanium	Hafnium	Indium	Lithium	Magnesium	Manganese	Molybdenum	Niobium	Rubidium	Strontium	Tantalum	Tellurium	Thorium	Tin	Titanium	Tungsten	Uranium	Vanadium	Zirconium
13J1							53		29.9	21	4.7			2130		40.8	20.4			1.01					3.3	12.9	116	662
13J2							51		22.3	15	4.0			7240		209	13.5			0.98					5.4	18.9	123	604
13L							93		22.4	4	2.9			15900		4.4	12.4			0.97					1.9	8.9	188	113
13M							86		23.2	3	3.3			15400		8.8	13.3			1.01					2.0	10.8	145	120
13N							60		16.9	7	3.5			8960		15.1	14.9			1.05					2.3	14.2	134	274
13O							36		14.7	20	5.8			6830		218	15.6			0.28					10.1	27.1	97	646
13P							95		25.8	13	4.8			9520		4.1	17.6			1.21					1.8	11.1	157	349
13Rt							119		12.1	11	3.9			3650		35.6	19.1			0.38					1.4	16.7	98	416
13Rm							38		5.8	4	1.3			2910		23.9	4.7			0.18					2.2	8.7	41	94.7

Tracy Mtn. REE Section 14

T.139N., R.101W., Sec.26, SW 1/4
Elevation at top 2,825 ft.

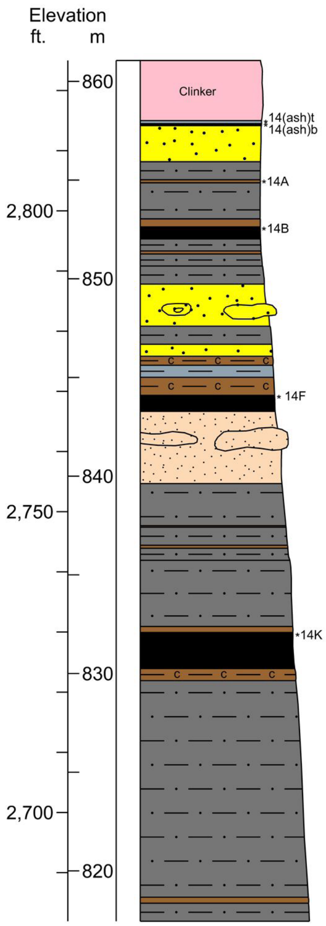

Sample ID	Lab Analysis (in µg/g)																Total REE	
	Cerium	Dysprosium	Erbium	Europium	Gadolinium	Holmium	Lanthanum	Lutetium	Neodymium	Praseodymium	Samarium	Scandium	Terbium	Thulium	Ytterbium	Yttrium	Whole coal	Ash
14(ash)t	37.6		2.18		3.4		19.2		16.5			13.6				24.2	*133*	*149*
14(ash)b	37.1		6.50		8.0		17.5		22.9			16.0				66.7	*209*	*264*
14A	65.1		3.60		6.9		27.9		36.2			17.7				25.8	*213*	*255*
14B	21.1		2.31		4.3		8.7		17.1			18.0				19.9	*108*	*319*
14F	57.7		3.63		6.6		25.2		30.1			16.1				28.7	*196*	*381*
14K	28.9		1.70		3.6		12.7		16.0			10.9				13.5	*102*	*389*

Sample ID	Lab Analysis (in µg/g)																										
	Antimony	Arsenic	Barium	Beryllium	Bismuth	Cesium	Chromium	Cobalt	Gallium	Germanium	Hafnium	Indium	Lithium	Magnesium	Manganese	Molybdenum	Niobium	Rubidium	Strontium	Tantalum	Tellurium	Thorium	Tin	Titanium	Tungsten	Uranium	Vanadium	Zirconium
14(ash)t	2.37	98.5	9550						13.8	3				28800		23.8	7.3								2.0	8.8	75	128
14(ash)b	4.66	86.7	5410						10.6	8				11300		120	7.0								27.4	34.1	63	254
14A	5.77	56.6	1580						23.1	6				15200		46.4	16.1								5.9	18.1	212	355
14B	3.00	295	811						4.6	2				17000		54.2	16.1								11.9	15.3	40	388
14F	9.53	58.0	600						17.1	12				6770		51.6	11.8								3.9	13.8	139	281
14K	3.19	41.7	706						5.6	4				2400		16.3	8.1								2.2	7.8	37	202

Tracy Mtn. REE Section 15

T.139N., R.101W., Sec.26,
Elevation at top 2,831 ft.

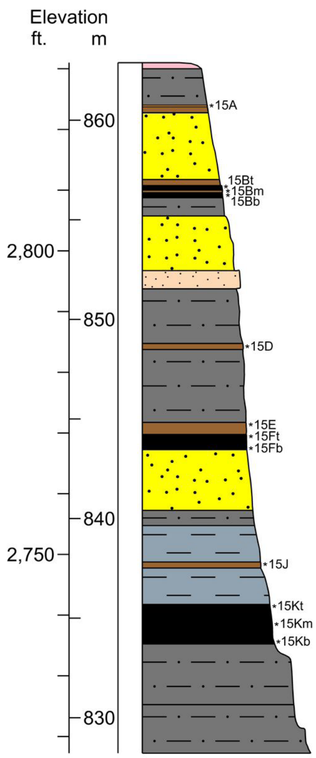

Sample ID	Lab Analysis (in µg/g) Cerium	Dysprosium	Erbium	Europium	Gadolinium	Holmium	Lanthanum	Lutetium	Neodymium	Praseodymium	Samarium	Scandium	Terbium	Thulium	Ytterbium	Yttrium	Total REE Whole coal	Total REE Ash
15A	55.0		2.54		6.0		26.0		32.7			13.5				19.7	*180*	*204*
15Bt	53.0	8.1	4.89	2.10	8.2	1.66	22.1	0.70	32.8	7.4	8.2	31.3	1.34	0.69	4.58	46.2	232	892
15Bm	84.8	11.9	7.59	2.02	11.0	2.57	40.1	0.95	35.8	9.4	7.3	12.0	1.87	1.03	6.02	93.8	328	1432
15Bb	99.2	12.2	6.31	3.32	14.0	2.28	36.1	0.78	59.1	13.9	13.9	18.2	2.19	0.85	5.13	51.5	339	575
15D	71.8		2.62		5.2		37.4		32.2			14.0				20.7	*209*	*223*
15E	71.9		3.05		5.6		34.3		33.6			13.9				23.1	*212*	*245*
15Ft	40.3		2.21		3.8		20.3		18.9			14.4				18.6	*136*	*236*
15Fb	46.1		3.26		5.7		20.5		24.7			12.8				25.6	*163*	*361*
15J	64.4		5.49		8.9		30.4		33.7			22.1				45.2	*248*	*573*
15Kt	13.0		0.67		1.5		6.3		7.2			5.0				5.3	*45*	*92*
15Km	9.1		0.40		0.8		4.6		4.1			0.9				4.4	*28*	*180*
15Kb	36.7		2.37		5.2		15.4		22.7			15.3				17.7	*136*	*446*

Sample ID	Lab Analysis (in µg/g)																											
	Antimony	Arsenic	Barium	Beryllium	Bismuth	Cesium	Chromium	Cobalt	Gallium	Germanium	Hafnium	Indium	Lithium	Magnesium	Manganese	Molybdenum	Niobium	Rubidium	Strontium	Tantalum	Tellurium	Thorium	Tin	Titanium	Tungsten	Uranium	Vanadium	Zirconium
15A	3.57	72.7	1580						20.6	6				11400		11.0	17.0								1.5	5.8	114	271
15Bt	1.94	15.2	1590						19.9	3				13900		18.9	19.3								2.5	21.4	98	542
15Bm	0.90	12.3	320						13.9	3				12100		16.3	17.9								5.3	10.7	17	157
15Bb	8.29	64.5	3640						18.8	8				7580		82.8	12.5								5.9	15.6	140	145
15D	2.88	6.3	591						28.3	3				14800		3.3	14.1								2.2	5.9	114	99.7
15E	3.55	12.6	971						26	5				14900		7.8	13.6								1.7	6.0	127	157
15Ft	8.00	48.2	228						17.9	10				6130		29.8	11.9								2.6	5.8	110	163
15Fb	3.61	29.1	417						14.8	12				8010		18.7	13.1								5.2	10.3	70	298
15J	16.6	72.7	368						17.6	14				7700		75.0	16.9								2.7	15.3	141	313
15Kt	4.95	315	4060						4.3	4				1990		22.4	6.3								1.9	2.2	48	103
15Km	0.30	16.5	222						4.1	1				2680		15.8	0.8								4.2	3.1	5	10.1
15Kb	10.9	104	626						12.6	27				3750		95.7	29.6								7.1	7.9	145	508

Appendix B - Analytical Results

Concentrations are reported on a whole rock basis as µg/g or parts per million

Sample ID	NDGS Field ID	Ash (wt%)	Cerium	Dysprosium	Erbium	Europium	Gadolinium	Holmium	Lanthanum	Lutetium	Neodymium	Praseodymium	Samarium	Scandium	Terbium	Thulium	Ytterbium	Yttrium	Antimony	Arsenic	Barium	Beryllium	Bismuth	Cesium	Chromium	Cobalt	Gallium	Germanium	Hafnium	Indium	Lithium	Magnesium	Manganese	Molybdenum	Niobium	Rubidium	Strontium	Tantalum	Tellurium	Thorium	Tin	Titanium	Tungsten	Uranium	Vanadium	Zirconium
1(sil)	225SIL	98.46%	41.1		1.28		2.1		22.4		16.6			6.2				10.7	1.44	2.8	367	0.5		5.29	36	1.9	10.2	2	2.8		33.3	1580	38	1.4	26.1	49	34	1.78		6.8		6930	3.7	3.1	54	98
1B1	225A	64.01%	191	18.8	10.1	5.37	21.8	3.6	83.1	1.33	97.7	24.1	22	30.6	3.34	1.38	8.72	88.7							76		23	7	6.3			8610		78.0	15.5			0.83					13.3	65.5	165	358
1B2	184A1	79.53%	124	11.1	6	3.16	13.0	2.1	57.6	0.79	61.7	15.1	13	22.3	1.96	0.83	5.37	53.2	7.33		4240	3.1		6.33	84		24	10	5.4		37.6	11100		47.8	13.8		420	1.02				2740	10.0	70.6	156	288
1F	225L	46.41%	38.8		3.03		6.3		15.2		25.3			18.2				24.6							55		10	15	8.7			8010		67.9	15.0			0.33					9.9	27.1	57	739
1I	225B	57.54%	116	21.1	13.0	4.68	21.9	4.5	58.9	1.73	70.3	15.7	17	32.7	3.46	1.74	10.9	112							157		25	42	10			6400		94.4	26.8			0.67					3.4	27.9	405	1150
1Ir	225BR	95.02%	52.9		2.29		4.4		29.1		24.4			15.2				20.5	1.99	16	3680	1.9		6.62	88	13	21	7	2.5		32.8	9090	157	4.5	13.4	96	173	0.97		9.8		4310	2.2	4.1	138	89.0
1K	225C	37.36%	18.9		1.81		2.6		8.1		10.2			4.9				20.0							8		5.5	3	2.9			7550		16.5	4.5			0.16					7.9	6.3	17	298
2A	184L	75.24%	61.5		5.80		8.6		31.8		32.6			22.8				43.0	22	392	11700	5.4	0.7	6.6	81	100	25	14	10	0.1	27	18600	1310	139	28.4	87	587	0.74	0.2	12	2.0	2420	56.6	18.9	184	480
2B1b	184A3b	80.40%	205	19	10.4	5	21.6	3.7	97.6	1.31	98.9	24.4	21	39.9	3.4	1.4	8.8	80.0	6.9	90	1390	5.6	0.7	9.9	118	9.8	35	20	8.2	0.1	55	11300	35	75.5	19.5	108	353	1.05	0.20	28	2.3	3250	18.3	106	206	503
2B1t	184A3t	74.38%	203	18	10.2	5.9	23.1	3.5	91.9	1.44	112	26.4	25	31.0	3.4	1.5	9.4	76.1	13	329	9830	5.0	0.6	5.4	89	9.5	33	13	13	0.1	56	11400	56	233	22.0	41	523	1.23	0.4	22	2.4	2540	24.6	100	241	775
2B2	184A2	69.90%	361	28.5	15.2	8.67	35.4	5.4	148	1.97	175	42.4	38	41.5	5.22	2.06	13.4	132	9.39	285	11500	7.6	0.9	5.77	110	9.5	44	15	15	0.1	60.4	15000	22	159	29.1	48	548	1.54	0.6	31	2.5	2830	31.2	157	201	959
2Fb	184MB	54.17%	62.4		4.38		8.3		24.0		35.3			18.0				34.1	6.49	48	486					5.7			5.3			4780		42.2									5.1	18.6		292
2Ft	184MA	41.38%	50.3		4.82		8.9		19.1		32.5			15.2				37.9	9.59	266	1650					11			6.9			6030		78.5									15.2	23.1		541
2G	184N	66.75%	34.1		3.86		4.0		17.5		15.7			12.0				33.8	6.22	43	1340					13			5.9			11800		35.7									2.8	26.9		299
2I	184B	55.67%	301	28.4	15.5	9.42	34.0	5.5	107	1.91	172	40.1	41	30.9	5.00	2.11	13.6	130	25.0	270	581	2.9	0.3	4.38	102	17	17.5	29	6.2	0.1	20.7	5310	86	58.5	13.4	45	255	0.56	0.1	14.2	1.4	1960	5.7	42.4	160	533
2K	184C	44.98%	31.6	2.9	1.73	0.75	3.1	0.6	13.9	0.26	15.6	4.0	3.4	6.9	0.48	0.25	1.70	14.0	4.88		517	1.9		1.33	19		10.5	10	3.3		9.7	3710		12.5	9.7		320	0.70				900	1.9	6.0	51	219
2N	184D	30.28%	9.9	2.6	1.95	0.53	2.1	0.6	5.2	0.34	5.7	1.3	1.6	11.9	0.39	0.30	2.04	15.5	6.95		775	1.9		0.14	11		6.3	11	2.4		1.3	4260		22.1	9.0		399	0.07				257	4.3	9.1	24	295
2Q	184E	47.92%	55.0	6.6	3.94	1.82	7.5	1.3	21.0	0.58	33.3	7.7	7.8	12.9	1.14	0.56	3.79	31.1	10.5		978	1.9		3.36	44		9.8	14	3.0		7.7	3010		68.3	10.9		204	0.32				1140	9.1	19.4	93	392
2R	184F	32.69%	20.2	2.5	1.36	0.79	3.0	0.5	7.9	0.18	13.5	3.1	3.3	5.9	0.44	0.19	1.20	11.8	6.11		986	1.1		0.87	25		4.3	14	1.9		3.4	1970		11.0	16.8		279	0.18				747	4.2	4.6	68	217
3A	208L	55.37%	53.3		9		10.9		26.8		30.2			32.7				72.7	16.4	698	16800					57			19			23200		126									83.5	44.4		870
3B1b	208AC	57.35%	122	13.3	7.7	3.47	14.8	2.6	58.2	1.05	62.3	15.2	14	26.7	2.33	1.06	6.80	67.6	9.18	42.0	1540	3.8	0.6	5.52	90	16	23	11	6.2	0.1	18.2	6470	29	62.8	11.5	66	482	0.61	0.2	11.5	1.4	2150	10.4	64.9	227	323
3B1m	208AB	69.34%	68.0		4.03		7.5		31.1		34.8			16.7				35.9	5.11	31	2780	3.1	0.7	6.37	50	6.3	32	6	4.8	0.1	46.0	5870	30	41.0	10.9	56	242	1.94	0.1	16	2.7	2380	8.4	32.7	126	193
3B1t	208AA	43.20%	141	14.7	8	4.27	17.4	2.8	53.2	1.06	81.0	19.2	19	28.2	2.66	1.10	7.00	64.8	6.17	87.0	4860	4.4	0.3	1.37	72	11	17.3	6	7.1	0.1	15.4	10300	46	48.1	16.2	11	471	0.45	0.2	12.4	1.1	1270	10.8	60.7	107	334
3B2b	208A2B	78.17%	128	13.3	7.9	3.64	14.3	2.7	62.8	1.10	63.7	15.6	14	31.5	2.26	1.08	7.03	65.1	13.1	267	13800					9.8			7.6			8130		107									10.9	94.8		494
3B2t	208A2A	79.58%	122	10.8	6.2	3.15	12.4	2.1	55.3	0.85	60.4	15.1	13	26.4	1.91	0.86	5.52	51.4	8.66	186	6280	4.6	0.8	7.65	79	12	31	9	7.4	0.1	58.7	9100	43	85.8	15.9	64	268	1.47	0.3	19	2.5	2790	11.0	74.9	185	389
3B3	208A3	58.67%	73.3		5.1		8.5		33.2		38.3			19.2				40.6	6.03	175	1590	4.0	0.5	4.80	54	26	22	7	6.1	0.1	29.0	9700	39	56.1	14.7	37	252	1.09	0.2	10.0	1.7	1900	9.8	114	117	297
3B4	208A4	73.52%	90.6	9.1	5.5	2.68	9.9	1.9	42.0	0.79	44.3	10.9	9.6	21.7	1.55	0.78	5.12	49.4	6.28	86	7370	4.2	0.5	8.97	80	18	32	8	6.3	0.1	38.1	10300	113	87.8	16.4	69	299	1.16	0.1	13.6	2.0	3000	13.4	76.0	181	283
3Fb	208MB	41.01%	29.8		3.75		4.7		14.5		14.9			17.4				32.7	6.18	33	1580					7.7			4.7			9170		44.1									7.1	12.1		284
3Ft	208MA	36.71%	34.9		4.70		6.5		15.9		20.6			14.1				41.7	7.06	49	1720					8.4			6.5			11300		75.2									12.7	24.5		418
3G	208N	68.67%	46.8		4.34		5.3		23.9		21.6			15.8				38.5	8.10	35	3210					31			5.2			15900		37.9									2.3	22.7		266
3I1	208B	55.97%	314	30.0	13.1	10.9	38.6	5.1	95.1	1.44	183	41.7	47	40.7	5.84	1.70	10.4	101	19.3	66	376	5.4	0.4	5.97	167	23	26	23	6.2	0.1	29.5	5210	86	64.0	9.7	56	199	0.57	0.1	22.4	1.6	2190	2.3	81.4	285	489
3I2	208B3	82.76%	161	15.5	7.10	5.33	19.1	2.7	63.6	0.83	91.2	21.7	23	26.1	2.98	0.96	5.80	59.8							129		30	5	3.3			5310		8.7	11.4			0.85					2.3	22.6	202	180
3J	208O	90.29%	51.8		1.91		3.4		26.9		21.8			18.0				15.6							90		26	2	3.4			11000		2.3	11.6			0.94					2.0	4.5	150	124
3K	208C	74.68%	20.3		0.83		1.5		10.2		8.9			8.7				6.8							21		22	3	3.8			7010		1.5	3.8			1.26					0.7	6.2	37	96
4B1b	209AB	87.13%	137	15.1	9	4.00	16.5	3.1	66.6	1.09	71.9	17.4	16	29.0	2.58	1.17	7.13	81.2	11.9	142	11200					12			6.7			10400		74.0									16.7	73.8		271
4B1t	209AA	86.29%	134	12.7	7.2	3.43	14.5	2.5	56.1	0.96	69.2	17.4	15	28.9	2.22	0.99	6.23	64.6	13.7	148	747	6.7	0.9	8.67	95	11	32	8	6.5	0.1	62.4	9990	58	125	20.9	65	275	1.46	0.6	27	2.7	3620	20.4	69.3	248	278
4B2	38B*	70.13%	127	14.0	7.9	3.63	15.4	2.8	60.2	1.04	64.4	15.8	15	23.4	2.41	1.08	6.87	65.0																												
4F1b	209MB	44.24%	45.8		4.17		6.9		19.6		25.0			13.9				29.6	8.47	93	553					8.5			6.0			8840		108									16.4	34.7		401
4F1t	209MA	63.81%	46.0		3.56		6.1		22.3		25.5			14.5				29.4	8.13	152	1860					10			7.5			9780		62.3									14.9	26.6		506
4F2	38A*	41.59%	44.7	7.8	4.65	1.64	7.6	1.6	17.2	0.67	26.4	6.2	6.6	13.4	1.28	0.66	4.27	33.0	7.04		4180	3.4		1.47	15		12.2	6	8.4		5.4	9420		99.8	3.6		434	0.17				506	19.3	21.6	58	617
4G1	209N	65.31%	34.3		4.82		4.9		19.0		16.0			13.1				46.2	12.0	52	9280					31			7.3			9040		32.6									6.3	13.0		395
4G2	38C	59.21%	32.7		4.44		4.5		15.8		14.9			14.4				38.3	5.35	31	6980					9.8			7.0			17800		11.3									3.0	23.0		397
4I1	209B	76.37%	224	20.6	9.5	6.41	24.3	3.6	96.9	1.00	112	28.4	26	37.0	3.85	1.23	7.22	88.5	7.65	36	5560	6.2	0.6	6.75	118	7.1	24	5	2.9	0.2	39.6	5380	69	14.2	9.5	68	190	0.65	0.10	29.6	1.8	2810	2.2	44.5	198	137
4I2	38D	81.95%	216	20.0	8.9	6.29	24.3	3.5	97.0	0.94	111	27.4	26	32.4	3.82	1.15	6.75	84.8	8.13	18	509	5.4	0.7	7.53	136	8.4	27	5	3.2	0.2	49.1	5190	63	13.4	10.8	81	85	0.77	0.1	25.7	2.0	3390	2.2	34.4	205	168
4J	209O	91.43%	52.6		2.04		4.0		25.7		23.6			17.0				16.5	2.18	12	937					6.1			3.3			9790		4.4									1.7	5.9		123
4Kb	209CB	16.51%	65.7	8.5	4.9	2.15	8.9	1.7	19.1	0.70	34.5	7.9	8.3	13.7	1.45	0.69	4.45	37.3	5.37	13	2730					12			3.2			2490		12.6									4.8	5.2		241
4Kt	209CA	60.45%	32.0		1.87		3.5		14.4		17.3			12.2				16.2	4.16	37	845					3.7			5.0			6540		7.0									2.4	7.4		285
5(nod)	224NOD	68.41%	11.8		0.62		1.2		8.1		5.7			2.9				7.2							20		4.6	<1	0.4			3930		<0.2	2.7			0.25					0.1	1.0	24	15
5Bb	224AB	84.35%	121	10.9	6.2	2.99	12.3	2.2	61.5	0.76	59.1	14.9	12	21.2	1.95	0.84	5.08	57.0							71		31	8	4.8			11700		86.7	13.3			1.42					11.6	111	189	228
5Bt	224AA	80.90%	251	20.3	10.5	6.01	25.2	3.7	112	1.27	130	32.5	28	32.9	3.79	1.39	8.47	89.0							86		29	9	7.5			14000		142	18.2			1.24					18.5	99.8	194	297
5E	224Q	78.11%	109	13.5	6.70	4.23	17.3	2.5	40.5	0.87	79.6	17.1	20	23.2	2.59	0.89	5.87	49.3							88		27	7	6.3			12300		29.8	15.0			1.03					3.0	31.4	213	345
5F1	224M	41.80%	42.6		3.90		9.6		13.4		40.1			14.3				30.3							36		8.3	4	6.0			6150		89.7	9.7			0.28					21.1	17.4	63	379
5F2	37L6	41.37%	46.6	9.8	5.1	2.81	12.3	1.8	14.1	0.66	48.7	9.1	13	19.8	1.79	0.68	4.50	36.8																												
5G	224N	43.25%	125	14.6	8.6	2.86	14.5	2.9	52.5	1.17	57.8	14.4	13	19.3	2.44	1.17	7.64	74.1							53		17.3	4	5.4			5110		50.1	16.6			0.74					2.6	15.5	84	261
5Ib	224BB	88.42%	142	10.0	4.87	3.10	12.2	1.8	68.6	0.58	65.5	16.8	14	21.3	1.87	0.66	4.03	45.7							100		25	4	3.1			7510		7.2	13.2			0.90					2.3	10.6	167	124
5Im	224BT	95.38%	79.8		2.38		6.0		38.8		35.3			12.0				21.9							66		17.8	3	2.3			4500		4.3	11.5			0.83					1.5	4.4	107	79
5Ir	224BR	92.40%	50.6		1.88		3.6		27.4		21.7			19.5				16.6							116		28	3	2.9			8930		6.5	14.2			0.91					2.5	3.8	207	98
5It	224BA	85.00%	141	11.3	5.5	3.36	13.6	2	67.6	0.65	65.1	16.6	14	23.6	2.09	0.73	4.38	52.7							117		35	5	3.0			6430		13.0	12.6			0.83					2.7	11.7	209	136
5K	224C	48.66%	29.9		1.77		3.7		13.7		16.5			7.5				16.8							24		12.8	8	4.4			5880		7.8	12.2			0.91					2.7	5.6	50	281
5L	224P	75.45%	37.5		2.39		3.3		19.6		17.2			16.2				20.5							98		24	28	4.8			18200		45.9	23.9			0.74					2.0	19.6	219	477
6B1	37L5A	88.23%	143	13.2	7.7	3.74	14.9	2.6	65.9	1.05	69.1	17.0	15	30.0	2.29	1.07	6.59	67.0							122		37	13	6.3			10600		105	20.1			1.18					20.3	69.4	268	302
6B2	38B2	80.89%	105	11.1	6.3	2.96	12.0	2.2	47.9	0.86	53.3	13.2	12	24.4	1.83	0.88	5.61	54.8	10.7	94	5740	4.5	0.9	8.32	87	26	22	7	6.4	0.1	58.3	15000	112	64.7	17.2	96	370	1.63	0.2	21	2.6	3000	16.5	63.9	200	331
6B3	223A	73.27%	159	17.4	10.5	4.36	18.6	3.6	78.1	1.39	77.6	19.0	17	30.9	2.97	1.43	8.98	105							70		32	7	7.8			13000		178	17.4			1.26					36.1	131	196	442

Sample ID	NDGS Field ID	Ash (wt%)	Cerium	Dysprosium	Erbium	Europium	Gadolinium	Holmium	Lanthanum	Lutetium	Neodymium	Praseodymium	Samarium	Scandium	Terbium	Thulium	Ytterbium	Yttrium	Antimony	Arsenic	Barium	Beryllium	Bismuth	Cesium	Chromium	Cobalt	Gallium	Germanium	Hafnium	Indium	Lithium	Magnesium	Manganese	Molybdenum	Niobium	Rubidium	Strontium	Tantalum	Tellurium	Thorium	Tin	Titanium	Tungsten	Uranium	Vanadium	Zirconium
6E	214M	65.60%	165	20.0	9.70	6.26	25.9	3.6	59.8	1.18	119	27.0	30	28.2	3.86	1.28	8.16	75.9	15.4	68	547					32			8.7			11900		51.3									4.5	49.2		524
6F1	37L4	32.04%	19.6	4.5	2.99	0.86	3.9	1	7.9	0.42	11.6	2.7	3.1	9.7	0.68	0.42	2.66	28.9	7.78	113	3050	3.7		0.64	13	8.3	10.7	6	4.7		6.1	8550		55.8	4.0		318	0.12				436	8.9	14.9	59	297
6F2	214M2	44.71%	47.2	10.8	7.5	1.72	9.0	2.4	19.5	1.09	26.7	6.3	6.8	19.6	1.60	1.06	6.76	71.0	9.29	55	600	6.5		1.19	23	30	17.5	6	6.5		8.7	9600		92.6	5.5		400	0.19				596	10.0	34.7	80	426
6F3	37L5	50.07%	83.7	12.7	6.6	3.24	14.6	2.4	30.1	0.82	57.9	12.9	14	19.4	2.28	0.87	5.47	57.8							27		8.9	5	5.9			7030		77.2	5.2			0.20					7.3	16.5	47	385
6G	214N	46.22%	114	13.7	8.3	2.63	13.2	2.8	54.6	1.15	53.9	13.6	12	21.0	2.26	1.16	7.47	73.6	4.50	34	1850					17			6.8			6670		26.1									2.5	23.7		320
6I	214B	90.75%	84.0		3.41		6.5		41.5		36.5			23.2				28.1							106		28	5	4.5			12500		6.4	13.9			1.03					2.2	15.6	202	254
6Ir	214BR	92.77%	61.9		2.37		5.0		32.1		28.5			15.0				21.2							84		21	3	2.8			20500		1.7	14.6			1.03					2.1	2.9	128	91
6J	214O	85.11%	49.4		2.30		4.1		24.0		22.6			18.6				18.4	6.80	24	3940					5.9			4.2			13500		11.2									1.9	12.3		214
6K1	214C	58.88%	19.6		1.03		1.8		9.5		9.5			7.6				8.8	4.30	38	7510					2			3.2			6730		8.3									1.1	5.0		158
6K2b	214C2b	23.52%	102	14	7.52	3.8	15.0	2.6	39.1	1.03	61.7	14.1	15	25.8	2.4	1.1	6.7	52.9									22	11				4280		9.8										8.0		487
6K2t	214C2t	67.22%	35.9		1.91		3.7		17.9		18.5			11.6				14.1									18	7				6630		9.8										10.3		204
7(bar)	223BAR	98.49%	12.6		0.57		1.2		6.6		6.3			3.1				5.3	0.29	1.7	32000	0.4		2.70	12	2.3	5.1	1	0.6		7.8	3150	84	0.5	3.2	28	524	0.24		1.9		930	0.5	1.7	27	20
7B	214A	82.78%	151	14.6	8.4	4.11	16.9	2.9	69.8	1.16	76.8	18.7	17	28.0	2.59	1.17	7.43	79.8	10.1	164	5630	6.6	0.9	7.62	99	15	33	8	7.4	0.1	76.6	8300	33	96.7	20.9	82	322	1.54	0.30	24	2.6	2990	20.7	58.8	214	359
7D	37O	27.05%	40.2	7.4	4.74	1.41	7.0	1.6	18.4	0.70	23.6	5.4	5.9	12.6	1.16	0.67	4.33	41.3																												
7E1b	223R	66.11%	91.9	11.4	5.7	3.80	15.0	2	31.7	0.75	72.2	15.3	18	27.1	2.21	0.76	4.98	42.9							107		18.0	6	7.3			10800		51.9	14.5			0.70					3.8	26.5	238	404
7E1t	223Q	63.27%	183	25.0	12.0	6.96	30.4	4.5	58.8	1.44	131	28.8	31	23.0	4.70	1.58	9.83	94.1							89		34	16	10			12200		124	31			0.80					12.6	34.9	382	720
7E2	37N	52.85%	216	30.8	13.9	9.85	40.0	5.3	61.1	1.71	175	37.6	46	33.3	5.79	1.84	11.5	93.0	22.6	107	4480	5.6	1.2	4.08	84	45	15.3	14	11	0.2	23.2	9430	43	131	25.8	46	163	0.56	0.3	16.0	2.2	1800	6.4	79.2	387	839
7F1	37L3	37.10%	95.5	17.6	8.8	4.75	21.0	3.2	28.7	1.13	81.8	16.8	21	20.9	3.15	1.17	7.48	68.8	11.2		11300	3.6		0.94	30		8.1	10	6.6		5.9	7790		110	6.4		203	0.16				520	17.1	25.0	74	372
7F2b	223MB	40.53%	69.9		6.5		10.2		29.6		37.0			23.6				61.7							38		13.8	4	4.2			7970		33.5	13.7			0.88					3.8	19.7	92	199
7F2t	223MA	44.90%	18.0		1.99		3.2		6.7		12.7			7.4				17.9							18		5.3	6	4.6			9040		144	6.5			0.15					10.3	7.3	40	324
7F3	37L2	40.07%	84.8	12.4	6.4	3.55	15.4	2.3	23.7	0.81	62.6	13.5	16	19.3	2.25	0.84	5.49	45.3																												
7F4b	37M*	54.63%	72.2	10.3	5.9	2.24	10.0	2.1	28.6	0.81	39.3	9.6	9.3	18.9	1.71	0.85	5.29	55.0																												
7F4t	37L*	40.07%	114	17.3	8.7	4.67	20.0	3.2	36.2	1.13	80.1	17.7	20		2.93	1.22	7.43	64.0																												
7F5	37L7	41.22%	44.6	7.5	4.20	1.88	8.4	1.5	17.0	0.61	33.1	7.0	8.3	15.7	1.27	0.59	3.82	33.5																												
7G1	223NII	63.27%	56.8		5.2		6.7		31.3		23.6			13.5				48.9							49		11.8	7	4.7			9030		28.5	20.7			0.82					3.1	7.7	156	212
7G2	223N	68.14%	38.9		3.67		4.4		22.0		16.0			10.3				34.4							47		12.7	7	4.5			6300		31.4	17.9			1.05					3.1	6.4	140	193
7HTm1	184G	49.74%	21.5		1.64		2.8		12.8		11.5			5.0				18.2	1.94	37	2030	1.6	0.2	1.71	23	6.1	6.3	4	1.3	0	11.9	4840	118	6.0	5.5	28	330	0.36	<0.1	3.5	0.8	1230	1.6	4.6	35	64
7HTm2	184H	30.10%	9.3		0.47		0.8		6.4		3.9			1.8				6.0	0.55	11	1620					2			0.8			4580		4.8									1.1	1.7		28
7HTm3	184I	17.60%	7.1		0.36		0.7		4.0		3.5			2.4				3.9	0.46	5.1	1780					3.1			0.7			3800		2.3									1.1	1.1		25
7J1	37K*	n/a	45.8	3.3	2.20	0.84	3.5	0.7	23.5	0.37	21.3	5.3	3.8		0.51	0.35	2.35	17.0																												
7J2	223B	88.47%	65.0		2.35		4.6		33.8		28.0			19.3				20.0							89		27	3	3.6			12600		1.7	13.3			0.96					1.9	6.9	147	154
7Kb	37J*	n/a	35.3	4.0	2.26	1.14	4.3	0.8	15.3	0.31	18.8	4.5	4.4		0.65	0.33	2.02	17.0																												
7Kt	37F*	59.28%	26.7	3.4	1.92	0.86	3.6	0.7	12.7	0.28	15.9	3.9	3.8		0.54	0.29	1.85	15.0																												
7M	223V	68.96%	57.9		3.34		5.4		28.1		26.9			19.2				25.1							88		20	46	4.0			7390		19.6	20.4			0.71					1.7	15.0	200	360
7N	37E*	29.37%	19.3	5.2	3.95	0.88	3.7	1.2	9.6	0.64	10.4	2.4	2.7		0.68	0.61	3.93	34.0																												
7O	223W	92.81%	99.6	10.1	5.5	2.89	11.9	1.9	44.1	0.75	54.6	12.9	12	10.5	1.83	0.76	4.84	45.1							56		16.0	4	3.1			6580		8.5	13.8			0.84					1.6	5.1	103	237
7Or	223WR	95.28%	70.8		2.80		5.7		37.4		32.8			13.4				25.7							78		20.0	3	3.3			13500		2.3	15.5			0.89					1.5	2.9	121	135
7P	223X	52.12%	48.6		3.19		6.5		19.3		29.7			14.1				25.3							49		11.1	25	3.5			4910		66.7	18.1			0.39					11.4	17.6	97	634
7Q	223Y	58.77%	31.7		3.26		3.2		17.6		14.5			16.4				26.2							65		19.9	59	4.1			6950		24.8	30			0.53					3.4	14.7	171	469
7R	37A*	n/a	28.5	3.0	1.47	1.13	3.8	0.6	11.4	0.18	18.2	4.1	4.4		0.53	0.20	1.25	12.0																												
7S	223Z	71.41%	54.8		2.77		5.7		23.4		28.8			16.9				22.0							81		19.4	36	2.8			7860		18.8	21.4			0.59					1.5	16.6	211	237
8(crb)	215Y	95.40%	66.2		2.78		5.3		36.0		29.1			12.1				29.4	3.15	19.0	618					37			3.0			8000		2.9									1.9	8.4		116
8(fe)	215Fe	89.67%	20.9		1.54		2.4		10.9		10.3			7.7				14.1	13.7	152	614					21			1.2			2650		31.3									2.3	22.9		50
8A	215L	71.56%	120	19.5	13.1	4.25	19.2	4.3	61.6	2.00	66.3	15.2	16	37.5	3.14	1.86	12.3	128	15.9	464	6020					253			12			23400		39.3									36.6	17.6		599
8B	215A	75.42%	101	9.1	5.4	2.73	11.1	1.8	46.6	0.78	51.7	12.5	11	20.2	1.65	0.74	4.77	49.5	5.59	146	4940	3.0	0.5	5.02	74	7.1	21	8	7.4	0.1	39.4	12500	230	48.8	22.2	60	360	1.06	0.20	14.4	1.9	2820	20.0	44.3	150	337
8C	215X	85.01%	163	21.0	12.5	4.76	23.4	4.5	79.7	1.50	84.1	20.0	18	32.4	3.60	1.60	9.38	143	14.0	33	724					15			7.3			13000		8.5									3.1	27.2		545
8D	215Z	91.54%	74.4		4.03		6.5		39.6		34.1			17.8				35.3	7.38	34	6920					20			6.6			17400		11.7									2.6	12.1		371
8F1	37L8	32.97%	42.5	8.8	4.89	2.24	10.0	1.7	14.5	0.70	36.7	7.5	9.9	17.1	1.52	0.69	4.59	34.0	6.74		3580	1.9		0.51	29		6.4	4	5.6		2.6	10400		73.1	5.3		132	0.15				599	14.6	19.9	55	345
8F2	215M	46.35%	30.5		3.63		6.0		10.4		21.9			10.6				31.8	6.88	291	17500					12			4.7			8400		53.2									10.0	10.4		332
8G	215N	66.69%	33.7		4.64		4.6		21.6		14.6			11.2				47.5	4.31	24	6200					13			4.7			7870		18.9										8.8		208
8I1	215B	83.31%	189	16.5	7.4	5.52	20.7	2.8	78.0	0.79	101	24.4	24	30.6	3.18	0.95	5.82	65.3	7.95	23	541	3.6	0.6	8.42	117	7.9	25	6	3.3	0.1	40.4	6450	56	14.1	11.6	87	107	0.88	0.1	45.9	2.2	3550	2.5	39.7	209	167
8I1r	215BR	91.92%	46.5		1.65		3.4		24.3		20.3			19.4				13.8							104		26	2	2.6			7100		8.9	12.2			0.78					2.1	5.7	181	80.0
8I2	215B2	58.94%	352	34.8	16.7	11.5	42.2	6.2	129	1.91	199	46.7	49	35.0	6.46	2.21	13.4	143							122		34	20	4.5			5240		47.0	9.7			0.53					2.2	60.4	230	391
8I2r	215B2R	92.65%	146	7.1	3.58	2.80	9.9	1.3	69.8	0.43	67.1	17.4	13	19.2	1.42	0.47	3.03	31.1							103		28	4	2.5			6390		2.9	12.8			0.83					2.2	4.6	172	77
8J	215O	80.78%	56.8		2.41		4.1		28.5		24.8			18.8				19.9							96		28	3	3.6			11500		2.8	11.6			0.96					1.9	8.4	162	181
8K	215C	53.24%	37.7		2.52		4.7		17.0		20.4			9.9				21.8							34		11.6	11	2.9			5270		8.7	6.4			0.50					1.2	4.6	72	194
9B	226A	65.69%	237	24.3	13.3	6.55	27.5	4.7	100	1.74	122	29.9	28	31.3	4.28	1.79	11.4	111							85		19.8	10	8.1			15300		175	20.2			0.85					22.2	200	155	413
9F	226L	44.54%	44.4		4.49		7.5		17.5		27.2			15.9				39.1							35		16.0	9	9.7			4590		69.1	10.4			0.23					14.9	26.3	99	741
9I	226B	38.57%	268	31.7	15.7	9.52	39.8	5.9	110	1.95	160	34.4	37	34.1	5.82	2.07	12.8	125							98		22	15	6.7			2360		134	18.2			0.26					4.7	51.3	216	697
9Ir	226BR	92.00%	226	14.8	7.5	5.32	19.1	2.7	101	0.90	111	28.2	23	20.4	2.84	1.00	6.28	68.8							117		33	8	2.9			5960		9.2	13.3			0.94					2.4	10.4	189	110
9K	226C	63.01%	26.4		1.42		2.7		11.9		13.6			8.0				11.6							25		14.3	7	2.9			6090		3.1	4.1			0.67					0.6	4.5	62	117
10(crb)	228L	79.96%	54.0		2.69		4.9		23.2		24.4			17.5				21.8							59		21	12	9.8			20500		71.6	23.1			0.88					30.1	25.0	103	539
10A	228X	89.02%	103	11.2	5.7	3.29	13.6	2	35.0	0.74	66.6	15.3	15	15.9	2.08	0.78	5.12	40.7							80		27	13	5.8			17400		13.6	21.3			0.96					5.9	22.0	236	280
10B	228A	75.31%	101	9.3	5.2	2.59	10.2	1.8	43.6	0.72	51.1	12.7	11	22.6	1.62	0.72	4.61	45.8							113		25	4	4.6			7750		27.9	14.3			1.05					3.9	46.6	249	222
10F	228Y	61.54%	51.3		3.03		5.8		23.2		27.6			13.3				26.4							55		16.4	12	5.6			7760		73.9	8.0			0.54					6.2	28.4	133	422
10G	228N	88.67%	88.5		4.33		7.3		43.6		39.7			13.9				37.0							48		34	4	5.7			5860		21.2	29.5			2.83					7.7	12.1	95	235
10J	228O	91.37%	49.1		1.91		3.2		24.8		20.9			17.7				15.2							85		27	3	3.6			10700		6.3	12.5			1.08					2.2	7.0	145	148

Sample ID	NDGS Field ID	Ash (wt%)	Cerium	Dysprosium	Erbium	Europium	Gadolinium	Holmium	Lanthanum	Lutetium	Neodymium	Praseodymium	Samarium	Scandium	Terbium	Thulium	Ytterbium	Yttrium	Antimony	Arsenic	Barium	Beryllium	Bismuth	Cesium	Chromium	Cobalt	Gallium	Germanium	Hafnium	Indium	Lithium	Magnesium	Manganese	Molybdenum	Niobium	Rubidium	Strontium	Tantalum	Tellurium	Thorium	Tin	Titanium	Tungsten	Uranium	Vanadium	Zirconium
10K	228C	67.86%	32.1		1.21		2.6		16.5		15.4			11.3				10.2							49		18.8	14	3.7			5940		7.7	13.0			1.22					2.0	6.6	120	229
11B1	229A	88.12%	49.6		2.32		3.5		25.1		20.1			18.7				14.4							108		25	3	5.3			11600		33.6	14.0			1.27					3.6	14.1	233	258
11B2	229N	85.83%	47.0		1.94		3.7		24.7		21.5			13.5				16.6							73		26	2	3.0			7600		6.3	9.3			1.22					1.9	7.7	147	132
11C	229Q	94.27%	74.6		2.81		6.2		35.0		34.6			10.8				25.3							50		17.8	2	2.7			8020		1.1	14.1			1.20					2.6	4.5	74	100
11J	229O	88.69%	39.9		1.76		2.8		20.2		17.4			11.5				14.3							71		16.4	7	3.0			10200		1.5	11.2			0.87					1.5	5.5	118	210
11K	229C	68.34%	19.9		1.04		2.2		9.1		11.2			9.5				8.6							25		15.8	11	3.0			6090		9.7	5.4			0.89					2.0	6.3	48	186
12E	235F	65.21%	31.2		1.89		2.4		16.8		13.3			10.5				16.2							67		14.7	15	3.2			11300		11.3	13.5			0.70					2.2	49.3	228	287
12F	235E	89.86%	43.4		1.37		2.6		22.0		18.9			9.3				11.1							56		17.2	3	2.9			8350		2.4	13.1			0.98					2.5	8.0	109	117
12G	235D	71.41%	28.8		1.14		2.1		12.6		12.2			7.5				11.0							13		14.0	4	2.8			11600		11.7	3.1			1.03					1.1	29.0	54	86
12L	235C	70.71%	40.4		2.44		4.2		19.4		21.2			13.4				17.9							73		22	64	5.0			6230		105	18.4			0.66					8.3	16.3	195	593
12P	235B	82.24%	83.3		4.90		9.3		40.0		42.3			16.4				39.6							97		23	30	3.5			7830		17.4	15.1			0.74					1.3	15.2	281	387
12R	235A	31.40%	20.6		1.42		3.4		7.2		15.8			4.7				12.9							29		4.5	6	2.3			2320		17.6	27.4			0.26					5.9	3.6	44	300
13J1	234A	88.38%	26.4		2.02		2.4		13.9		11.1			13.2				17.6							53		30	21	4.7			2130		40.8	20.4			1.01					3.3	12.9	116	662
13J2	234A2	84.36%	39.1		2.84		3.8		21.1		17.5			16.7				27.8							51		22	15	4.0			7240		209	13.5			0.98					5.4	18.9	123	604
13L	234B	93.12%	53.6		2.32		4.5		28.8		24.6			14.0				21.2							93		22	4	2.9			15900		4.4	12.4			0.97					1.9	8.9	188	113
13M	234C	94.09%	60.0		2.00		4.3		31.4		26.5			14.9				18.3							86		23	3	3.3			15400		8.8	13.3			1.01					2.0	10.8	145	120
13N	234D	86.97%	41.4		1.83		2.8		22.7		18.1			10.3				15.3							60		16.9	7	3.5			8960		15.1	14.9			1.05					2.3	14.2	134	274
13O	234E	54.19%	27.4		2.37		3.5		14.2		14.6			11.5				21.1							36		14.7	20	5.8			6830		218	15.6			0.28					10.1	27.1	97	646
13P	234F	86.91%	78.3		3.34		6.5		41.5		35.9			17.9				29.5							95		26	13	4.8			9520		4.1	17.6			1.21					1.8	11.1	157	349
13Rm	234H	39.10%	17.1		1.09		2.2		7.4		10.5			5.3				9.3							38		5.8	4	1.3			2910		23.9	4.7			0.18					2.2	8.7	41	95
13Rt	234G	50.08%	39.4		2.03		4.9		17.0		25.4			13.8				15.9							119		12.1	11	3.9			3650		35.6	19.1			0.38					1.4	16.7	98	416
14(ash)b	237AshB	79.30%	37.1		6.50		8.0		17.5		22.9			16.0				66.7	4.66	87	5410						10.6	8				11300		120	7.0								27.4	34.1	63	254
14(ash)t	237Ash	89.17%	37.6		2.18		3.4		19.2		16.5			13.6				24.2	2.37	99	9550						13.8	3				28800		23.8	7.3								2.0	8.8	75	128
14A	237A	83.46%	65.1		3.60		6.9		27.9		36.2			17.7				25.8	5.77	57	1580						23	6				15200		46.4	16.1								5.9	18.1	212	355
14B	237B	33.87%	21.1		2.31		4.3		8.7		17.1			18.0				19.9	3.00	295	811						4.6	2				17000		54.2	16.1								11.9	15.3	40	388
14F	237E	51.52%	57.7		3.63		6.6		25.2		30.1			16.1				28.7	9.53	58.0	600						17.1	12				6770		51.6	11.8								3.9	13.8	139	281
14K	237G	26.21%	28.9		1.70		3.6		12.7		16.0			10.9				13.5	3.19	42	706						5.6	4				2400		16.3	8.1								2.2	7.8	37	202
15A	236A	88.42%	55.0		2.54		6.0		26.0		32.7			13.5				19.7	3.57	73	1580						21	6				11400		11.0	17.0								1.5	5.8	114	271
15Bb	236BC	58.96%	99.2	12.2	6.3	3.32	14.0	2.3	36.1	0.78	59.1	13.9	14	18.2	2.19	0.85	5.13	51.5	8.29	65	3640						18.8	8				7580		82.8	12.5								5.9	15.6	140	145
15Bm	236BB	22.91%	84.8	11.9	7.6	2.02	11.0	2.6	40.1	0.95	35.8	9.4	7.3	12.0	1.87	1.03	6.02	93.8	0.90	12	320						13.9	3				12100		16.3	17.9								5.3	10.7	17	157
15Bt	236BA	26.06%	53.0	8.1	4.89	2.10	8.2	1.7	22.1	0.70	32.8	7.4	8.2	31.3	1.34	0.69	4.58	46.2	1.94	15	1590						19.9	3				13900		18.9	19.3								2.5	21.4	98	542
15D	236C	93.66%	71.8		2.62		5.2		37.4		32.2			14.0				20.7	2.88	6.3	591						28	3				14800		3.3	14.1								2.2	5.9	114	100
15E	236D	86.58%	71.9		3.05		5.6		34.3		33.6			13.9				23.1	3.55	13	971						26	5				14900		7.8	13.6								1.7	6.0	127	157
15Fb	236EB	45.15%	46.1		3.26		5.7		20.5		24.7			12.8				25.6	3.61	29	417						14.8	12				8010		18.7	13.1								5.2	10.3	70	298
15Ft	236EA	57.42%	40.3		2.21		3.8		20.3		18.9			14.4				18.6	8.00	48	228						17.9	10				6130		29.8	11.9								2.6	5.8	110	163
15J	236F	43.24%	64.4		5.5		8.9		30.4		33.7			22.1				45.2	16.6	73	368						17.6	14				7700		75.0	16.9								2.7	15.3	141	313
15Kb	236GC	30.47%	36.7		2.37		5.2		15.4		22.7			15.3				17.7	10.9	104	626						12.6	27				3750		95.7	29.6								7.1	7.9	145	508
15Km	236GB	15.47%	9.1		0.40		0.8		4.6		4.1			0.9				4.4	0.30	17	222						4.1	1				2680		15.8	0.8								4.2	3.1	5	10
15Kt	236GA	49.09%	13.0		0.67		1.5		6.3		7.2			5.0				5.3	4.95	315	4060						4.3	4				1990		22.4	6.3								1.9	2.2	48	103

* REE data for 9 samples previously reported in Kruger and others (2017), pages 71-72.